A CALDERA SEQUENCE IN THE EARLY PRECAMBRIAN, FAVOURABLE LAKE VOLCANIC COMPLEX, NORTHWESTERN ONTARIO

A Thesis

Presented to the

Faculty of Graduate Studies

of

The University of Manitoba

In Partial Fulfillment

of the Requirements

for the degree

Master of Science

by

PETER STANLEY BUCK

February, 1978

A CALDERA SEQUENCE IN THE EARLY PRECAMBRIAN, FAVOURABLE LAKE VOLCANIC COMPLEX, NORTHWESTERN ONTARIO

BY

PETER STANLEY BUCK

A dissertation submitted to the Faculty of Graduate Studies of the University of Manitoba in partial fulfillment of the requirements of the degree of

MASTER OF SCIENCE

ABSTRACT

A steeply overturned, Early Precambrian, felsic to intermediate vent facies metavolcanic formation occupies a caldera or volcanic graben in the eastern part of the Favourable Lake metavolcanic-metasedimentary belt, northwestern Ontario. The caldera has a restricted extent with well defined margins and in the exposed cross section is about 6.2 km long and up to 1870 m deep. The formation, informally termed formation H, consists dominantly of andesitic and dacitic pyroclastic rocks and flows and minor volcanic epiclastic rocks regionally metamorphosed to low or middle greenschist facies. Formation H is subdivided into four members that represent major volcanic pulses.

The caldera or volcanic graben was initiated during the final stages of growth of a subaqueous to subaerial mafic shield volcano. Collapse continued during subsequent felsic to intermediate, dominantly explosive, subaerial volcanism which infilled the depression. Source vents, as indicated by the distribution of flows and coarse pyroclastic rocks, were near the margins of the caldera. Collapse appears to have been coeval with felsic to intermediate volcanism, and this probably caused the collapse and withdrawal of support from the magma chamber. The formation is thickest in the central and southern parts, and the magnitude of collapse is greatest along the southern boundary; collapse probably simulated a trap-door movement. Following volcanism, formation H underwent a period of rapid erosion, and coarse sandstone and conglomerate were deposited in an alluvial fan and shallow-water environment bounded by the margins of the caldera.

Metavolcanic formation H differs texturally, mineralogically, and chemically from other felsic to intermediate, greenschist-facies metavolcanic rocks in the area in poorer preservation of primary textures,

higher biotite content, local preservation of primary plagioclase composition, local presence of garnet, widespread occurrence of pyrite and pyrrhotite, presence of muscovite-rich buff alteration zones, and greater metasomatic changes in major element compositions. Graphical plots employing major elements and normative mineral compositions show a wide scatter due to metasomatic changes, but the formation H rocks retain calc-alkaline chemical characteristics. The most obvious chemical changes are depleted CaO and total alkalies, and both depleted and enriched Na_2O and K_2O compared to unaltered Precambrian and Cenozoic felsic to intermediate calc-alkaline rocks. Changes in SiO_2, MgO and FeO (total) may also occur, but are difficult to detect. These features suggest that formation H underwent a period of pervasive synvolcanic metamorphism and metasomatism, in the form of hot-spring and fumarolic activity, prior to the regional greenschist metamorphic event. Local muscovite-rich, buff alteration zones occur in several proximal vent facies sequences and have undergone stronger chemical changes and recrystallization than the bulk of the formation; they are probably zones of more intense fumarolic or hot-spring activity related to source vents.

CONTENTS

LIST OF FIGURES

LIST OF TABLES

INTRODUCTION

GENERAL STATEMENT

In the eastern part of the Early Precambrian, isoclinally folded, Favourable Lake metavolcanic-metasedimentary belt northwestern Ontario, (Fig. 1), five volcanic cycles have been recognized (Ayres, 1977). Most cycles comprise an early mafic effusive phase and a later, dominantly pyroclastic, felsic to intermediate phase. In the second cycle the later phase consists of a lower mafic to intermediate sequence, informally termed formation G, overlain by a felsic to intermediate sequence, informally termed formation H, which has a restricted field occurrence within an overturned structural depression that appears to have formed by volcanic collapse. Gold, silver, lead, and zinc bearing quartz veins have been mined from the upper part of the formation (Ayres, in preparation). This study focuses on several aspects of formation H: 1) characteristics, origin, facies, and environment of emplacement of volcanic products, 2) the origin of the structural depression and its relationship to volcanism, and 3) metasomatism.

Most studies of Early Precambrian volcanism have been more concerned with the stratigraphic framework than with the details of the stratigraphy (e.g. Goodwin, 1967; Goodwin and Ridler, 1970; Wilson et al, 1974). The emphasis has been on broad stratigraphic, lithologic and chemical changes, and their implication regarding volcanic evolution of metavolcanic-metasedimentary belts, tectonics and metallogenesis. These studies are necessary but should be complemented by detailed stratigraphic studies. This study shows the importance of detailed work for accurately solving fundamental volcanological and geochemical problems such as those stated above.

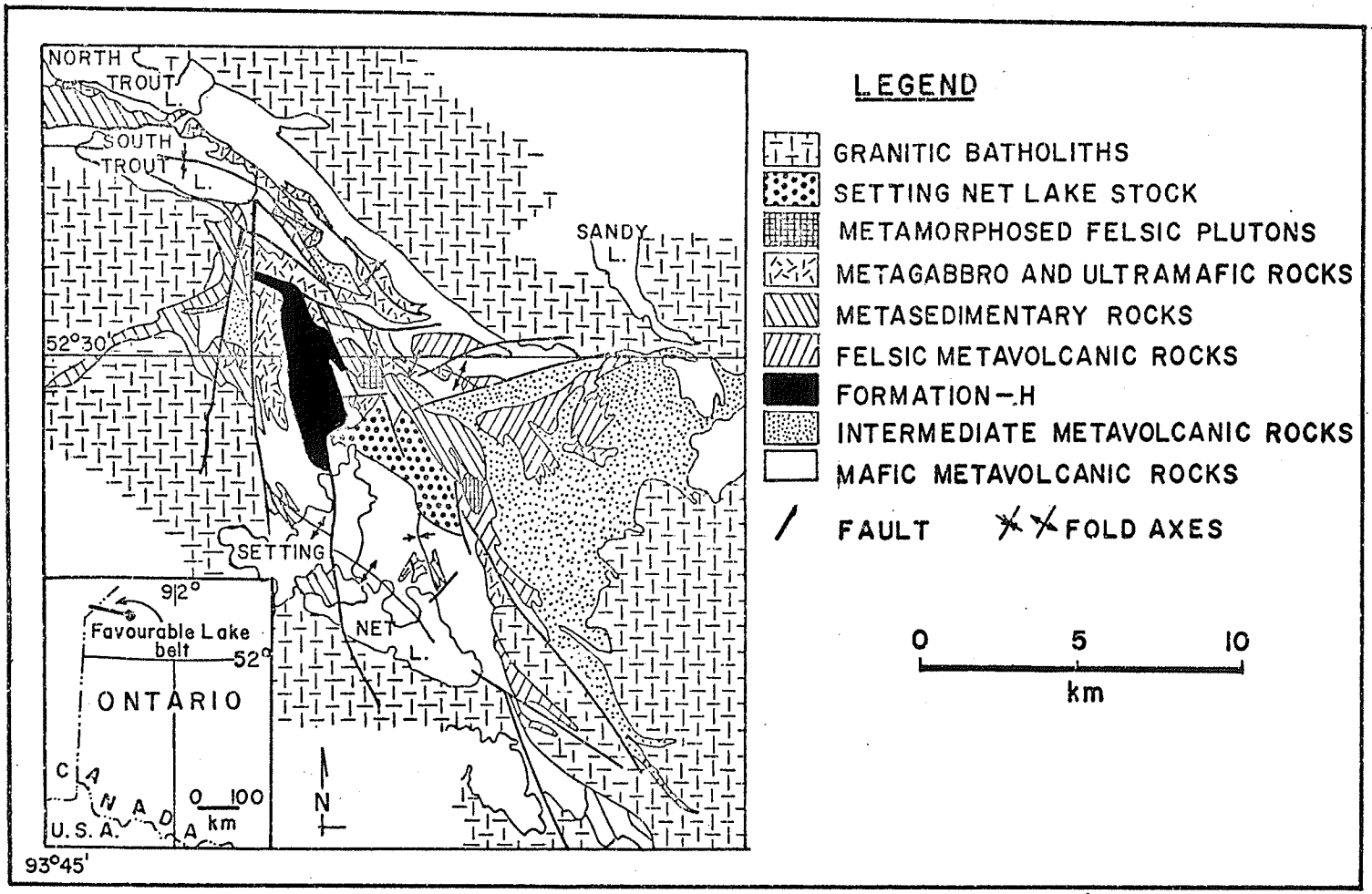

Fig. 1. Generalized geological map and location of the eastern part of the Favourable Lake metavolcanic-metasedimentary belt (Ayres, 1977).

In addition, this study is unique because volcanic collapse structures have not been recorded in other Early Precambrian volcances.

ACKNOWLEDGEMENTS

Research for this thesis was carried out under the direction of Professor L.D. Ayres, whom I wish to thank for assistance and for critically reading and improving early versions of the manuscript. I am also grateful to Professor A.C. Turnock for reviewing and improving early versions of the manuscript. Special thanks to my wife Roslyn for providing capable field assistance, encouragement, and for typing the manuscript. The author is sincerely grateful to Mr. R. Woodall, Western Mining Corp. Ltd. for encouragement and interest prior to and during the study. Numerous fruitful discussions and assistance by fellow students and staff are gratefully acknowledged.

The author acknowledges the co-operation of Zahavy Mines Ltd. for free access in the area and for furnishing diamond drill core.

The study was generously supported by the National Research Council of Canada Operating Grant A8996 and by funds from Western Mining Corp. Ltd., a University of Manitoba Fellowship and a Manitoba Graduate Assistantship.

METHODS OF STUDY

The eastern part of the Favourable Lake metavolcanic-metasedimentary belt was mapped between 1965 and 1972 by Ayres (1970, 1972, 1974) at a scale of 1:15,840 for the Ontario Division

of Mines. This mapping outlined the basic stratigraphy of the belt (Ayres, 1977) and the possible caldera origin of formation H.

In the summer of 1974, the author spent two months re-examining and mapping formation H in detail. Data was compiled on 1:7920 aerial photographs enlarged from 1:15,840. This phase of the program delineated the stratigraphy and established the genesis of some units. A further two weeks were spent in the field during the summer of 1975 to study specific problem areas that arose from the initial field and laboratory study.

About 450 samples were collected and about 250 of these were studied in thin-section. Detailed macroscopic studies were made of fragmental rocks and some of these samples were studied by etching sawn surfaces with HF solution for thirty seconds to accentuate textures. Twenty-four samples were modally and chemically analysed and two additional analyses were provided by Ayres. Chemical analyses were done by rapid methods : Si, Al, Fe (total), Mg, Ca, K, Ti and Mn, were determined by X-ray fluorescence spectrometry; P_2O_5 by colorimetry; FeO by decomposition of the sample in HF and 1:4 H_2SO_4 solution titrated with $K_2Cr_2O_7$ (sodium diphenylamine sulphanate was used as indicator); and H_2O (total), S and CO_2 by induction furnace procedures.

NOMENCLATURE AND CLASSIFICATION

Metavolcanic Rocks

Modal colour index (Ayres, 1969) is a useful field and laboratory criteria for compositional classification of metavolcanic rocks. Colour index is the total amount of ferromagnesium minerals: actinolite, hornblende, biotite, chlorite, chloritoid, garnet, pyroxenes and olivine. It is an approximate measure of chemical composition because: 1) minerals forming the colour index contain most of the iron and magnesium in metavolcanic rocks, and 2) iron and magnesium decrease with increasing silica content. Ayres (1969) defined three colour index groups for subalkaline rocks:

Compositional Group	Colour Index
mafic	greater than 35
intermediate	15 to 35
felsic	less than 15

Correlation of these groups with chemical data by Ayres (1969) showed that the boundaries between these three groups are in the andesite and dacite fields.

In this study colour index could not be precisely used because of the fine-grain size of the rocks, rapid variations in the field and heterolithic nature of some units. Petrographic and field study found that colour indicies are in the mafic to intermediate range for formation G rocks, and in the felsic to intermediate range (2 to 35) for most formation H rocks. Petrographic measurements of colour index for formation H felsic to intermediate metavolcanic rocks may have errors of as much as 20 percent because of fine-grain size.

Volcaniclastic Rocks

At present there are no formally established classification schemes or nomenclature for volcaniclastic rocks. This has led to confusion and different usage of terms by different authors. To alleviate this problem most recent studies in North America, including this study, adopt classification schemes and nomenclature of Fisher (1960b, 1961, 1966) and Parsons (1969).

The term "volcaniclastic" as defined by Fisher (1961, 1966) embraces the entire spectrum of clastic rocks composed in part, or entirely of volcanic fragments formed by any mechanism or origin, and emplaced in any physiographic environment. Volcaniclastic rocks can be classified both genetically and on the basis of particle size. Of these two classifications, the genetic is the more useful for determining facies and the nature and environment of volcanism.

Parsons (1969) genetically subdivided volcaniclastic rocks into autoclastic, alloclastic, pyroclastic, and epiclastic types. Hyaloclastite is treated as a pyroclastic rock by Parsons (1969) but should be considered as a separate and distinct type. Criteria for genetic subdivision (Parsons, 1969) of volcaniclastic rocks include: 1) Size, shape, composition, texture and abundance of fragments, 2) composition, texture, and amount of matrix, 3) sorting, and 4) primary structural features. The five genetic types listed in Figure 2 will be defined (after Fisher, 1960b, 1961, 1966; Parsons, 1969; and Macdonald, 1972) to alleviate any confusion in nomenclature.

Autoclastic (Fig. 2) refers to brecciation of solid or

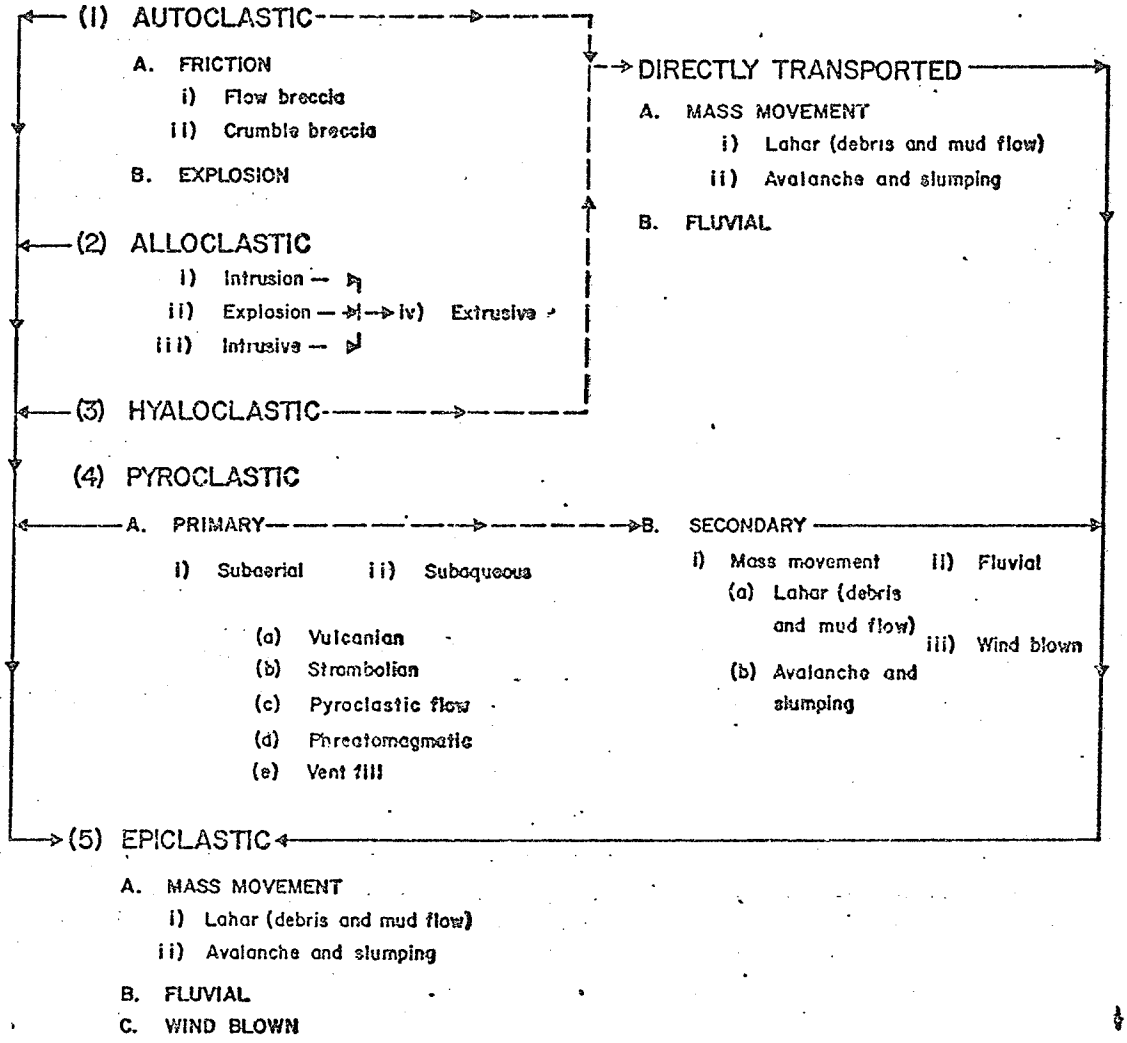

Fig. 2 Volcaniclastic cycle and types of volcaniclastic rock types (Parsons, 1969) and their subdivision. The dashed lines denote rapid and restricted transport of unconsolidated volcanic fragments during the eruption phase. Much of this movement is triggered by processes related to volcanism, such as rainfall, earthquakes and unstable slopes. The continuous lines denote erosion of consolidated volcanic rocks and transport of resultant fragments to form epiclastic volcanic rocks. All processes and rock types are gradational.

semi-solid lava by explosive disruption by gases contained within a lava flow, by gravity collapse and flowage of domes and of flows, or by a combination of these processes (Fisher, 1960b; Parson, 1969).

Alloclastic (Fig. 2) refers to brecciation of pre-existing rock or solid or semi-solid magma by volcanic processes beneath the earth's surface. Alloclastic rocks are of three basic types: 1) intrusion breccia formed by forceful injection of magma into wallrock, 2) explosion breccia formed by explosive disruption of wallrocks and magma, and 3) intrusive breccia formed by movement and injection of the other two types. All three types may be extruded to form fragmental flows (Parsons, 1969).

Hyaloclastic breccias are formed by the flaking off, or decrepitation, of the surface of lava by sudden chilling in water and in places is closely associated with pillowed flows (Macdonald, 1972).

Unconsolidated autoclastic, extruded alloclastic, and hyaloclastic rocks may be transported rapidly from the original site of emplacement by fluvial or mass movement processes shortly after initial emplacement (Fig. 2). Recognition of such transported deposits would be difficult and is beyond the scope of this study.

Pyroclastic rocks are produced by explosive ejection of fragments from a vent, and comprise two major groups: primary and secondary (Fig. 2; Fisher, 1961, 1966). In primary pyroclastic rocks the fragments were not moved from the original site of emplacement prior to lithification, whereas in secondary pyroclastic rocks the fragments were moved short distances by fluvial, mass movement and atmospheric processes prior to lithification but during the eruption stage.

Primary pyroclastic rocks are subdivided into five basic genetic types (Fig. 2) depending on the mechanism and energy of the explosion (Parsons, 1969). Most of these can form in both subaerial or subaqueous environments.

Secondary pyroclastic rocks are subdivided according to the depositional process (Fig. 2). Mass movement types can occur in subaerial or subaqueous environments and form by movement of large volumes of particles in: 1) debris or mudflows formed by saturation and viscous movement of debris (lahars), and 2) avalanches or slumping. Fluvial types are stream or alluvial deposits if formed under subaerial conditions or marine sediments if deposited under subaqueous conditions. Atmospheric types form by the movement of particles by wind with deposition in either subaerial or subaqueous environments. The amount of transportation is such that the pyroclastic origin of the clasts can still be recognised. With additional transport secondary pyroclastic rocks grade into epiclastic rocks in which the pyroclastic origin of the clasts can no longer be determined. Restricted transport of unconsolidated or poorly consolidated alloclastic breccias could lead to major problems in distinguishing secondary alloclastic deposits from secondary pyroclastic rocks.

Pyroclastic fragments are further classified on their mode of origin (Macdonald, 1972, p. 123). Essential fragments are derived from the magma source and may be either magmatic or fragments of solidified magma; they are partly or entirely glassy. Accessory fragments are derived from pre-existing rocks formed by the volcano during previous eruptions; they are termed lithic and are partly

or wholly crystalline. Accidental fragments are derived from non-volcanic rocks or volcanic rocks formed during periods of volcanism preceding the birth of the volcano from which they were ejected.

Epiclastic volcanic rocks (Fig. 2) are mechanically deposited sediments consisting of weathered and eroded products of pre-existing, consolidated or unconsolidated volcanic rocks (Fisher, 1961, 1966) plus a variable proportion of non-volcanic clasts. As for secondary pyroclastic rocks, epiclastic rocks are subdivided according to the processes by which detritus was deposited: mass movement, fluvial, and atmospheric (Fig. 2). It is important to note that epiclastic and pyroclastic rocks differ in amount of transport and in some cases, processes of fragmentation but not necessarily in processes of deposition (Fisher, 1966). Epiclastic should not be interchanged with sedimentary which includes pyroclastic and epiclastic products and thus, does not imply special compositions of the clasts or special processes of formation.

Most stratovolcanoes consist of "vent or cone complex facies" and "alluvial or epiclastic facies" as shown in Figure 3 (Parsons, 1969; Smedes and Prostka, 1972). The vent facies consists of flows, high level intrusions and primary and secondary pyroclastic rocks in varying proportions. Outward from the volcanic centre the vent facies interfingers and grades into alluvial facies aprons of epiclastic volcanic rocks and airfall tuff, pyroclastic flows and some lahars. The alluvial facies is characterised by a decrease in section thickness, bed thickness, and clast size, and an increase in sorting and rounding away from the volcanic centres, as described by Smedes and Prostka

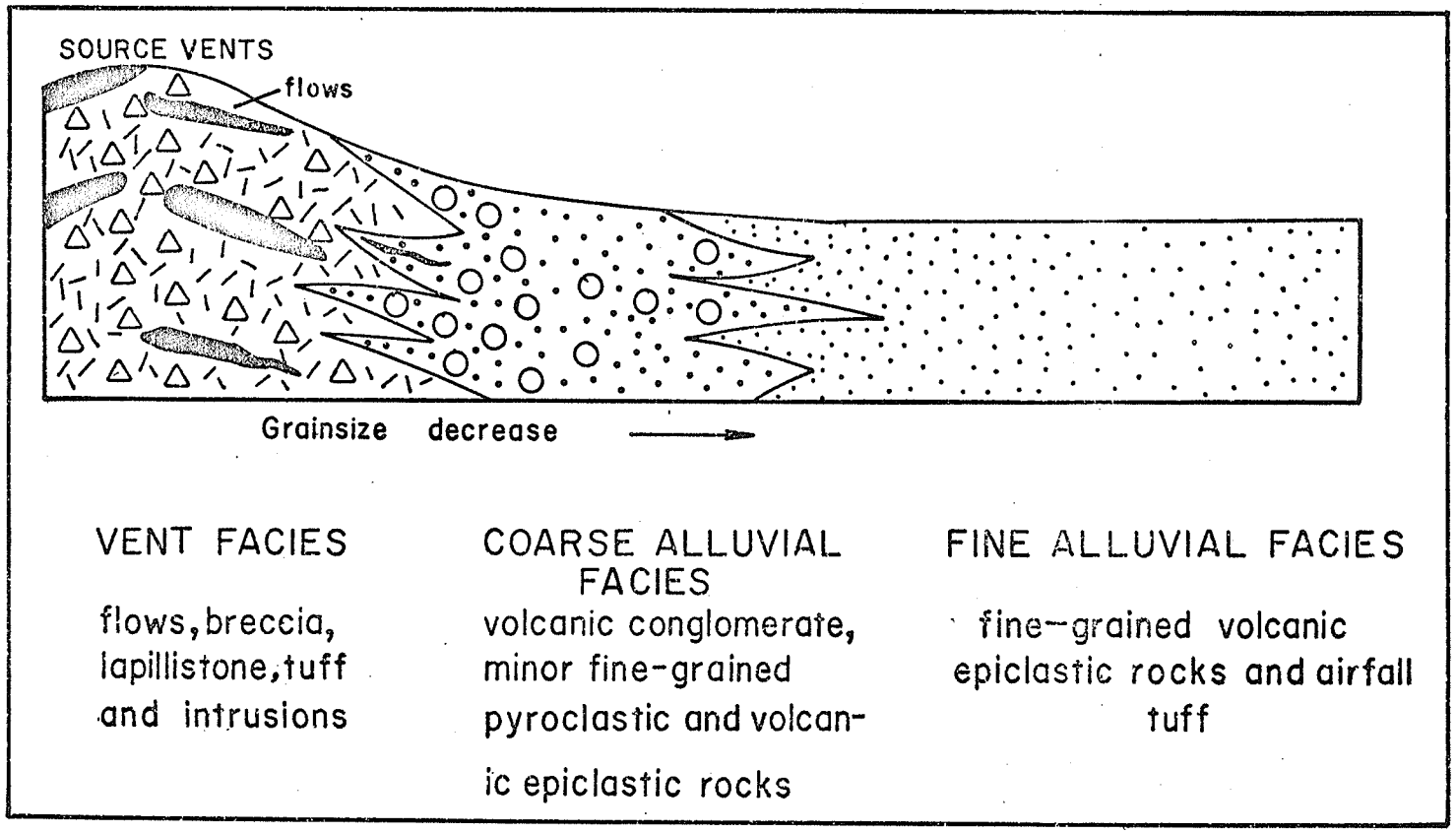

Fig 3. Schematic cross-section showing vent and alluvial facies of a stratovolcano (Smedes and Prostka, 1972).

(1972) in the Absaroka volcanic field, Wyoming and Montana. Thus, vent facies grades into coarse-grained alluvial facies which in turn grades into fine-grained alluvial facies (Fig. 3). Because pyroclastic and epiclastic rocks form the bulk of most felsic and intermediate volcanoes, their distinction is critical for determining facies and consequently the size, morphology, and vent area of a volcano.

The fragmental rocks in formation H are largely primary and secondary pyroclastic rocks with some epiclastic units, minor autoclastic breccia, and rare alloclastic breccia (Table 2). In formation H genetic classification of the primary pyroclastic rocks, and distinction among primary pyroclastic, secondary pyroclastic and epiclastic rocks, particularly fine-grained types, are difficult. These difficulties arise because of 1) destruction of primary textures by metamorphism, 2) gradational nature of pyroclastic and epiclastic rocks, 3) absence of the third dimension because of a homoclinal section, and 4) discontinuous outcrop. Consequently in this study no further genetic subdivision of primary pyroclastic rocks is made. Secondary pyroclastic rocks are subdivided into fluvial and mass movement types.

The pyroclastic and epiclastic rocks of formation H are further subdivided into non-genetic, particle-size categories. Several different particle size classifications have been proposed for both pyroclastic and epiclastic rocks (Figher 1966). Because of the gradational nature of pyroclastic and epiclastic rocks, identical size categories must be used for both rock types (Fisher, 1961, 1966). The Wentworth scale (1922) for sediments and its modification for pyroclastic rocks

TABLE 1. Grade size limits and names of consolidated and unconsolidated volcaniclastic debris

GRADE SIZE LIMITS (mm)	PYROCLASTIC		EPICLASTIC	
	Unconsolidated Fragments	Consolidated Deposits	Unconsolidated Fragments	Consolidated Deposits
	Fisher, 1961		Wentworth, 1922	Fisher, 1961
-256	blocks and bombs	breccia and agglomerate	boulders	volcanic boulder conglomerate
			cobble	volcanic cobble conglomerate
- 64	lapilli	lapillistone	pebble	volcanic pebble conglomerate
- 2	ash	tuff	sand	volcanic sandstone
-1/16			silt	volcanic siltstone
-1/256			clay	volcanic claystone

TABLE 2. Volcaniclastic rock types in formation H and basic criteria for recognition (after Parsons, 1969)

VOLCANICLASTIC ROCK TYPES	FRAGMENT CHARACTERISTICS	MATRIX	STRUCTURAL FEATURES
(1) AUTOCLASTIC Flow breccia	Angular; monolithic; same composition as massive flow; no sorting.	Same composition as fragments if derived from the flow. May also be of different composition if derived from eruptions of ash, weathering, or chemical precipitates.	No bedding; may be bounded on one or both sides by a massive flow zone.
(2) ALLOCLASTIC Intrusive breccia	Angular to subangular; monolithic to heterolithic; no sorting.	Variable and of igneous origin.	No stratification; discordant with adjacent units.
(3) PYROCLASTIC (A) Primary (i) Tuff	Angular to subangular; monolithic to heterolithic; essential, accessory and minor accidental fragments; glassy, pumiceous and vesicular rock fragments, glass shards, and crystals in variable proportions; poor to good sorting.	Minor or absent.	Massive to well bedded; extensive units; normal and reversed vertical grading and lateral grading.
(ii) Coarse-grained rocks	Angular to rounded; monolithic to heterolithic; crystalline and glassy rock fragments; essential, accessory and accidental fragments; bombs may occur in varying proportions; wide size range; poor sorting.	Clastic or tuffaceous; rock fragments similar in composition as coarse fraction, glass shards and minor crystals, variable abundance from less than 20 percent up to 70 percent.	Massive to well bedded; local normal and reversed grading; lenticular units near vents.
(B) Secondary (i) Fluvial tuff and fine-grained lapillistone	Subangular to rounded; monolithic to heterolithic; dominantly rock fragments; crystals, no vesicular fragments; glass shards absent or minor; moderate to good sorting.	Minor or absent.	Massive to well bedded; normal grading.

TABLE 2 (continued)

VOLCANICLASTIC ROCK TYPES	FRAGMENT CHARACTERISTICS	MATRIX	STRUCTURAL FEATURES
(ii) Laharic lapilli-tuff	Angular to subangular; hetero-lithic; dense crystalline fragments; pumice and glass shards rare or absent; poor sorting due to bimodal size distribution of larger fragments and matrix.	Clastic; same composition as rock fragments; crystal clasts can be common; up to 75 percent; sand to clay size.	No bedding; forms stratigraphic unit.
(4) EPICLASTIC Volcanic sandstone	Subangular to rounded; hetero-lithic; rock fragments and crystals in varying proportions; no glass shards or vesicular fragments; poor to good sorting.	Same composition as fragments; variable content; silt and sand size.	Well bedded; sedimentary structures.

(Fisher, 1961) is the classification used herein. Grade size limits and end-member terms for rocks and unconsolidated material are listed in Table 1. Mixture terms, lapilli-tuff and tuff-breccia, are commonly applied to pyroclastic rocks with fragments coarser than 2mm and abundant tuffaceous matrix. Precise boundaries for end-member and mixture terms are not formally defined and therefore depend on individual choice. In this study mixture terms are given to rocks containing 30 to 70 percent tuffaceous material in addition to lapilli (lapilli-tuff) or blocks (tuff-breccia).

Table 2 gives the genetic types and broad size cagetories of volcaniclastic rocks in formation H and basic criteria for subdivision.

REGIONAL GEOLOGICAL SETTING

The Favourable Lake belt (Fig. 1) is an isoclinally folded sequence of Early Precambrian metavolcanic, metasedimentary, and metagabbroic rocks flanked by intrusive granitic batholiths. The belt has a west- to northwest-trend, ranges in width from 3 to 13 km and extends from Northwind Lake, northwestern Ontario, 160 km westward into eastern Manitoba. It is widest and most complex at the east end (Fig. 1, Ayres, in preparation) and it is in this area that recent geological investigations have been concentrated (this study; Ayres, 1970, 1972, 1974, 1977; Raudsepp, 1975). Metamorphic grade ranges from greenschist to amphibolite facies (Ayres, 1974, in preparation).

The metavolcanic-metasedimentary sequence has a thickness of 7.5 km and despite the disruptive effects of widespread faulting, isoclinal faulting, and numerous metagabbro intrusions, 15 formations have been recognised (Table 3). The formations have been given informal alphabet designations (Table 3) for three main reasons (Ayres, 1977): 1) the stratigraphy is tentative, 2) the formations are restricted to the Favourable Lake metavolcanic-metasedimentary belt and consequently have restricted geographic distribution, and 3) even if formal nomenclature was warranted, there are insufficient geographic names in the area to name all the formations. The formations represent parts of five volcanic cycles, the middle three of which are characterised by progressive compositional change from early effusive mafic volcanism to later explosive felsic to intermediate volcanism (Table 3). In cycle 3 the felsic to intermediate phase is not exposed, and instead, volcanic sedimentary rocks derived in part from concomitant felsic to intermediate volcanism form the upper part of the cycle. The mafic flow sequence is missing in cycle 1 and is presumed to have been removed by emplacement of granitic batholiths (Ayres, 1977). Cycle 5 unconformably overlies the other cycles and is largely intermediate metavolcanics.

Numerous gabbro, peridotite, and pyroxenite sills and dikes intruded the volcanic-sedimentary sequence prior to regional metamorphism and are probably related to mafic volcanism. These form both single-phase complexes, as at the base of formations G and H in cycle 2 (Fig. 5), or multiphase complexes as in cycle 3 (Raudsepp, 1975).

TABLE 3. Stratigraphy in the eastern part of the Favourable Lake belt (after Ayres, 1977)

Cycle 5

Formation P - intermediate pyroclastic rocks and sandstone

Cycle 4

Formation N - felsic to intermediate tuff and sandstone

Formation M - mafic flows

Cycle 3

Formation L - intermediate lapilli-tuff

Formation K - sandstone and conglomerate

Formation J - mafic flows

Cycle 2

Formation I - siltstone, sandstone and conglomerate

Formation H - felsic to intermediate pyroclastic rocks and flows

Formation G - mafic to intermediate pyroclastic rocks and flows

Formation F - marble, chert and siltstone

Formation E - mafic flows

Cycle 1

Formation D - argillite, siltstone and sandstone

Formation C - felsic flows

Formation B - mafic flows

Formation A - intermediate to felsic flows and pyroclastic rocks

Felsic to intermediate intrusive activity began during volcanism with emplacement of sills and dikes that may be feeders for volcanism. Several of these have been located in formation H (Fig. 5). Major felsic to intermediate intrusive activity that resulted in the emplacement of granitic batholiths post-dates volcanism and was probably coeval with folding and metamorphism.

Igneous activity ended with intrusion of post-batholith unmetamorphosed intermediate to ultramafic dikes and sills. One of these intrusions, a north-northeast-trending diabase dike occurs in formations G and H just west of Borthwick Creek (Fig. 5).

CALDERA SEQUENCE

INTRODUCTION

Cycle 2 comprises five north-northwest- to northwest-trending formations with an aggregate thickness of 2300m (Table 3, Fig. 4). Formation E, the lowermost formation, is up to 2200m thick and comprises pillowed and massive mafic flows. It appears to represent a subaqueous shield volcano erupted on the flank of an older strata-volcano represented by cycle 1 (Ayres, 1977). These mafic flows are separated from overlying felsic to intermediate metavolcanic rocks of formations G, H and I, by thin, discontinuous siltstone, chert, and marble units of formation F that appears to represent a quiescence in volcanism.

Formation H, the southern part of formation G, and the northern part of formation I occupy a caldera in formation E, steeply overturned to the west by regional isoclinal folding (Figs. 4 and 5). These formations have a maximum thickness of 1870m and are termed the caldera sequence (Fig. 5). Formation H, which has a maximum thickness of 1400m, is the dominant caldera-filling phase in the present cross-section. The present exposure of the caldera sequence represents a near-vertical cross-section through the caldera.

In the south, the caldera sequence is abruptly truncated by east-trending faults and by the Setting Net Lake stock which appears to have been intruded along part of the caldera margin. In the north, the sequence thins and is truncated by a northeast-trending fault (Fig. 5). The upper surface of the caldera sequence was originally sub-horizontal. The relationship of the caldera sequence with underlying formations E and F is obscured by the Setting Net Creek fault,

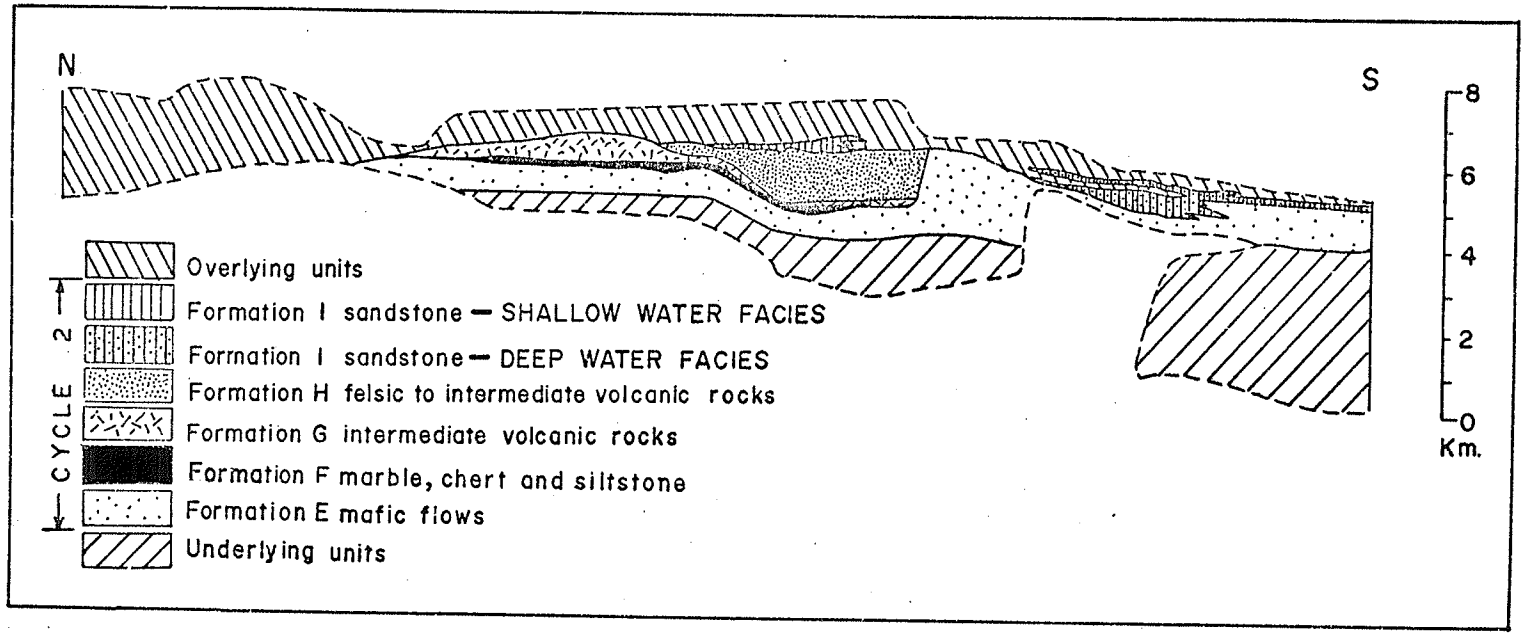

Fig. 4. Reconstructed cross section of the volcanic sequence emphasizing the second volcanic cycle and showing the restricted occurrence of formation H and the shallow-water facies of formation I outlining the caldera (after Ayres, 1977).

slightly discordant metagabbro and metaquartz diorite sills, and thick overburden. Formation F is only present at the northern end of the caldera.

That part of formation G north of the caldera (Fig. 4) is a lenticular unit of monolithologic and heterolithologic volcaniclastic rocks up to 450m thick (Ayres, 1977). It consists of two facies: 1) a thicker, near-vent and partially reworked sequence of thick-bedded breccia and tuff-breccia, and 2) a thinner marginal sequence of well-bedded tuff and tuffaceous sandstone, which appear to be the reworked alluvial equivalent to the coarser breccia. The southern part of formation G, occupying the caldera, appears to be related to a second vent near the south end of the caldera.

Metasedimentary formation I comprises a proximal facies and a distal greywacke facies, separated by a lateral distance of 2 km. Both facies consist partly of detritus eroded from formation H. The proximal facies was deposited in an alluvial fan and shallow-water environment at the top of the caldera and is co-extensive with, and unconformably overlies formation H. The greywacke facies is a marine turbidite, and it appears to be a more distal equivalent of the proximal facies, deposited south of the caldera on the outer slope of a shield volcano represented by formation E (Ayres, 1977).

All members of the caldera sequence have been metamorphosed under regional greenschist facies conditions. Formation H however, differs mineralogically, texturally and chemically from other felsic to intermediate formations of similar metamorphic grade elsewhere in the Favourable Lake metavolcanic-metasedimentary belt. These differences, which will be amplified below, suggest that formation H

underwent volcanic-related metasomatism prior to regional greenschist facies metamorphism. Also, this metasomatism affected formation G and the basal conglomerate of formation I within the caldera.

FORMATION G

Within the caldera, mafic to intermediate metavolcanic formation G has a maximum thickness of 270m in the south and gradually thins northward (Fig. 5). It consists of metamorphosed basaltic and andesitic proximal vent-facies flows in the south and distal vent-facies pyroclastic rocks in the north. Modal analyses are listed in Table 4, the metamorphic mineral parageneses in Table 5, and chemical analyses in Table 11.

In the south the flow sequence is abruptly truncated by the Setting Net Lake stock but in the north it interfingers with formation H forming two tongues each with a maximum thickness of 120m (Fig. 5). The upper tongue has a blunt northern termination that may be a primary feature or a result of subsequent faulting. The lower tongue appears to thin northward, and interfinger with distal vent facies pyroclastic rocks, but this relationship is uncertain because of disruption by a metagabbro intrusion (Fig. 5).

Individual flows could not be defined in the field because of their: 1) fine-grain size, 2) uniform appearance, 3) absence of brecciated margins, and 4) poor exposure. However, petrographic study showed variable textures and colour indices that may indicate the presence of several flows in each tongue. The precise number of flows and flow thicknesses could not be defined. Both aphyric and porphyritic flows are present, with aphyric flows predominating. Aphyric flows can be subdivided into three broad types, on the basis of colour index, the petrographic characteristics which are summarized

TABLE 4. Modal analyses of samples from formations G and H

	FORMATION G				FORMATION H																		
					FLOWS										VOLCANICLASTIC ROCKS									QUARTZ DIORITE	
	158	160	199	71	18	19	37	38	261	394	423	426	445	476	478	95	183	224	228	268	285	308	382	H3/22	84	398
Plagioclase phenocrysts–total	—	—	—	—	35·0	9·0	—	21·6	25·6	15·9	10·0	18·0	15·6	21·1	9·0	—	2·0	4·9	9·0	1·4	—	—	7·5	10·3	—	—
–plagioclase	—	—	—	—	24·0	3·0	—	17·5	20·0	10·5	—	7·9	13·7	18·0	7·6	—	2·0	4·0	8·0	1·3	—	—	6·0	9·0	—	—
–biotite	—	—	—	—	9·0	tr	—	4·1	4·0	3·6	—	9·5	—	2·8	1·0	—	tr	0·6	1·0	—	—	—	0·3	0·5	—	—
–sericite	—	—	—	—	—	6·0	—	—	0·3	1·6	10·0	—	1·5	—	0·2	—	—	0·3	tr	0·1	—	—	—	0·2	—	—
–chlorite	—	—	—	—	2·0	—	—	—	0·3	—	—	0·1	0·3	—	—	—	—	—	—	—	—	—	1·0	—	—	—
–epidote	—	—	—	—	—	tr	—	—	1·0	tr	—	0·5	0·1	0·3	0·2	—	—	—	—	—	—	—	0·2	0·5	—	—
–carbonate	—	—	—	—	—	—	—	—	—	—	—	—	—	—	tr	—	—	—	—	—	—	—	—	0·1	—	—
Actinolite phenocrysts–total	—	2·5	—	—	—	—	—	—	—	—	—	—	—	—	—	—	—	—	—	—	—	—	—	—	—	—
–actinolite	—	2·0	—	—	—	—	—	—	—	—	—	—	—	—	—	—	—	—	—	—	—	—	—	—	—	—
–pyrite	—	0·5	—	—	—	—	—	—	—	—	—	—	—	—	—	—	—	—	—	—	—	—	—	—	—	—
Plagioclase	40·0	33·0	35·5	40·0	—	—	63·1	—	—	—	—	—	—	—	—	—	—	—	—	—	5·5	—	—	—	44·6	44·3
Undifferentiated quartz and feldspar	—	—	—	—	46·0	56·0	—	49·5	56·0	32·3	52·0	46·3	60·0	51·0	53·0	50·0	53·0	59·0	55·0	55·3	42·0	48·0	53·0	40·0	—	—
Quartz	tr	tr	—	24·0	—	—	14·8	0·3	—	—	—	—	3·0	—	—	—	—	—	—	—	14·6	—	—	—	33·2	27·4
Biotite	3·6	3·0	3·0	—	8·0	2·0	18·9	28·2	11·0	14·0	—	32·0	0·6	25·0	29·0	43·0	39·0	30·0	31·0	4·5	23·6	4·0	4·0	43·0	16·1	13·4
Sericite	—	—	—	—	—	24·0	tr	—	1·0	29·0	32·0	—	11·0	tr	3·4	—	—	0·3	0·2	32·0	0·3	31·0	—	—	0·7	4·0
Chlorite	—	0·4	8·0	30·0	8·0	—	0·8	tr	1·0	2·0	4·0	1·0	6·0	1·9	0·8	3·0	tr	0·5	0·2	0·3	1·0	6·0	28·0	3·0	4·2	3·1
Actinolite	52·0	49·6	36·0	6·0	—	—	—	—	—	—	—	—	—	—	—	—	—	—	—	—	—	—	—	—	—	—
Epidote and clinozoisite	5·0	8·0	11·0	—	—	tr	—	—	3·0	1·8	1·0	1·0	1·0	0·4	—	2·0	—	4·0	2·0	1·5	10·3	1·0	0·2	2·4	0·1	5·6
Carbonate	—	1·0	2·0	—	—	—	0·5	0·1	—	—	—	—	—	—	—	—	tr	—	—	—	—	0·3	—	tr	—	tr
Tourmaline	—	—	—	—	tr	—	tr	tr	tr	—	—	—	—	—	tr	tr	—	—	—	—	0·1	—	—	—	—	—
Apatite	—	—	—	—	tr	tr	—	tr	tr	tr	tr	—	0·1	tr	0·1	—	tr	0·1	0·1	—	—	—	—	—	0·2	0·2
Zircon	—	—	—	—	—	—	—	—	—	—	tr	—	—	—	tr	—	tr	0·1	—	—	—	—	—	—	tr	tr
Leucoxene	—	—	—	—	—	—	—	—	—	—	tr	—	tr	—	—	—	—	—	—	—	—	—	—	—	—	—
Pyrite and pyrrhotite	tr	2·5	0·5	—	3·0	tr	0·9	tr	—	0·5	—	0·2	0·5	—	0·7	tr	—	—	0·5	0·1	0·3	1·4	0·2	—	—	1·0
Fe–Ti oxide	tr	—	1·0		tr	tr	1·0	0·3	2·0	1·0	1·0	1·0	2·0	1·0	—	tr	—	0·1	—	3·0	1·6	—	2·0	tr	0·9	1·0
Hematite	—	—	—	—	—	—	—	—	0·4	—	—	—	—	0·1	—	—	—	—	—	—	0·2	0·3	0·1	—	—	—
Vein–quartz	—	—	—	—	tr	8·0	—	—	tr	2·0	—	—	—	0·5	3·0	1·0	2·0	1·0	1·5	0·2	0·5	8·0	3·0	—	—	—
–biotite	—	—	—	—	tr	1·0	—	—	—	1·5	—	0·5	—	—	1·0	tr	4·0	—	0·5	0·2	—	—	1·0	0·8	—	—
–epidote	—	—	2·0		—	—	—	—	—	—	—	—	—	—	—	1·0	—	—	—	0·4	—	—	—	tr	—	—
–plagioclase	—	—	0·5	—	—	—	—	—	—	—	—	—	—	—	—	—	—	—	—	—	—	—	—	—	—	—
–chlorite	—	—	—	—	—	—	—	—	—	tr	—	—	—	—	—	tr	—	—	tr	0·1	—	—	1·0	0·5	—	—
–pyrite	—	—	0·5	—	—	—	—	—	—	—	—	—	—	—	—	—	—	—	tr	—	—	—	—	—	—	—
–Fe–Ti oxide	—	—	—	—	—	—	—	—	—	—	—	—	—	—	—	—	—	—	—	1·0	—	—	—	—	—	—
Modal plagioclase composition	—	—	—	—	An_{0-3}	—	An_{15-30}	An_{34}	An_{0-3}	—	—	An_{0}	An_{0}	An_{0-20}		—	—	—	—	—	—	—	An_{0}	—	An_{0-5}	An_{0-5}
Modal colour index	55·6	53·0	47·0	36·0	27·0	2·0	19·7	32·0	16·3	19·6	4·0	42·6	7·1	29·7	30·8	46·0	39·0	30·5	31·2	4·8	24·6	10·0	32·0	46·0	20·3	16·5

TABLE 4 (continued)

Notes

1. Modal analyses determined petrographically, except for 71 which was determined by X-ray diffraction

2. FORMATION G. Flows, proximal vent facies: 158,160, 199

   Primary lapillistone, distal vent facies: 71

3. FORMATION H. Flows, proximal vent facies
   member H-2: 394
   member H-4: (northern facies) 18,19,37,38,476, 478
   (southern facies) 261,423,426,445

   Volcaniclastic rocks,
   Primary tuff — proximal vent facies
   member H-1: H3/22
   member H-4: 268
   — distal vent facies
   member H-1: 95
   member H-3: 228
   Fluvial tuff — distal to proximal vent facies
   member H-4: 285
   — distal vent facies
   member H-3: 224
   Fine primary lapilli-tuff — distal vent facies
   member H-2: 183
   Primary breccia fragment — proximal vent facies
   member H-4: 308
   Volcanic litharenite — proximal to distal vent facies
   member H-2: 382

   Quartz diorite, northern pluton: 398
   southern pluton: 84

4. FORMATION H BUFF ALTERATION ZONES.
   Flows : 19, 394, 423
   Breccia: 308
   Tuff: H3/22

5. Chemical analyses for all samples are presented in Table II.

6. Sample locations are plotted on Figure 5.

TABLE 5. Metamorphic mineral assemblages

A. INTERMEDIATE TO MAFIC FLOWS AND PYROCLASTIC ROCKS IN FORMATION G

actinolite + albite + epidote ± chlorite ± quartz ± biotite ± carbonate

B. FELSIC TO INTERMEDIATE FLOWS, PYROCLASTIC AND INTRUSIVE ROCKS IN FORMATION H

1) biotite + albite + quartz + epidote ± chlorite ± muscovite

2) chlorite + biotite + albite + quartz + muscovite

3) muscovite + albite + quartz ± epidote ± biotite ± chlorite; rare garnet and actinolite

in Table 6 along with those for porphyritic flows. There are no obvious mineralogical differences, apart from relative abundances of minerals, between the flow types.

Aphyric flows and the groundmass of porphyritic flows consist of discrete, uniformly distributed plagioclase crystals enclosed by an interlocking mat of acicular actinolite and minor chlorite. Primary, euhedral, tabular plagioclase shapes are preserved by pseudomorphic aggregates of albite with or without some epidote and chlorite. Several samples with a grain size less than 0.2mm contain acicular albite which appears to have partly preserved features, such as swallow tail crystal shapes indicative of quench origin. The actinolite mat lacks obvious primary textures. However, the enclosure of plagioclase crystals by this mat may be indicative of primary ophitic, subophitic or isogranular textures. Porphyritic rocks contain up to 5 percent 0.5 to 2mm, tabular, euhedral to anhedral aggregates of actinolite which are probably pseudomorphs after primary pyroxene phenocrysts, and up to 10 percent tabular aggregates of epidote that may be pseudomorphs after plagioclase phenocrysts. Rare rounded vesicles and quartz amygdules were observed.

Pillows are conspicuously absent, and flow brecciation was only observed in a lenticular inclusion in the metagabbro sill.

A subvertical mafic to intermediate dike, about 10m wide occurs in the lower part of formation H immediately overlying formation G near the southern margin of the caldera (Fig. 5). Macroscopically the dike is mineralogically and texturally similar to the aphyric flows. The presence of the dike may indicate renewed mafic to intermediate volcanism higher in the sequence, although no comparable flow or pyroclastic units were found in formation H.

TABLE 6. Characteristics of mafic to intermediate flow types in formation G

FLOW TYPES (colour indices)	GROSS MINERALOGY	GRAIN SIZE (mm)	OTHER FEATURES	FIELD APPEARANCE
1. APHYRIC (15 to 35) 2. APHYRIC (35 to 50) 3. APHYRIC (> 50)	(i) Interlocking mat of acicular actinolite laths enclosing euhedral, tabular and rarely acicular plagioclase. (ii) Some of the actinolite have isolated chlorite rims. (iii) Plagioclase is pseudomorphously recrystallized to aggregates of albite ± epidote granules and ± chlorite. Poorly preserved primary twinning. (iv) Porphyroblasts of epidote and clinozoisite. (v) Disseminated pyrite. (vi) Patchy biotite distribution.	less than 0.5	Veins of pyrite, epidote clinozoisite, actinolite and albite.	Uniformly fine-grained without obvious textural distinctions. No obvious contacts or pillows and only rare flow breccia.
4. PORPHYRITIC (35 to 50)	(i) Up to 5 percent euhedral to anhedral pyroxene phenocrysts pseudomorphously replaced by actinolite and pyrite. (ii) Up to 10 percent tabular aggregates of epidote that probably pseudomorph euhedral plagioclase phenocrysts. (iii) Groundmass similar to aphyric flows	phenocrysts up to 2 groundmass less than 0.5		

The northern distal vent facies is 20 to 200m thick, although relations at the north end of the unit are disrupted by metagabbro and quartz diorite plutons. It is mainly primary monolitholigic to heterolithologic lapillistone and minor tuff, except at the northend where tuff appears to predominate. South of Borthwick Creek, relations between formations G and H are obscured by the discordant quartz diorite sill and poor outcrop, but the formations apparently interfinger. North of Borthwick Creek, contact relations are better exposed and the formations are in sharp contact, except locally where there is minor interlayering of pyroclastic rocks with volcanic sandstone and argillaceous rocks of formation H.

Also, north of Borthwick Creek, formation G pyroclastic rocks become less mafic and consist of alternating intermediate and felsic to intermediate layers that may have been derived from two volcanic sources. Unlike adjacent formation H, most of the facies appear to have been strongly deformed. Two well-developed, discordant secondary foliations are present, and fragments are strongly flattened with indices of elongation of as much as 5:1. Although deformation hampers study of the fragments, they appear to have been originally rounded to angular and poorly to moderately sorted; they ranged in size from less than 2mm in tuff to 30mm in lapillistone. Metamorphic recrystallization and fine internal grain size of fragments hampers determination of fragment compositions. Fragments are aphyric and consist of varying proportions of chlorite, actinolite and albite, in heterolithologic units, and of either actinolite or chlorite in monolithologic units. Because of recrystallization the matrix is difficult to identify, but is commonly less than 5 percent and has a metamorphic mineralogy similar to the fragments.

North of Borthwick Creek, some beds contain actinolite-rich fragments in a fine-grained quartz matrix that may be recrystallized chert.

FORMATION H

Introduction

Formation H has a strike length of 6.2 km and varies in thickness from 1400m in the south to about 300m in the north (Fig. 5). It consists dominantly of metamorphosed felsic to intermediate pyroclastic rocks and flows of andesitic and dacitic composition. The major lithofacies (Fig. 5) are: 1) 15 percent flows, 2) 22 percent primary tuff, 3) 8 percent fluvial tuff, 4) 7 percent undifferentiated tuff, 5) 21 percent primary lapilli-tuff and lapillistone, 6) 2 percent fluvial lapillistone, 7) 4 percent undifferentiated lapillistone, 8) 19 percent laharic lapilli-tuff and tuff-breccia, 9) 1 percent primary breccia and agglomerate, 10) 1 percent volcanic epiclastic rocks, and 11) minor intrusive breccia. The formation also contains minor conglomerate, chert, and ferruginous chert. In addition, the quartz diorite sill at the base of formation H is interpreted, from field relations and textural features to be an integral part of the volcanism that produced formation H. The dominance of primary pyroclastic rocks, flows, and high-level quartz-diorite intrusions, with respect to epiclastic volcanic rocks indicate that formation H is a vent facies.

The formation is subdivided into four members (Figs. 5 and 6) each of which represents a major pulse of volcanism. Members are informally designated H-1 to H-4.

Contacts between individual pyroclastic and some epiclastic units are difficult to define because of: 1) fine-grain size of some units 2) destruction of primary textures by recrystallization, 3) paucity of

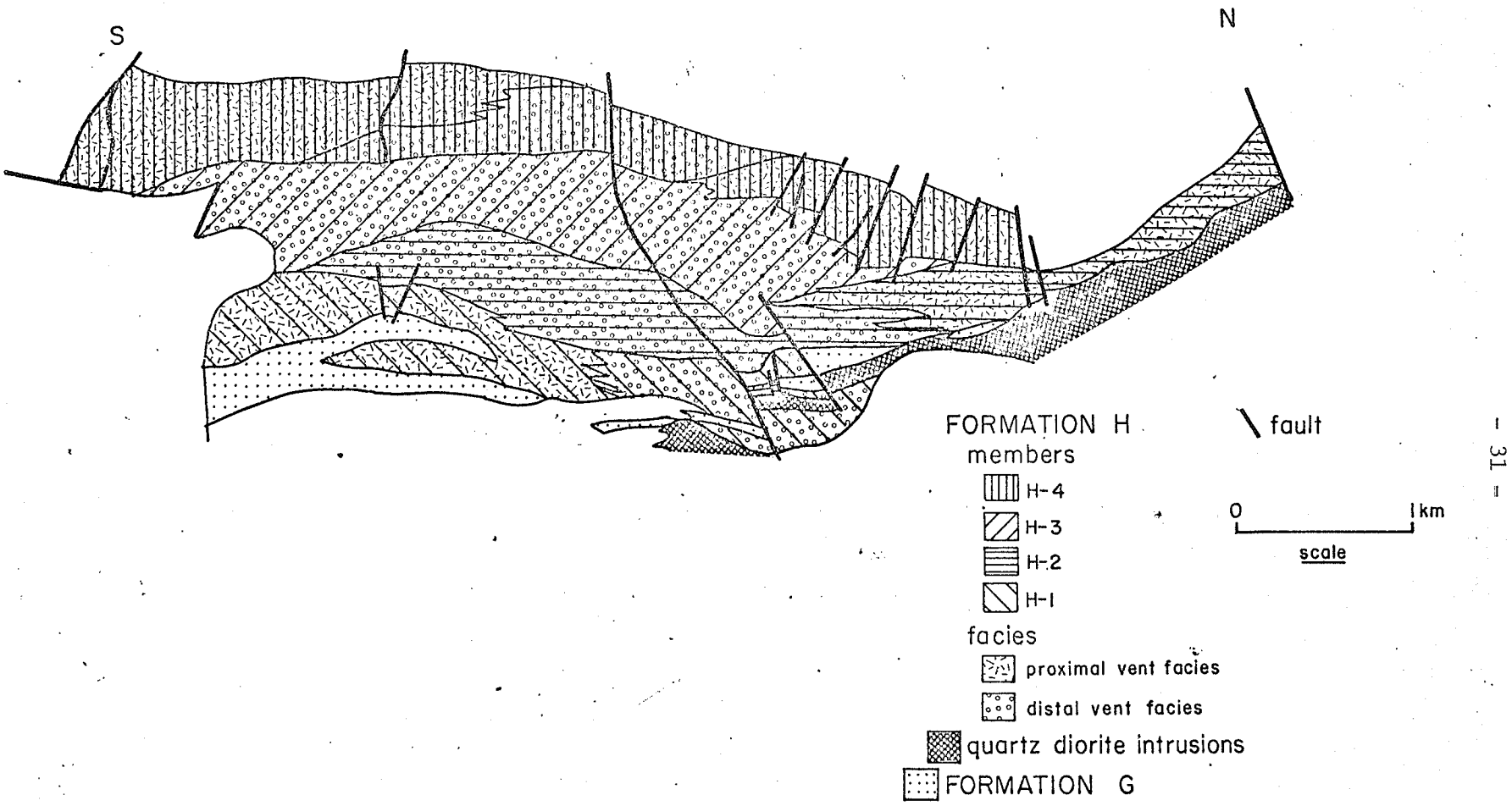

Fig. 6. Distribution of members and facies in formation H. Refer to Figure 5 for lithologies.

diagnostic features, such as unique fragment types that distinguish individual units, 4) rapid lateral and diffuse vertical grain size variations, or 5) limited exposure. Consequently map boundaries, particularly in the southern part of formation H (Fig. 5), are arbitrary and based on major clast size changes determined from both field and petrographic study.

Units tend to be lensoidal (Fig. 5) reflecting restricted distribution of volcanic products, irregularities in primary volcanic surfaces, and perhaps erosion during volcanism. Most units have north-northwesterly trends and dip steeply between 70° east and 70° west. The northern end of the formation (Fig. 5) is gently folded about a near-vertical axis producing northwesterly trends. Well defined bedding planes were observed only in a few pyroclastic and epiclastic units because most units are either characterised by gradual grain size changes or have thick bedding. Thin bedding (less than 1 m thick) defined by compositional or grain size variations is best developed in fluvial tuff and lapillistone, and in epiclastic volcanic rocks. Graded beds were observed in only a few epiclastic and pyroclastic units. Normal graded beds in epiclastic units face westward, but both normal and reversed graded beds were observed in primary pyroclastic units. Members H-1, H-2, and H-4, are characterised by crude normal or reversed grading.

The volcanic rocks have been recrystallized to fine-grained aggregates of quartz, plagioclase, and micas which resulted in partial to complete destruction of primary textures, especially in fine-grained pyroclastic and epiclastic rocks. Primary volcanic minerals are poorly preserved. Minor relict primary plagioclase with compositions between

An_{20} and An_{35} was observed (Table 4) but most plagioclase is replaced pseusomorphously by albite, biotite, chlorite, and muscovite. Quartz phenocrysts are rare and are generally recrystallized to monocrystalline aggregates. Three metamorphic mineral assemblages can be identified (Table 5). Assemblage (1), which is characterised by a high biotite content, is most common. Assemblage (2) is of minor importance and is intimately associated with assemblage (1). Assemblage (3) is muscovite-rich and occurs near vents as large irregular zones discordant with the stratigraphy, as small irregular zones in flows, as reaction rims on bombs in agglomerate, and as thin selvages adjacent to quartz veins. These zones are termed buff alteration. Minor minerals in all assemblages are apatite, zircon, tourmaline, pyrite, pyrrhotite, iron-titanium oxide, leucoxene and rarely carbonate. Modal analyses are presented in Table 4.

The strong degree of recrystallization and the occurrence of mineral assemblages (1) and (3) are unique to formation H and do not characterise other felsic to intermediate rocks of similar metamorphic grade outside the caldera which will be discussed in a later section. These features together with chemistry (Table 11), indicate that formation H underwent metasomatism during volcanism. Assemblage (1) probably represents a pervasive hot-spring and fumarolic alteration whereas assemblage (3) represents locally intense hot-spring and fumarolic activity close to vents.

Lithology

Flows

Felsic to intermediate flows (Fig. 5) are commonly lenticular, between 10 and 90 m thick, and between 400 and 1320 m long; they commonly form sequences up to 140 m thick. The high thickness: length ratio is probably indicative of high flow viscosities and most flows are probably close to source vents. In flow sequences, individual flows can be accurately defined only where they are separated by thin pyroclastic units or have brecciated margins. Chilled contacts were observed rarely. Where these features are absent, textural and mineralogical variations indicate the presence of two or more flows, but flow contacts are difficult to define. Consequently, boundaries between flows in Figure 5 are commonly arbitrary and are only drawn where diagnostic evidence are present and textural variations can be traced along strike for more than several tens of metres. Modal analyses of flows are presented in Table 4 and chemical analyses in Table 11.

Both porphyritic and aphyric flows are present and their petrographic characteristics are listed in Table 7. Porphyritic flows form about 80 percent of all flows. Porphyritic flows can be broadly subdivided into two types: 1) those containing only plagioclase phenocrysts and forming about 90 percent of porphyritic flows, and 2) those containing both plagioclase and quartz phenocrysts (Table 7). In all porphyritic flows, plagioclase phenocrysts have a uniform size (0.1 - 5mm) and distribution (Fig. 7), and random and/or preferred orientations. Although recrystallized, their primary, euhedral, tabular shapes are well

TABLE 7. Characteristics of felsic to intermediate flows

FLOW TYPE	COLOUR INDEX	% PHENOCRYSTS	% GROUNDMASS	PRIMARY TEXTURAL CHARACTERISTICS	METAMORPHIC CHARACTERISTICS		OTHER FEATURES	PRIMARY INTERNAL STRUCTURES
					Plagioclase	Groundmass		
1. PORPHYRITIC with plagioclase phenocrysts	5 to 30	10 to 35	65 to 90	Euhedral plagioclase phenocrysts (0.1 to 3 mm)	(1) Pseudomorphously recrystallized to albite, ± muscovite, ± biotite, ± epidote. (2) Locally muscovite rich. (3) Poor to well preserved albite twinning (4) Local relict primary plagioclase with oligoclase to andesine composition.	(1) Fine-grained (less than 0.1 mm) undifferentiated quartz and plagioclase, biotite, chlorite, muscovite, epidote and rare local garnet and tourmaline. Fine-grain size and lack of primary textures suggests that it may have been glassy (2) Locally muscovite rich.	Sparse, irregular to tabular, 0.25 to 2 mm patches of biotite which may be recrystallized mafic phenocrysts.	(1) 1 to 3 mm wide flow layers with variable grain size, phenocryst content and phenocryst orientation. (2) Foliations and lineations defined by preferred orientation of plagioclase phenocrysts either throughout the flow or, at the flow base. (3) Trends of these structures are discordant to tectonic structures, and vary from parallel to discordant with flow contacts.
2. PORPHYRITIC with plagioclase and quartz, phenocrysts		Quartz 1 to 5; plagioclase; 5 to 15	83 to 94	(1) Euhedral plagioclase phenocrysts (0.1 to 3 mm) (2) Recrystallized subhedral, corroded quartz phenocrysts (0.25 to 0.50 mm)				
3. APHYRIC				(1) 85 to 90 percent interlocking subhedral to euhedral plagioclase (0.1 to 1 mm) (2) 10 to 15 percent anhedral quartz (0.05 mm to 0.5 mm)				Local preferred orientation of plagioclase in the central part of the flow or near the flow base.

preserved by pseudomorphs of albite, epidote, muscovite and biotite. Primary oligoclase-andesine (An_{20} - An_{35}) phenocrysts are preserved in parts of several flows. Quartz phenocrysts have uniform size (0.25 to 0.50 mm) and distribution throughout a flow and despite recrystallization have well preserved primary subhedral, corroded, equant shapes.

In strongly altered flows, plagioclase phenocrysts are largely replaced by muscovite and may be difficult to distinguish from the groundmass which is also replaced dominantly by muscovite. In some flows biotite is the major replacement mineral of plagioclase, forming 25 to 50 percent of the pseudomorphs (Table 4). In addition, biotite forms irregular to tabular aggregates (0.25 to 2 mm) that may be completely replaced plagioclase phenocrysts or mafic phenocrysts.

The groundmass in all porphyritic flows has recrystallized to fine-grained (less than 0.1 mm) quartz, plagioclase, biotite, chlorite, muscovite, epidote, trace garnet and tourmaline, and rare actinolite. Biotite forms 10 to 40 percent of the groundmass (Table 4). The high biotite content in the groundmass and plagioclase pseudomorphs of some flows is one of the unique features of formation H (both flows and pyroclastic rocks). Such abundant biotite does not appear to be a normal metamorphic effect because it is rare in flows and pyroclastic rocks of similar composition and metamorphic grade, outside of the caldera (Ayres, pers. comm.). As discussed in a later section its presence in formation H may be the result of hydrothermal alteration.

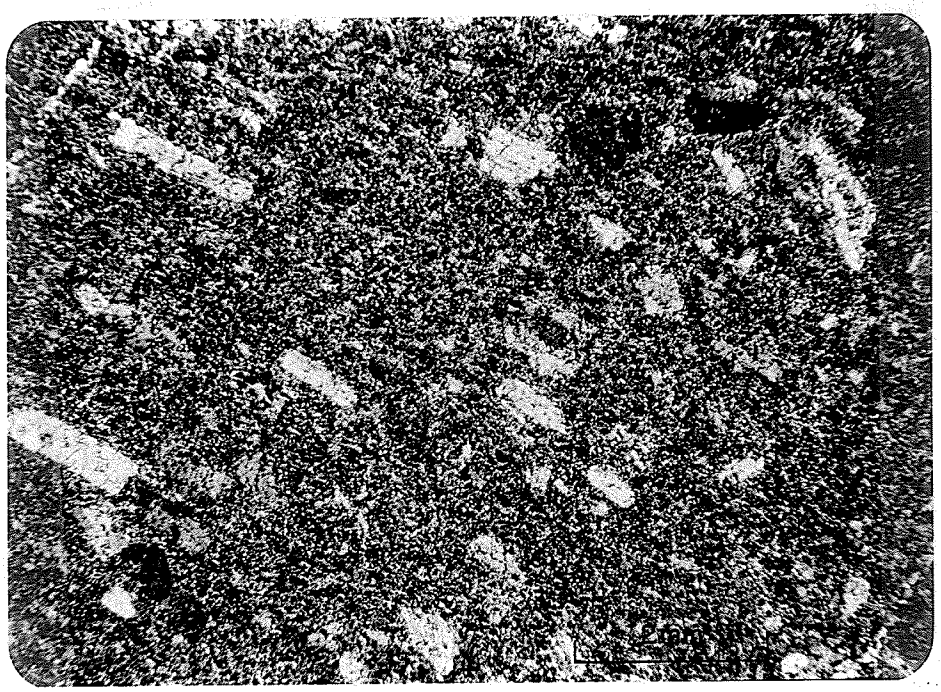

Fig. 7. Photomicrograph of a porphyritic felsic to intermediate flow with uniformly distributed and aligned plagioclase phenocrysts and a fine-grained recrystallized groundmass of plagioclase and quartz, that may have been originally glassy. Plagioclase phenocrysts are replaced pseudomorphously by albite and minor sericite, chlorite and biotite. Crossed nicols.

In strongly altered flows muscovite is a major component of the groundmass.

The lack of preserved primary textures and the uniformly fine-grain size of the groundmass suggest that it may have been originally glassy. Crystallization of most phenocrysts prior to extrusion and formation of a glassy groundmass after extrusion could account for the uniform distribution and size of phenocrysts in flows.

Aphyric flows contain 85 to 90 percent randomly oriented or aligned, subhedral to euhedral, 0.1 to 1 mm plagioclase and 10 to 15 percent anhedral, 0.05 - 0.5 mm quartz. Plagioclase has been replaced pseudomorphously as described above and in Table 7 for plagioclase phenocrysts in porphyritic flows. Circular biotite aggregates (0.25 to 1 mm) may be completely replaced plagioclase or mafic crystals.

Primary flow foliation, lineation, and layering are well developed within and near the margins of some flows and are distinctly different from, and are commonly discordant to, poorly developed metamorphic foliation and lineation produced by micaceous minerals. Primary foliation and lineation are defined by aligned plagioclase crystals and may be present in all flow types (Table 7). Flow layers are only present in porphyritic flows and are 1 to 3 mm thick; they are recognised by: 1) healed parting planes, 2) variation in composition, 3) variation in phenocryst size, 4) variation in phenocryst content, and 5) variation in phenocryst alignment, whereby different layers show different average orientation directions of plagioclase phenocrysts with regard to layer orientation. At the base of flows the attitude of

foliations, lineations and layers vary from parallel to the basal contact to as much as 40° discordant. Parallelism of these structures would be expected near the basal contact because of marginal shear between the viscous flow and underlying surface. The origin of the discordant trends is unknown, although they probably reflect shear directions during magma flow. Primary flow foliation and lineation were observed in the central parts of only a few flows, where they are parallel or slightly discordant to flow contacts. In the central and upper parts of one flow, in the southern part of member H-4, inclined layering locally folded into a detached antiform was observed. Similar inclined and folded flow layers have been found in Cenozoic rhyolite flows (Christiansen and Lipman, 1966) and can be used to determine flow directions. However, there is insufficient data to apply this criteria to the caldera flows.

Autobrecciation occurs as marginal zones up to 4 m thick in most flows. It occurs less commonly as isolated lenticular zones up to 3 m thick within flows and comprises the entire thickness, of part of one flow in member H-4 near the mine. The latter example maybe a flowfront or margin, but this cannot be proven here because of faulting. Autobreccia zones are monolithic; the fragments are identical in mineralogy and texture to the massive flow zone, angular to subangular, 5 cm to 0.5 m in size, and poorly sorted (Table 8). Matrix is less than 10 percent and its primary nature is indeterminate because of replacement by quartz, muscovite, actinolite, pyrite, and pyrrhotite. The breccia grades into the massive flow zone. Rare spines projecting 1 m into the brecciated

top, from the upper surface of the massive flow zone were observed in one flow in the southern part of member H-4.

Tuff

Tuff forms lenticular units ranging in thickness from less than 1 m to 300 m and up to 1800 m long. Units appear to be thickly bedded, with bedding thicknesses greater than 1 m. Thin bedding (6 cm to 1 m), and normal grading were rarely observed. Tuffs are subdivided into primary and secondary types; their characteristics are listed in Table 8, modal analyses in Table 4, and chemical analyses in Table 11.

Primary Tuff: Primary tuff contains 10 to 50 percent identifiable essential and accessory rock fragments, and 50 to 90 percent matrix-like material (Table 8). Most identifiable rock fragments are felsic to intermediate, porphyritic and aphyric varieties, and tuff may be heterolithic or monolithic depending on the degree of textural variation. Other fragment types occur locally (Table 8). Porphyritic fragments contain plagioclase phenocrysts that are replaced pseudomorphously by single grains of albite or aggregates of albite, biotite and muscovite. Aphyric fragments, the groundmass in porphyritic fragments, pyroclastic fragments, pumiceous fragments, amygdaloidal fragments, and the matrix-like material have recrystallized to fine-grained (less than 0.05 mm) quartz, plagioclase, muscovite and biotite. The secondary mineralogy and fine-grain size within these fragments suggest that they may have been originally glassy, with the matrix-like material representing granules and shards of glass whose borders are no longer identifiable because of

TABLE 8. Volcaniclastic rock types in formation H and their characteristics

ROCK TYPES	FRAGMENTS				SORTING	MATRIX	STRUCTURAL FEATURES	FIELD RELATIONS
	Type & abundance	Origins	Size	Shape				
1. Autoclastic Brecciated flows	90%; monolithic; same mineralogy and textures as the massive flow zone.	Flow	2 cm to 0.5 m	Angular to sub-angular.	nonsorted	10 percent; indeterminate because of replacement by quartz, actinolite and Fe-sulphides.	1. No bedding. 2. Occurs at flow margins, as lenticular, concordant and discordant zones within flows, and rarely involves the entire flow. 3. Grades into the massive flow zone.	In proximal vent facies.
2. Alloclastic Intrusive breccia	70 to 80%; monolithic to heterolithic, felsic to intermediate, varying from porphyritic with a diversity of textures to aphyric; minor quartz and sedimentary fragments.	Pre-existing rocks around the vent.	1 to 15 cm	Subangular.	nonsorted	20 to 30 percent; vuggy and smokey quartz of probable hydrothermal origin.	1. Discordant to adjacent units. 2. Sharp and diffuse contacts. 3. Fragments adjacent to contacts may be elongated and aligned parallel to contacts. 4. Absence of tectonic cataclasis and schistosity.	
3. Pyroclastic A. Primary (i) Tuff, fine lapilli-tuff, and fine lapilli-stone	10 to 50% identifiable rock fragments in tuff, 30 to 70% in lapilli-tuff, and greater than 70% in lapillistone. In order of decreasing abundance the main fragment types are: 1. Felsic to intermediate, porphyritic with euhedral pseudomorphosed plagioclase phenocrysts (1 mm) in a fine-grained groundmass. 2. Felsic aphyric composed dominantly of quartz and plagioclase. 3. Quartz-dioritic. 4. Biotite-rich Rare types are: 5. Felsic to intermediate tuff. 6. Mafic to intermediate. 7. Felsic to intermediate, amygdaloidal. 8. Pumiceous. 9. Sedimentary. 10. Plagioclase crystals. Monolithic units: contain only type 1 or type 2. Heterolithic units: contain 2 or more fragment types. Tuff: also contains 50 to 90% matrix-like material that probably represents glass shards and granules of similar size as the identifiable fragments but are not texturally preserved because of recrystallization to fine-grained quartz, plagioclase, biotite, sericite and epidote.	Essential: 3, 4, 8, and 10. Accessory: 5, 6, and 9. Essential or Accessory: 1, 2, and 7.	Tuff: < 2 mm; types 5, 7, and 8 up to 4 mm. Lapilli-tuff: 1 mm to 3 cm, with 30 to 70% between 2 mm and 2 cm. Lapillistone: 1 mm to 3 cm with > 70% between 2 mm and 3 cm.	Rock fragments: angular to sub-angular; types 4 and rarely 2 have concave borders because of vesicle controlled breakage; Pumice: collapsed to form lenses. Crystals: broken and corners may or may not be rounded.	Tuff: Indeterminate because grain size of glass particles is not known. Lapilli-tuff and Lapillistone: poor to good.	Tuff: absent if the fine-grained matrix-like material was originally glass particles of the same size as identifiable fragments. Lapilli-tuff and Lapillistone: 30 to 70% in lapilli-tuff and < 30% in lapillistone; composed of fragments similar to the coarser fraction and possible glass; identifiable fragments < 2 mm in size.	1. Extensive and lenticular units. 2. Massive to thick bedding, generally > 1 m; rare thin to thick bedding between 6 cm and 1 m. 3. Rare normal grading.	1. Proximal vent facies: associated with flows and coarse-grained primary pyroclastic rocks. 2. Distal vent facies: associated with fine-grained primary and secondary lapilli-tuff and lapillistone and secondary tuff.

TABLE 8 (continued)

ROCK TYPES	FRAGMENTS				SORTING	MATRIX	STRUCTURAL FEATURES	FIELD RELATIONS
	Type & abundance	Origins	Size	Shape				
3. Pyroclastic cont'd (ii) Coarse lapilli-stone, breccia and agglo-merate	>80%. In order of decreasing abundance the fragment types are: 1. Felsic to intermediate, porphyritic with euhedral pseudomorphosed plagioclase phenocrysts (1 mm) in a fine-grained groundmass. 2. Felsic aphyric composed of dominantly quartz and plagioclase. Rare types are: 3. Mafic to intermediate. 4. Sedimentary. Monolithic types: rare; comprise either type 1 or type 2 fragments Heterolithic types: mixtures of type 1 and 2 or only type 1 with a diversity of textures.	Essential: bombs. Accessory: 3, 2, and 4. Essential and Accessory: 1 and 2. Monolitic units contain essential fragments and heterolithic units contain essential and accessory fragments,	Lapillistone: 2 to 10 cm with >70% between 2 and 6.4 cm. Breccia: 5 to 160 cm. Agglomerate: bombs up to 30 cm in diameter, and blocks up to 3 m.	Lapilli and blocks: sub-angular to angular. Bombs: rounded.	Poor.	<20%; lack of data on fragment types, but they probably include rock fragments, and minor crystals and recryst-allized glass fragments <2 mm in size.	1. Lenticular units. 2. Massive to well stratified with layers up to 1 m thick defined by variation in fragment sizes. 3. Local normal and reverse graded layers.	Proximal vent facies co-extensive with flows.
B. Secondary (i) Fluvial tuff and fine lapilli-stone	>90%; monolithic to hetero-lithic, identifiable rock frag-ments of types 1, 2, 3 and 10 as in primary tuff, lapilli-tuff and fine lapillistone; type 10 (plagioclase crystals) is minor.	Derived from primary tuff, lapilli-tuff and fine lapillistone, and therefore the origins are as for these rock types.	Tuff: 2 mm. Lapillistone: 2 mm to 1.5 cm.	Subangular to rounded.	Moderate.	Tuff: 0 to 5%. Lapillistone: < 10%; Composition is masked by recrystallisation, but it probably consists of rock fragments and crystals <2 mm in size.	As for primary tuff.	Proximal and distal vent facies with greater abundance in distal vent facies.
(ii) Laharic lapilli-tuff, lapilli-stone and tuff-breccia	30 to 70% in lapilli-tuff and tuff-breccia; 70 to 80% in lapillistone; heterolithic; types 1, 2 and 3 as in primary coarse lapillistone, breccia and agglomerate, with types 1 and 2 predominating.	Derived from mass movement of unconsol-idated primary pyroclastic material, and therefore the original origins are the same as for the primary pyro-clastic source rocks.	Bimodal; coarse fraction 1 to 7 cm in lapilli-tuff and lapillistone and 3 to 15 cm in tuff breccia.	Subangular.	nonsorted	Lapilli-tuff and tuff-breccia: 30 to 70% Lapillistone: 20 to 30% Rock fragments and minor crystals < 2 mm in size.	1. No bedding or grading. 2. Lenticular units of varying lateral extent.	Distal vent facies.
4. Epiclastic Volcanic sandstone	80 to 95% rock fragments, up to 15% plagioclase crystals and up to 10% quartz crystals; litharenite has <5% plagioclase crystals and feldspathic litharenite has 5 to 15% plagioclase crystals; hetero-lithic; rock fragments are similar to types 1 and 2 in primary tuff.	Volcanic provenance; Exact nature of source rocks is indeterminate.	< 2 mm.	Subangular to rounded.	Good.	< 5% indeterminate because of recrystall-ization.	1. Thin lenticular units. 2. Poor to good bedding with thicknesses ranging from 0.3 to 30 cm. 3. Normal grading. 4. Scour, flame and slump structures.	Proximal and distal vent facies with greater abundance in distal vent facies.

recrystallization. Biotite content is variable and can be as high as 30 to 45 percent (Table 4). In places it is the sole mineral replacing rock fragments (Table 8) and it is commonly a major component of the matrix-like material. The high biotite content and its distribution are unique to formation H, and as discussed for felsic to intermediate flows are possibly due to hydrothermal alteration. Amygdules in felsic to intermediate fragments are composed of quartz and epidote.

Mafic to intermediate fragments have colour indices between 15 and 35 and are mineralogically and texturally similar to aphyric, mafic to intermediate flows of formation G. They are probably accessory.

Separate plagioclase crystals, which are replaced pseudomorphously by albite and minor biotite and muscovite, are normally a minor constituent. However, near the quartz diorite sill (Fig. 5) some tuff units contain abundant phenocrysts and glomerocrysts of plagioclase and fragments of fine to medium-grained equigranular interlocking plagioclase. The restricted occurrence of these fragment types and their resemblance to plagioclase in the quartz diorite sill, suggests a genetic relationship. The sill was probably emplaced during early stages of caldera filling and was a high-level magma chamber feeding pyroclastic eruptions higher in the sequence.

Rock fragments are angular to subangular, although boundaries of most felsic to intermediate fragments are partly masked by recrystallization. Figures 8a and 8b show a monolithic tuff with well preserved, recrystallized, dominantly aphyric rock fragments. Tuff units containing porphyritic fragments with poorly preserved fragment boundaries, plagioclase crystals, and a high matrix content

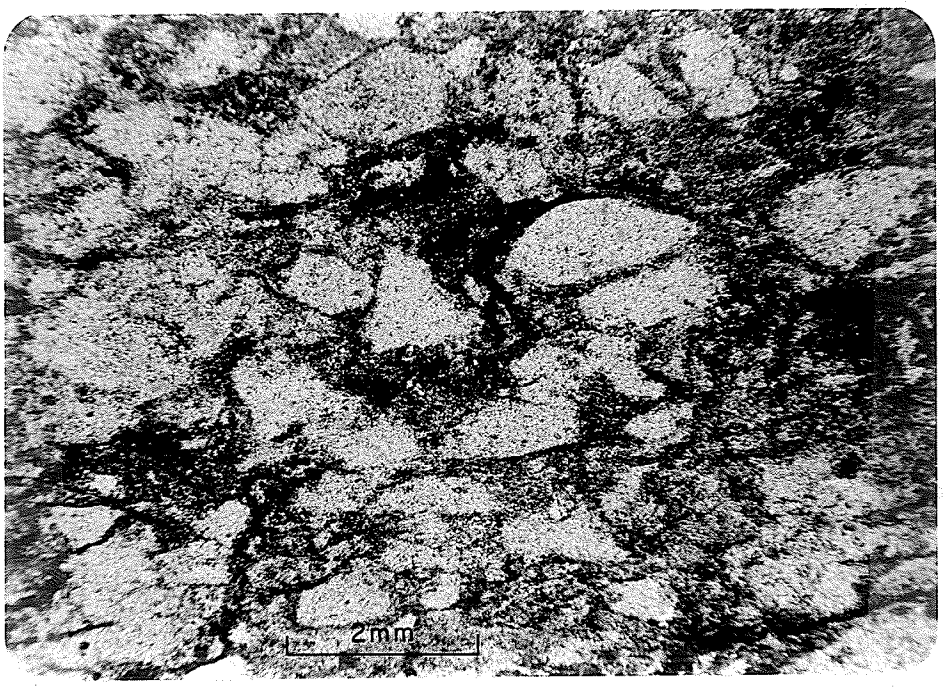

Fig. 8a. Photomicrograph of primary tuff, from a stratified primary tuff-lapillistone unit, with poor to moderately sorted angular rock fragments. Concave boundaries probably formed by conchoidal fracture. The fine-grained biotite-rich matrix may have been originally glassy. Plane light.

Fig. 8 b. As 8 a but under crossed nicols showing fine-grained recrystallization of fragments. Fine and uniform grain-size within fragments shows that they were monolithic and possibly glassy.

of what may have been primary glass shards superficially resemble porphyritic felsic to intermediate flows, but they can be distinguished from flows by criteria listed in Table 9. Some aphyric, felsic and biotite-rich fragments have concave boundaries and equant to 'Y' shapes (Fig. 9) due to vesicle controlled breakage. Flattening of these clasts was not observed. Pumice forms flattened, elongated fragments with wispy ends and an internal foliation formed by vesicle collapse (Fig. 10).

Fragments are normally less than 2 mm except for pyroclastic, amygdaloidal and pumiceous fragments which are up to 4 mm. Sorting is commonly indeterminate because of the high content of matrix-like material and destruction of primary textures in this phase. Tuff containing a high proportion (up to 70 percent) of rock fragments appears to be poorly to moderately sorted.

Secondary Tuff: Secondary tuff is monolithic to heterolithic and contains more than 90 percent subangular to rounded, moderately to well sorted identifiable rock fragments, minor plagioclase crystals and less than 5 percent matrix (Table 8). The rock fragments are felsic to intermediate, porphyritic and aphyric types. Other fragment types that are found in primary tuff (Table 8) are absent in secondary tuff. The nature of the matrix is difficult to determine because of recrystallization, but it seems to consist of rock fragments and minor plagioclase crystals with perhaps minor glass shards and granules.

A most significant feature of secondary tuff, distinguishing it from primary tuff, is its well preserved primary texture. This reflects the high content of crystalline rock fragments and the

TABLE 9. Textural criteria distinguishing between strongly recrystallized, massive felsic to intermediate tuff units and porphyritic felsic to intermediate flows

	TUFF	FLOWS
1.	Variable phenocryst content and size in adjacent samples.	Relatively uniform phenocryst content and size in adjacent samples.
2.	Non-uniform phenocryst distribution in individual thin sections.	Uniform phenocryst distribution in individual thin sections.
3.	Abrupt textural variations in thin section.	No textural variations.
4.	Strong local concentration and size variation of phenocrysts due to their occurrence mainly in clasts.	No concentrations except in some flow layers.
5.	Variable phenocryst shape due to fragmentation.	Commonly euhedral, no evidence of fragmentation.
6.	Rare rounded plagioclase glomerocrysts lacking protrusions of individual crystals.	Rare well developed plagioclase glomerocrysts, with angular crystal corners projecting into groundmass.
7.	Absence of phenocryst alignment.	Plagioclase phenocryst alignment is common.
8.	Stronger recrystallization with poor to moderate preservation of primary textures.	Moderate recrystallization with good preservation of primary textures.
9.	Irregular weathered outcrop surface in some units.	Smooth weathered outcrop surface with fine grained aphyric or porphyritic textures.

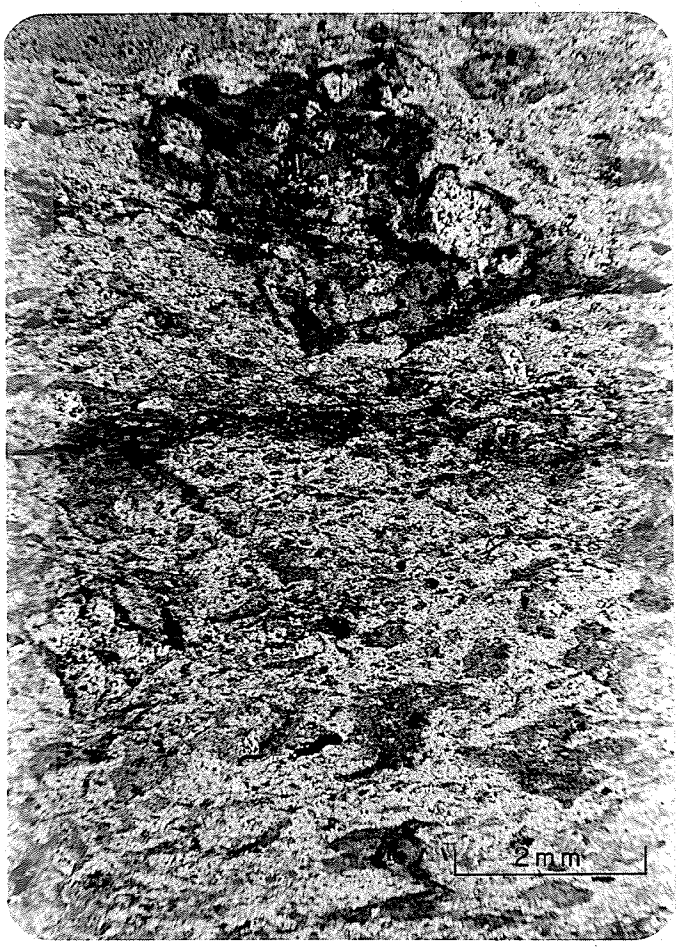

Fig. 9. Photomicrograph of primary tuff with partly preserved primary texture. An amygdaloidal lapillus at the top and smaller biotite-rich, ash-sized aggregates (darker grey) are the only identifiable rock fragments. Note the concave borders in some biotite-rich fragments suggesting that shape was partly vesicle controlled. Light-coloured, matrix-like material lacks primary texture and may have been originally glass. Plane light.

Fig. 10. Photomicrograph of primary tuff with an elongated flattened pumice fragment in the centre. The vague internal foliation may have been formed by vesicle collapse. Plane light.

paucity or absence of a fine-grained recrystallized phase representing possible original glass shards and granules.

The occurrence of secondary tuff in the vent facies, the high content, rounded shape, and moderate sorting of rock fragments, the similarity of fragments to the dominant identifiable rock fragment types in primary tuff, the absence or paucity of glass shards and granules, and the low content of matrix suggest that the rock fragments in secondary tuff were derived from poorly consolidated primary tuff by fluvial processes during the eruption phase.

Lapilli-tuff, Lapillistone, Breccia and Agglomerate

Primary Types: Primary lapilli-tuff, lapillistone, breccia and agglomerate occur as lenticular units up to 300 m thick and 1780 m long. Both monolithic and heterolithic units are present, with heterolithic units up to 50 m thick commonly occurring near the base of pyroclastic accumulations, the upper parts of which are monolithic units and flows. The basal contact of the heterolithic units with underlying tuff or flows is sharp; the upper contact with overlying flows is sharp and with overlying monolithic pyroclastic units either sharp or gradational. In some accumulations, there is no variation in absolute fragment size range but in others the upper monolithic units are coarser than the basal heterolithic units. Where present this reverse grading may indicate that the initial phase of the eruption was more explosive. Bedding, with thicknesses less than 1 m, and both normal and reversed grading are locally present.

In the following discussion and in Table 8 the characteristics of fine lapillistone (2 mm to 2 cm lapilli) and coarse

lapillistone (2 to 6.4 cm lapilli) are treated separately because of differences in the range of fragment types. Fine lapillistone is discussed with fine lapilli-tuff and coarse lapillistone with breccia and agglomerate because of similar ranges of fragment types in the two groups. No coarse lapilli-tuff was observed.

Fine lapilli-tuff and lapillistone are monolithic to heterolithic and consist of subangular to angular, poorly to well sorted, identifiable rock fragments and plagioclase crystals, and fine-grained (less than 0.05 mm) aggregates of quartz, plagioclase, muscovite, and biotite, that may be recrystallized glass granules and shards. The rock fragments include all types found in tuff (Table 8) with felsic to intermediate, porphyritic and aphyric varieties being most common. Monolithic units contain only aphyric fragments, as shown for a tuff in Figure 8b, and heterolithic units contain both aphyric and porphyritic fragments. Lapilli-tuff and lapillistone consist of two gradational particle size fractions: 1) lapilli consisting of 2 mm to 2 cm rock fragments, and 2) ash matrix of less than 2 mm rock fragments, which have similar compositions and textures to the lapilli, recrystallized glass shards and granules, and rare plagioclase crystals. Of the two fractions, matrix forms 30 to 70 percent in lapilli-tuff and less than 30 percent in lapillistone.

Coarse lapillistone, breccia, and agglomerate (Table 8) are monolithic to heterolithic and consist of two, commonly gradational poorly sorted size fractions. The coarse fraction 2 to 10 cm forms more than 80 percent of the unit. It comprises subangular to angular

lapilli in lapillistone, 5 to 160 cm subangular to angular lapilli and blocks in breccia, and rounded bombs (Fig. 11) up to 30 cm and subangular to angular blocks up to 3 m (Figs. 11 and 12) in agglomerate. The fine fraction forms less than 20 percent of the unit and is an ash (less than 2 mm) matrix. The matrix is poorly known because of difficulty in sampling glaciated outcrops, but it probably consists of rock fragments, rare plagioclase crystals and recrystallized glass particles, similar to matrix in lapilli-tuff and fine lapillistone. The term agglomerate is used for units with more than 10 percent bombs; the maximum content of bombs in agglomerate is about 40 percent. Agglomerate is confined to the northern part of member H-4 (Fig. 5). The range of fragment types is more limited than in primary tuff, lapilli-tuff, and fine lapillistone, but, as in these rock units, felsic to intermediate, porphyritic and aphyric types predominate (Table 8).

Monolithic units contain aphyric fragments and heterolithic units contain both aphyric and porphyritic fragments. The bombs in agglomerate are fine-grained and commonly characterised by distinct internal concentric layering with layers up to 0.5 cm thick and by a 1 to 5 cm thick outer rim (Fig. 11). All of the layers, including the outer rim, differ in colour indices and in content of muscovite, actinolite and to a lesser extent garnet. The outer rim is characterised by a high muscovite content and the presence of actinolite and/or garnet, minerals that are rare elsewhere in the formation. The rounded shape of the bombs and the presence of concentric layering in most bombs suggests: 1) the bombs are essential and originated as clots of ejected magma, and

Fig. 11. Rounded bomb (30 cm diameter) with reaction rim and internal concentric layers in agglomerate in the northern proximal vent facies of member H-4 about 300 m southwest of the No. 1 shaft.

Fig. 12. Subangular block in agglomerate; northern proximal vent facies of member H-4, about 300 m southwest of the No. 1 shaft.

2) that the layering is primary, with the outer rim forming either by rapid cooling or alteration shortly after deposition and the internal layering by the cooling process. The present mineralogy of the layers, however, formed by subsequent metamorphism. Some of the blocks in agglomerate have well developed flow layering.

The origin of the subangular to angular fragments is more difficult to determine than the bombs in agglomerate. The occurrence of heterolithic units at the base, and monolithic units nearer the top of pyroclastic accumulations, suggests a common evolutionary cycle. The heterolithic fragments produced by the initial phase of eruption could have several origins: 1) slumped earlier formed pyroclastic and autoclastic breccias around the vent prior to the eruptive phase; the fragments would be dominantly accessory, 2) blasted and ejected from pre-existing pyroclastic and autoclastic breccias and flows within and around the vent during the earliest phase of the eruption; the fragments would be dominantly accessory, 3) a combination of 2) above with fragments from the magma; the fragments would be accessory and essential, and 4) a combination of all of the above sources. Of the above 2) was probably the dominant process. As eruption proceeded, the magmatic component increased in importance and the monolithic units were derived largely from the magma; fragments are dominantly essential. The mixture of bombs and blocks in agglomerate may have resulted from slumping around the vent during an eruption or more probably be magmatic, with the blocks derived from a slightly more viscous magma.

Secondary Types: The coarser secondary pyroclastic rocks comprise both fluvial and laharic units and their characteristics are listed

in Table 8. Fluvial units consist of lapillistone whereas laharic units consist dominantly of lapilli-tuff and minor tuff-breccia and lapillistone. Laharic units are more common than fluvial units, and consequently coarse secondary pyroclastic rocks as a whole have a higher lapilli-tuff to lapillistone ratio than coarse primary pyroclastic rocks. Also, coarse secondary pyroclastic rocks have a lower maximum size range of fragments.

Fluvial lapillistone units are up to 100 m thick and 1500 m long. They occur with fluvial tuff and primary tuff and fine lapillistone in the distal vent facies (Fig. 5) and as thin lenses, which could not be mapped because of their poor exposure, in laharic sequences. They are heterolithic to monolithic and consist of more than 90 percent subangular to rounded, moderately sorted, 2 mm to 1.5 cm rock fragments and less than 10 percent tuffaceous matrix. The rock fragments are dominantly felsic to intermediate porphyritic and aphyric varieties similar to the dominant fragment types in primary lapillistone. The nature of the matrix is masked by recrystallization, but it probably consists dominantly of rock fragments and minor plagioclase crystals. No single criterion sufficiently distinguishes secondary lapillistone from primary lapillistone, but rather a combination of criteria including better sorting, greater rounding of fragments lower maximum size range of the rock fragments, and the absence of fine-grained recrystallized glass fragments.

Heterolithic laharic units and sequences range in thickness from 20 to 470 m and in length from 180 to 2800 m. Internal bedding is absent and no grading was observed. In contrast to other

pyroclastic rocks, lahars have a bimodal fragment size distribution (Fig. 13) comprising a 1 to 15 cm coarse fraction and a fine-fraction or matrix less than 2 mm in size. The matrix forms 30 to 70 percent of lapilli-tuff (Fig. 13) and tuff-breccia and 20 to 30 percent of lapillistone. Both fractions comprise similar subangular to rounded rock fragments, the only difference being in size. The matrix also contains minor rounded plagioclase crystals; no glass fragments were observed. The rock fragments are dominantly felsic to intermediate, porphyritic and aphyric types (Table 8) similar to fragment types in coarser primary pyroclastic rocks. Some laharic units contain up to 15 percent mafic to intermediate fragments, whereas in coarser primary pyroclastic rocks this fragment type is rare.

It is difficult to unequivocally determine the origin of the fragments, particularly the mafic to intermediate fragments, the presence of which is probably significant. The occurrence of the mafic to intermediate fragments may indicate rapid erosion of parts of formation H thereby exposing formation G, collapse of the mafic wall rocks of the caldera, renewed mafic to intermediate volcanism in the caldera, or transport of material into the caldera from the dissected formation G cone north of the caldera. None of these processes can be proven or disproven, although the rarity of intermediate to mafic fragments in other pyroclastic units supports an extra-caldera origin. Despite the problems of

Fig. 13. Weathered surface of laharic lapilli-tuff showing bimodal grain-size distribution of subangular lapilli in tuffaceous matrix; central part of the upper laharic sequence in member H-2.

determining the origin of the fragments, lahars are classified as pyroclastic, formed by mass movement of pyroclastic fragments, rather than epiclastic for the following reasons: 1) the predominance of felsic to intermediate fragments identical to fragments in primary pyroclastic rocks, 2) the lack of evidence for formation of the fragments by erosion, 3) the lack of intercalated volcanic epiclastic rocks, as occurs in the alluvial or epiclastic facies of most stratovolcanoes, and 4) the relatively close proximity to flows and primary pyroclastic rocks.

Volcanic Epiclastic Units

Volcanic epiclastic rocks comprise volcanic argillite and sandstone (Fig. 5). The characteristics of argillite are not included in Table 8 because petrographic data is limited and primary textures have been completely destroyed by recrystallization.

Volcanic Argillite: These units are up to 60 m thick but their strike length is unknown because of faulting. As used herein, argillite includes siltstone and claystone and is characterised by well developed layering and moderately developed bedding plane foliation.

It consists of alternating layers with different proportions of plagioclase, biotite, quartz, actinolite, epidote, chlorite and pyrite. The layers are less than 2 mm thick and represent primary compositionally different beds. In places argillite is graphitic.

Argillite is classified as volcanic because of its restricted occurrence in vent sequences (Fig. 5). It probably formed by the settling of fine windblown ash or fluvial silt and clay in shallow water.

Volcanic Sandstone: These units have maximum thicknesses of 37 m

and strike lengths of 500 m. They contain rounded, moderately to well sorted sand-sized material comprising 80 to 95 percent heterolithic felsic to intermediate porphyritic and aphyric volcanic clasts, up to 15 percent plagioclase, and up to 10 percent quartz; matrix forms less than 5 percent of the sandstone (Table 8). Plagioclase clasts and plagioclase phenocrysts in volcanic fragments are replaced pseudomorphously by single grains of albite rather than aggregates. These pseudomorphs have better developed twinning than plagioclase clasts and phenocrysts in tuff and most flows where pseudomorphs are albite aggregates. Quartz occurs as single grains and as recrystallized polycrystalline aggregates. Volcanic sandstone can be petrographically subdivided into litharenite and feldspathic litharenite, with feldspathic litharenite containing 5 to 15 percent plagioclase clasts (Fig. 14) and litharenite containing less than 5 percent plagioclase clasts. Clast sorting and rounding are better developed in feldspathic litharenite than in litharenite. The better sorting and rounding implies that the increase in plagioclase is due to more reworking rather than to differences in provenance. Plagioclase is more resistant to abrasion than rock clasts and its abundance is thus an indicator of maturity (Pettijohn et al. 1972).

Volcanic sandstones have poorly to well developed bedding with thicknesses ranging from 0.3 to 30 cm. Normal graded bedding is developed on a local scale and indicates that beds face west. Primary scour, flame and slump structures are present but were observed only in thin-section.

Designation of the sandstone as epiclastic is based on fragment heterogeneity, better rounding and sorting, better developed bedding, and higher content of plagioclase clasts and in places

Fig. 14. Photomicrograph of volcanic feldspathic litharenite showing broken and rounded plagioclase clasts that were originally phenocrysts. The fine-grained material between crystal clasts are sand-sized rock fragments but their boundaries are not distinguishable under crossed nicols.

quartz clasts compared to secondary tuff. The nature of the fragments indicates the provenance for the sandstone was volcanic.

Alloclastic Units

Two discordant intrusive breccia units between 3.5 and 5 m wide have been traced for strike lengths of 100 to 160 m, in the northern proximal vent facies of member H-4, north and south of the mine workings (Fig. 5). The units are 45 to 75° discordant to host rocks. The contacts of the northern unit are sharp whereas those of the southern unit are sharp to diffuse. They are monolithic to heterolithic and consist of dominantly subangular, nonsorted, felsic to intermediate aphyric and porphyritic volcanic fragments between 1 and 15 cm in size (Table 8). Locally, the fragments adjacent to the contacts are elongated and aligned parallel to the contact whereas in the centre of the units, fragments are equant. Matrix forms 20 to 30 percent of the unit and consists of vuggy or smokey quartz.

The matrix is probably of hydrothermal origin and could have provided the medium for mobilization and intrusion of the fragments. Alternatively, the matrix may have been deposited from fumarolic activity after the intrusion of the breccia replacing the original matrix. The shape and composition of the fragments, alignment of fragments adjacent to contacts, sharp and discordant contacts, the apparent restricted occurrence of these units to proximal vent facies, and possibly the nature of the matrix, indicate that the units are intrusive breccias related to volcanism and may form part of original vents. They are not tectonic breccias.

Conglomerate, Chert and Ferruginous Chert

Only one small conglomerate unit, 10 to 40 m thick; was found in formation H. It is in the lower lahar sequence in member H-2 (Fig. 5). It consists of 40 percent, well rounded pebbles and cobbles, 1 to 10 cm in diameter, and 60 percent medium to coarse-grained sandstone matrix. The conglomerate was not classified as volcanic because volcanic clasts were not unequivocally recognized. The pebbles and cobbles are medium-grained with felsic and felsic to intermediate compositions suggesting that they may have been derived from quartz diorite plutons. Bedding is well developed, with larger pebbles and cobbles in beds 10 to 18 cm thick and small pebbles in beds 1 to 2 cm thick.

Chert and ferruginous chert units range in thickness from 20 to 50 m, have strike lengths of 600 m, and are closely associated with volcanic argillite and proximal and distal vent facies pyroclastic rocks in member H - 1 (Fig. 5). Chert consists of alternating fine-grained, granular, quartz layers 2 mm to 2 cm thick and actinolite plus chlorite layers less than 1 mm thick.

Ferruginous chert comprises alternating layers consisting of: 1) 75 to 80 percent actinolite, 5 to 10 percent epidote and clinozoisite and 10 to 15 percent disseminated and finely layered pyrite and pyrrhotite, in 2 to 4 cm thick layers, and 2) 83 percent quartz, 5 percent biotite, 2 percent disseminated pyrite and pyrrhotite, and 10 percent disseminated or finely layered actinolite, in 1 mm to 2 cm thick layers.

Quartz Diorite

Metamorphosed quartz diorite forms two sill-like plutons

which have a maximum thickness of 400 m and a combined strike length of 3.5 km in formation G and the northern part of formation H (Fig. 5). Narrow sills and dikes up to 10 m thick occur elsewhere in formation H. The main plutons may be part of a single pluton or two separate plutons, but poor exposure and faulting in the Borthwick Creek area hampers determination of their relationship. Quartz diorite was metamorphosed under greenschist facies conditions similar to those that affected the country rocks.

The plutons have sharp, sinuous to straight, chilled upper contacts, although chilling is difficult to document because grain size variations near the contact are masked by metamorphic effects. The lower contacts are not exposed. The plutons are slightly discordant to the metavolcanic sequence and contain lenticular to irregular inclusions of both formation G and formation H. They are composite intrusions but phases are not shown on Fig. 5 because of poor exposure and the restricted occurrence of some phases. Contacts between phases vary from sharp and sinuous to straight with chilled and unchilled margins, to diffuse where phase boundaries can be inferred only by rapid textural changes.

Primary porphyritic, equigranular and granophyric textures are commonly preserved with porphyritic phases predominating in the southern pluton and equigranular phases in the northern pluton. Equigranular phases range in grainsize from 0.1 to 1.75 mm and consist of interlocking, subhedral, tabular plagioclase and interstitial anhedral quartz. Granophyric intergrowths of quartz and plagioclase occur in parts of the northern pluton. The

plagioclase was originally oligoclase to andesine (An_{20} to An_{35}) but is largely replaced pseudomorphously by albite, minor biotite, muscovite, epidote, and chlorite, and rare carbonate. Locally, muscovite is the major pseudomorphous phase. Two modal and chemical analyses of rocks from equigranular phases, one from the southern pluton (sample 84) and the other from the northern pluton (sample 398), and presented in Tables 4 and 11 respectively. They show that these rocks are mineralogically and chemically similar in both plutons.

Porphyritic phases contain 15 to 35 percent euhedral, tabular, 1 to 3 mm long plagioclase phenocrysts, 1 to 5 percent, subhedral to rounded, 0.5 to 4 mm quartz phenocrysts, and 60 to 85 percent groundmass. Plagioclase phenocrysts were originally oligoclase to andesine (An_{20} to An_{35}) but are largely replaced pseudomorphously by albite, minor biotite, muscovite, and epidote, and rare carbonate. Muscovite locally is the major pseudomorphous phase. The groundmass consists of albite and quartz, minor epidote, chlorite, biotite, and muscovite, and trace Fe-Ti oxide, pyrite or pyrrhotite and apatite. Groundmass textures are partly recrystallized, but where primary, they consist of subhedral to euhedral plagioclase and anhedral quartz with a grain size up to 0.75 mm. Where recrystallized, groundmass grain size is less than 0.1 mm, and the fine grain size may indicate that parts of the groundmass were originally glassy.

The plutons are part of formation H because: 1) their occurrence is restricted to formation H and therefore the caldera, 2) they are compositionally similar to formation H, 3) they appear to have been the source for some of the rock fragments

in adjacent primary tuff units, the conglomerate in the lahar sequence in member H-2, and metasedimentary rocks in formation I where it overlies formation H, 4) the presence of granophyric texture, the possible presence of original glassy groundmass, and chilled contacts suggest that the plutons were emplaced at a high crustal level close to the surface, and 5) they have undergone metasomation which was restricted to formation H.

Stratigraphy

Subdivision of formation H into four vent facies members (Figs. 5 and 6), termed H-1, H-2, H-3 and H-4, assists understanding of the lithologic complexities, deciphering of the history of volcanism, and location of source vents. Members are defined by major, systematic vertical lithologic and genetic variations; each member represents a major pulse of volcanism. Most member boundaries are relatively well defined because vertical changes are commonly abrupt. However, there are areas, for example the top of member H-2, where lithologic changes appear gradational and the member boundary is arbitrarily defined.

Members H-1, H-2 and H-4 are further subdivided (Fig. 6), using lateral lithologic and genetic variations and proximity of source vents, into: 1) a proximal vent facies comprising flows and primary breccia, agglomerate, lapillistone, lapilli-tuff and tuff, in varying proportions, and only minor secondary pyroclastic rocks and volcanic epiclastic rocks, and 2) a distal vent facies comprising primary tuff, fluvial tuff, fine primary and fluvial lapillistone and lapilli-tuff, and laharic lapilli-tuff, lapillistone

and tuff-breccia in varying proportions, minor epiclastic volcanic rocks, and rare flows and coarse primary pyroclastic rocks.

Facies boundaries (Fig. 6) within members are arbitrarily defined because lateral changes are gradational. Member H - 3 comprises only distal vent facies. The characteristics of the members are summarized in Table 10.

Coarse alluvial facies consisting dominantly of volcanic conglomerate and fine alluvial facies comprising volcanic sandstone and siltstone and airfall tuff (Smedes and Prostka, 1972) do not occur in the formation.

Member H - 1

Member H - 1 (Table 10) is the lowermost member and is confined to the south and central parts of the caldera where it overlies and interfingers with formation G (Fig. 5). The restricted extent appears to be mainly controlled by pre-existing topography, but a smaller caldera size during early felsic to intermediate volcanism also may have played a role. The southern portion of the member (Fig. 5) is abruptly truncated by the Setting Net Lake stock, which may have been intruded along the margin of the caldera; and the northern portion is disrupted by quartz diorite and metagabbro sills.

There appears to be a northward decrease in both clast size and thickness of individual units and an increase in volcanic epiclastic units, suggesting that the member consists of a southern proximal vent facies and a northern distal vent facies (Figs. 5 and 6).

TABLE 10. Characteristics of the members in formation H

MEMBER	MAXIMUM THICKNESS (M)	MEASURED AREAL PROPORTIONS OF ROCK TYPES (%)	FACIES AND ROCK TYPE DISTRIBUTION
H - 1	400	25 primary tuff, 13 fluvial tuff, 41 primary lapilli-tuff and lapillistone, 17 fluvial lapillistone, minor breccia, 2 argillite, 2 chert and ferruginous chert, minor flows	1. Proximal vent facies in the south: dominantly primary tuff and lapillistone, fluvial tuff and lapillistone, with minor flows, chert, ferruginous chert and argillite. 2. Distal vent facies in the north: dominantly primary tuff and lapilli-tuff, and fluvial tuff and lapillistone, and minor primary lapillistone and breccia, chert, ferruginous chert, argillite and flows.
H - 2	470	5 primary and secondary tuff, 4 primary lapilli-tuff and lapillistone, 70 laharic lapilli-tuff, lapillistone and tuff-breccia, 4 volcanic sandstone, 17 flows	1. Proximal vent facies in the north: dominantly flows and interflow primary tuff, lapilli-tuff and lapillistone, with minor volcanic sandstone. 2. Distal vent facies in the south dominantly laharic lapilli-tuff, lapillistone and tuff breccia with minor primary and secondary tuff.
H - 3	700	12 primary tuff, 6 fluvial tuff, 48 undifferentiated tuff, 12 primary lapillistone, 16 undifferentiated lappistone, 6 flows, minor breccia	Entirely distal vent facies with flows concentrated in the central part.
H - 4	600	29 primary tuff, 26 primary lapillistone, minor secondary lapillistone, 10 laharic lapilli-tuff and tuff-breccia, 2 primary breccia and agglomerate, 33 flows	1. Proximal vent facies at the north and south ends: primary tuff, lapillistone, breccia and agglomerate, and flows, and with minor laharic lapillistone. Breccia and agglomerate are more common in the northern facies and flows more common in the southern facies. 2. Central distal vent facies: laharic lapilli-tuff and tuff-breccia, and primary and fluvial tuff.

Southern Proximal Vent Facies: This facies is divided into two units by several mafic to intermediate flows of formation G that form a northward terminating tongue (Figs. 5 and 6). The lower unit, composed of fluvial tuff and lapillistone, wedges out southward against mafic to intermediate flows of formation G. It may have been deposited on a northward-facing slope formed by eruption of the underlying flows. Vents responsible for this unit were probably not in the immediate vicinity. The upper unit is more directly vent related and comprises a sequence of primary lapillistone overlain, in the south, by primary tuff with minor intercalated flows. Chert, ferruginous chert, and volcanic argillite, in places graphitic, form lenses up to 50 m thick at or near the base of both units. These sedimentary units appear to represent periods of quiescence that broadly correspond to the transition from effusive mafic to intermediate volcanism of formation G to explosive felsic to intermediate volcanism of formation H. Silica in chert and ferruginous chert may have been derived from fumarolic or hot spring activity during quiescent periods.

The distribution of the primary lapillistone, which ranges in thickness from 40 to 200 m (Fig. 5), appears to be controlled by pre-existing topography. The unit is thickest north of the hill formed by the mafic to intermediate flow tongue. North of the flow front, there is a lateral gradation in clast size and composition, and in the abundance of matrix-like material that probably represents recrystallized glass shards. Maximum clast size decreases from 30 mm in the south to less than 3 mm in the north, where the unit is more tuffaceous. There is a concomitant change in clast composition from monolithic with dominantly rock fragments and minor matrix,

similar to but coarser than the tuff in Figures 8a and ib, to heterolithic with dominantly recrystallized vitric fragments. Fragments in the southern part of the unit are entirely aphyric felsic to intermediate types (Fig. 8b) but in the northern part biotite-rich, amygdaloidal, and pumiceous fragments (Fig. 10) are present. The unit also contains well developed normal graded beds that range in thickness from 6 cm to 1 m.

South of the flow front the lapillistone thins and is heterolithic with a maximum fragment size of 30 mm. Fragments observed in this part of the unit include porphyritic and aphyric felsic to intermediate types and minor mafic to intermediate types and chert derived from the immediate basement rocks.

The lateral changes in the lapillistone indicate that the southern part of the unit was closer to the vent. The overlying tuff, which represents the end of a caldera filling event thickens southward and may have banked up against the caldera wall. It contains less than 20 percent identifiable fragments; glass shards, subsequently recrystallized, were probably the major fragment type. The degree of reworking, as shown by textural changes (Table 8) increases upward and was concomitant with waning volcanism.

Northern Distal Vent Facies: This facies interfingers with pyroclastic rocks of formation G and, although it is poorly exposed and disrupted by faults and the quartz diorite and gabbro intrusions, it appears to thin northward (Figs. 5 and 6). The facies comprises thin interlayered lenses of primary and secondary tuff, lapilli-tuff and lapillistone, volcanic argillite and litharenite, and minor heterolithic breccia and felsic to intermediate flows.

Deposition appears to have occurred at lower topographic levels than the southern proximal vent facies because of greater reworking with some of the material derived from the proximal vent facies.

Some primary tuff units near the base of the facies and near the quartz diorite sill (Fig. 5) contain clasts derived from the sill, suggesting that the sill was emplaced close to the surface, perhaps as a dome, and was the source for some of the lower units. The restricted occurrence of thin, coarse lapillistone and breccia units close to the sill supports this proposal. The observed upper contacts of the quartz diorite appear to be intrusive indicating that the vent was not in the presently exposed section through the caldera; but could not have been far removed. This possible vent may have been subsidiary to the main vent further south.

Near the top of the facies some primary tuff units that overly the formation G pyroclastic lenses have well defined, alternating mafic to intermediate, and felsic to intermediate beds. These units interfinger with volcanic argillite and litharenite. Although it is difficult to determine the origin of the tuff units from criteria listed in Table 8, it is proposed that the compositional bedding reflects local subaqueous emplacement of airfall fragments from two separate volcanic centres.

Member H-2

Member H-2 (Table 10) is the only member at the north end of the caldera, it extends most of the way across the caldera to pinch out near the presumed south margin. The northern end of the member overlies quartz diorite and is truncated by a north to northeast trending fault (Figs. 5 and 6). The lateral extent of the member indicates that at this stage the caldera had almost reached its maximum dimensions.

The restricted extent of flows and primary lapilli-tuff and lapillistone to the northern part of the member and of laharic lapilli-tuff to the south indicates that the member comprises a northern proximal vent facies and southern distal vent facies (Figs. 5 and 6).

Northern Proximal Vent Facies: In this facies a basal primary tuff, lapilli-tuff, and lapillistone sequence is overlain by a sequence of porphyritic to aphyric felsic to intermediate flows with thin interflow units of primary tuff, lapilli-tuff and lapillistone.

At the south end of this facies, at least four flows are present and the flow sequence has a maximum thickness of 300 m. Only one flow is known to extend to the north margin of the caldera (Fig. 5). The flow sequence rapidly thins and pinches out southwards, where it is intertongued with litharenite, feldspathic litharenite, and laharic lapilli-tuff of the southern distal facies. The restricted extent of the flows indicates closeness to source vents and that the source vents apparently do not coincide with the existing caldera margin.

The origin of tuff and lapilli-tuff is variable, particularly in the south where they appear to be mixed primary and secondary types. Further north the pyroclastic rocks appear to be dominantly primary.

Southern Distal Vent Facies: This facies is more extensive than the northern proximal vent facies and consists dominantly of laharic lapilli-tuff with minor intercalated tuff, volcanic litharenite, feldspathic litharenite, and conglomerate (Fig. 5).

Two laharic sequences, which differ in textural variability and range of fragment composition, can be recognized south of the fault along Borthwick Creek. In places, lenses of tuff and fine-grained lapilli-

stone, of possible primary origin, occur between the two sequences. Although the nature of the laharic sequence north of Borthwick Creek is poorly understood because of poor exposure, it appears to be equivalent to the upper sequence south of the fault. Stratigraphic relations north of the fault indicate that the lower flows of the proximal vent facies are coeval with, and the upper flows younger than, the upper laharic sequence. Thus the lower sequence south of and terminated by the fault, would be older than the flows.

The lower sequence is heterolithic lapilli-tuff, lapillistone and tuff-breccia that contain felsic to intermediate fragments, (Table 8), have a bimodal grain size distribution, and have a chaotic stratification with abrupt vertical and lateral grain size changes. In the northern part of the sequence, lapilli-tuff and lapillistone predominate and have a coarse size fraction between 30 and 64 mm, and 20 to 30 percent tuffaceous matrix; some lapillistone lenses may be fluvial. In the south the lahars are dominantly lapilli-tuff and tuff-breccia with fragments up to 150 mm and 30 to 50 percent matrix. They interfinger, near the base, with underlying tuffaceous rocks of member H-1.

The lahars are probably subaerial because the chaotic stratification implies that individual units were emplaced in channels eroded into underlying laharic units, similar to the situation described by Waldron (1967) at Irazú Volcano, Costa Rica. The northward thickening of the lower sequence (Fig. 5) appears to be controlled by pre-existing topography with emplacement confined to a depression in member H-1. This depression was formed by preferential deposition of mafic to intermediate flows of formation G

and primary tuff of member H-1 near the margin of the caldera, possibly aided by collapse in the centre of the caldera. The northward decrease in overall grain size, emplacement of the sequence in a depression, suggest a southern source. The exact provenance is unknown but the similarity of fragments to those in coarse primary lapillistone and breccia suggests that the source is a coarse proximal vent facies not exposed in the present section.

In contrast to the lower sequence, the upper sequence is characterized by gradual grain size changes and individual units are more continuous along strike. It has a bimodal clast size distribution with 40 percent tuffaceous matrix and 60 percent lithic fragments. Seventy-five percent of the fragments are felsic to intermediate, similar to those in the lower sequence, but twenty-five percent are mafic to intermediate, and appear to have been derived from formation G; such mafic to intermediate fragments are rare in the lower sequence. The size of the clasts gradually varies along strike but the size variation is opposite to that observed in the lower sequence. In the north, south of Borthwick Creek, clasts range from 5 to 64 mm whereas in the south they are 2 to 30 mm. The provenance for the upper sequence is difficult to determine without knowledge of the third dimension, but several comments can be made. Firstly, the flow relations which support a build-up of material to the north and the southward decrease in grain size indicate a potential northern source. Secondly, the high proportion of mafic to intermediate clasts indicates that the provenance is not the proximal vent facies exposed in the present cross-section because no formation G units are exposed in the cross-section at this stratigraphic level.

A potential source is unconsolidated coarse intermediate pyroclastics and these units are exposed immediately below member H-2.

Member H-3

Member H-3 (Table 10) is confined to the south and central parts of the caldera. The southern end is abruptly truncated by an east-trending fault, that appears to be a primary boundary fault of the caldera, and by the Setting Net Lake stock which appears to have been intruded along the boundary fault (Fig. 5). The northern part of the member pinches out.

The member consists mainly of pyroclastic rocks, but genetic and grain size subdivision of the pyroclastic rocks is difficult because of poor exposure, rapid vertical and lateral grain size variations, and metamorphism. Consequently, unit boundaries shown on Fig. 5 are arbitrary and reflect broad scale, grain size changes. Genetic subdivision into primary and secondary types is based on petrographic data because diagnostic macroscopic features were not observed. Despite these problems the member is considered to be entirely distal vent facies because of the predominance of tuff, the fine-grain size of lapilli-tuff and lapillistone, and the paucity of flows (Figs. 5 and 6, Table 10).

The upper unit of the member is poorly exposed north of Borthwick Creek. This unit has been designated as undifferentiated tuff (Fig. 5) because of its poor exposure and the predominance of tuff in the few outcrops south of the Creek.

The central part of the member near Borthwick Creek is an interlayered sequence of porphyritic flows, primary and undifferentiated tuff, lapillistone and rare breccia. To the south the sequence is generally similar, although flows and undiffenentiated pyroclastic rocks are less abundant. The maximum fragment size in the pyroclastic

rocks is 3 cm.

Near Borthwick Creek the discordant attitude of the flows define (Fig. 5) a northward facing slope caused by progressive northward expansion of the pyroclastic sequence. The marked northward increase in thickness of the overlying undifferentiated tuff is partly due to this northward slope, but it may also reflect, inpart, a depression in member H-2. The rapid thinning of the undifferentiated tuff further north reflects the positive topographic expression of the proximal vent facies flows of member H-2. Although the depression in member H-2 may have been exaggerated by later faults, it is probable that it formed by post-depositional collapse before deposition of member H-3 and the build-up of flows to the north. The discordant attitude of the flows indicates a progressive build-up of the member from south to north.

The northward expansion of the member was caused by the restriction of early volcanism to the southern part of the caldera and the build up of material against the margin, followed by a northward shift in vent positions as volcanism continued.

Member H-4

Member H-4 (Table 10) occupies most of the upper part of the caldera (Figs. 5 and 6). It is thickest at the south end where it is truncated by an east-trending fault that appears to represent the original boundary of the caldera. The northern end of the member is uncertain, but it appears to be truncated abruptly by a post-caldera fault (Fig. 5).

The member is a diverse sequence comprising proximal vent facies at the north and south ends, separated by a central distal vent facies (Fig. 6). This relationship suggests that source vents

were at the north and south ends of the caldera. Contact relations between the facies provide insight into the development of the member. To the south the distal vent facies underlies and grades into the proximal vent facies, whereas to the north it appears to overlie the proximal vent facies. Thus, volcanism was not coeval throughout the member but progressed from north to south.

Flows and primary lapillistone predominate in both proximal vent facies, but the northern facies differs from the southern facies in having less primary tuff and flows, and more primary breccia and agglomerate.

Northern Proximal Vent Facies: Primary lapillistone, breccia, and agglomerate units separated in places by flows form most of this facies (Fig. 5). The proportion of breccia and agglomerate is greater here than anywhere else in the present cross-section of the caldera. The lateral extent of many units cannot be determined because of offset along numerous east-trending faults (Fig. 5). As shown by the contact between formations H and I and by unit boundaries, the faults produced only limited vertical offset (horizontal in reference to the present ground surface). However, the apparent lack of correlation between the fault blocks indicates that units must be lenticular and that there must be considerable horizontal offset (vertical in reference to the present ground surface) along the faults. The faults are post-caldera but are synvolcanic because many faults contain quartz veins that are probably related to late-stage hydrothermal activity.

The coarser nature of the pyroclastic rocks, as compared to other proximal vent facies units in the formation, indicates either

that the area is closer to the vent, or a waning in intensity of volcanism, or perhaps both. The coarsest units are in the southern part of the facies near the No. 1 Shaft (Fig. 5) and there is a progressive decrease in grain size northward. Southward there is an abrupt transition to the distal vent facies.

The coarsest and best exposed agglomerate unit is at the top of the facies about 300 m south of the No. 1 Shaft (Fig. 5); it is 80 m thick and overlies sharply a thin tuff unit. The agglomerate is variable in texture and composition. The lower 5 to 7 m comprises angular, heterolithic, felsic to intermediate lapilli; the angularity and heterolithic nature of the fragments and the lack of bombs suggest that many of the early erupted fragments were derived from older units rather than new magma. The central zone appears to be monolithic and consists of rounded bombs and angular to subangular blocks; this suggests that as the eruption continued, the magma became the major source for ejecta. The upper 3 to 5 m is a mixed zone that includes fragments from the basal brecciated zone of the overlying flow. Mixing was probably caused by friction during movement of the flow over unconsolidated ejecta.

The coarse pyroclastic unit north of the No. 1 Shaft (Fig. 5) comprises interlayered breccia, agglomerate, coarse (3 to 6 cm) lapillistone, and minor fine (2 to 4 mm lapillistone. The breccia and coarse lapillistone appear to be heterolithic with angular to subangular, poorly sorted fragments. Fine lapillistone forms, well bedded lenses, up to 3 m thick and 6 to 9 m long, that appear to have infilled depressions in the irregular surface of the breccia

and coarse lapillistone. Rock fragments in these lenses are subangular to rounded and well sorted; these features indicate some reworking possibly by fluvial processes.

This unit is transected by two generations of minor east-trending faults. Early faults have tightly healed, irregular surfaces deflected by the fragments and have only minor quartz infilling and cataclastic textures; they are probably penecontemporaneous with deposition. Late faults have straight surfaces that transect fragments and have prominent quartz infilling and cataclastic textures; they are synvolcanic but post-lithification.

The lapillistone units (Fig. 5) are heterolithic and contain only sparse blocks. Lapilli-tuff and tuff are relatively rare and form isolated massive lenses up to 40 m thick, mainly in the northern part of the facies.

Discordant, intrusive alloclastic breccias that may represent source vents were found 180 m south of the No. 1 Shaft and 150 m north of the No. 2 Shaft (Fig. 5). The units trend between 90° and 120°, are about 3 m wide, and have been traced for distances of 150 m. Although outcrop exposure is poor, the southern unit may be associated with, and represent the source vent for, the overlying coarse breccia and agglomerate unit.

Another feature indicating closeness to source vents is the close association of flows and coarse pyroclastic rocks (Fig. 5). Flows are most common in the south of the facies and this feature together with the southward increase in grain size in the pyroclastic rocks, points to southern source vents which would have been near

the centre of the caldera. The abrupt transition to the south with the distal vent facies reflects the younger age of the distal vent facies and progressive burial of the volcanic edifice represented by the proximal vent facies. The trend of the uppermost flow in the south part of the proximal vent facies represents the initial dip of the edifice.

Central Distal Vent Facies. This facies is poorly exposed and little known. It appears to comprise a lower sequence of fluvial tuff in the south and laharic lapilli-tuff and tuff-breccia in the north, both of which are overlain by an upper tuffaceous sequence.

Southern Proximal Vent Facies: Lenticular, porphyritic flows with a maximum thickness of 150 m and an average thickness of 30 m are present throughout the facies. In the uppermost flow sequence there is an abrupt lateral textural change that appears to indicate the presence of two or more lenticular flows and, or ash-flow tuff units separated by a steep contact (Fig. 5). Both units have the same general thickness. The northern two outcrops are texturally uniform with 20 percent plagioclase phenocrysts and appear to be a lenticular flow about 1200 m long and 80 m thick. In the southern two outcrops the sequence has a variable phenocryst content: quartz phenocrysts are ubiquitous but there is a variable quartz to plagioclase phenocryst ratio. In addition, minor accessory rock fragments are locally present, and the groundmass is very fine-grained and was probably glassy. Based on phenocryst contents, one interpretation, as shown on Figure 5 is that the southern sequence comprises three flows with slightly different phenocryst contents. Boundaries between flows were not observed in the field. An alternative interpretation is that the unit represents an ash-flow

tuff sequence deposited in a depression between the porphyritic flow on the north and the caldera wall on the south. This interpretation is supported by the variable phenocryst population (Ross and Smith, 1961; Lipman et al. 1966; Williams and McBirney, 1969), the presence of accessory clasts, and the similarity in thickness of the southern unit and the northern flow, although the similar thickness could be the result of subsequent erosion. Broken phenocrysts which would be diagnostic of ash flow origin were not identified in the unit because recrystallization has largely destroyed grain boundaries. On the basis of the limited data, the author prefers the ash flow origin, although the units are shown as flows on Figure 5, because the data are inadequate to introduce a new lithologic unit. This is the only place in formation H where ash-flow tuff has been tentatively identified.

Both primary tuff and lapillistone show an upward progression from heterolithic to monolithic. The basal tuff unit (Fig. 5) is heterolithic and contains pyroclastic, sedimentary, and mafic to intermediate fragments in addition to the dominant aphyric and porphyritic felsic to intermediate fragments. Tuff units higher in the sequence (Fig. 5) contain only aphyric and porphyritic felsic to intermediate fragments, but this tuff is termed monolithic because many seemingly aphyric, ash-sized fragments may have been derived from sparsely porphyritic units.

Heterolithic lapillistone contains both aphyric and porphyritic fragments with variable phenocryst contents. The basal lapillistone unit contains fragments of the immediately underlying flow sequence which is characterized by well developed flow foliation. Monolithic units higher in the sequence contain only porphyritic fragments and are

difficult to distinguish from flow breccia.

The vertical change from heterolithic to monolithic suggests that early eruptions ejected fragments of pre-existing rock from within the vent in addition to new magma, but as volcanism proceeded the magma became the sole source for ejecta.

The southern part of the two uppermost lapillistone units (Fig. 5) appear to have been reworked, possibly as lahars. They contain rounded, heterolithic fragments and up to 30 percent matrix.

The extreme south end of the facies is a wedge-shaped fault block (Fig. 5), of porphyritic flows and thin interflow primary tuff units. This cannot be directly related to the remainder of the facies.

FORMATION I - SEDIMENTARY ROCKS

There are two distinct facies of formation I (Fig. 4): a northern shallow-water facies that is coextensive with formation H (Fig. 5) and a southern deep-water facies that is physically separated from both the northern facies and formation H (Ayres, in preparation). The northern facies comprises a lower sandstone and conglomerate member, that ranges in thickness from 0 to 100 m, and an upper sequence of argillite, siltstone, intermediate to mafic tuff, chert, and ferruginous chert with an average thickness of 50 m. The southern facies is a turbidite sequence of greywacke and minor conglomerate and is at least 2.5 km south of the caldera. Although formation I was not part of the present study, a summary of the sandstone and conglomerate of the northern facies is included here because they appear to have been derived from formation H and deposited in the caldera.

The northern facies unconformably overlies formation H. North

of Borthwick Lake, deposition and facies relationships in the lower sandstone and conglomerate member were partly controlled by topographic irregularities in the underlying volcanic surface (Fig. 5); relief on this surface was up to 125 m. The irregular surface is probably a combination of volcanic constructional processes, offset on early faults, and minor erosion. South of Borthwick Lake (Fig. 5), the lower member has a more regular thickness, lacks rapid facies changes, and appears to have been deposited on a relatively smooth surface that may be a primary volcanic surface resulting from extrusion of flows and/or ash flows. Deposition of the sandstone and conglomerate appears to have smoothed out the topographic irregularities north of Borthwick Lake.

The sandstone north of Borthwick Lake is feldspathic litharenite and litharenite (Ayres, in preparation) and is characterised by, 1) a high content of rounded volcanic fragments of medium to coarse sand size, 2) a low content of rounded to angular, sand-size quartz and plagioclase, with a high quartz to plagioclase ratio, 3) dispersed rounded volcanic pebbles, 4) a low matrix content, 5) rare rounded to subangular chert clasts and 6) a well preserved primary texture. Volcanic fragments are mainly aphyric to locally porphyritic and felsic to intermediate. Quartz, although commonly recrystallized, consists of mono- and polycrystalline varieties, indicating a composite provenance. Limited chemical study by Ayres (in preparation) showed that the sandstone is chemically similar to volcanic rocks of formation H. The sandstone has well developed bedding, in part graded, with thicknesses between 1 cm and 9.6 m. Local cross-bedding, ripple marks, and flame structures were observed.

The conglomerate is interbedded with the sandstone and contacts are sharp to gradational. Based on dominant clast types, two distinct types of conglomerate can be distinguished: volcaniclastic conglomerate and porphyry conglomerate (Ayres, in preparation). The volcaniclastic conglomerate is a polymictic pebble to boulder paraconglomerate consisting of 30 to 60 percent rounded clasts in a medium to coarse sand matrix that contains ubiquitous pyrite. Fine-grained, aphyric to porphyritic, felsic to intermediate volcanic clasts, that are identical to lithologies in formation H, form 80 to 90 percent of the clast population. Minor clast types include chert, white vein quartz, green mica schist, and mafic to intermediate volcanic rocks. Porphyry conglomerate is a polymictic cobble to boulder orthoconglomerate consisting of 70 to 80 percent, rounded to subangular clasts in a quartz-poor sandy matrix. Aphyric to porphyritic, felsic to intermediate clasts predominate but they have a greater compositional heterogeneity than clasts in volcaniclastic conglomerate and do not resemble lithologies found in the exposed section of formation H. Minor clasts are similar to those in the volcaniclastic conglomerate. Porphry conglomerate is restricted to the top of the sandstone and conglomerate member and is only 15 m thick. The abrupt change in the nature of the conglomerate presumably reflects a change in provenance and/or transport regimes. Bedding is poorly developed in all conglomerate.

South of Borthwick Lake, the lower member consists dominantly of sandstone, and conglomerate is less abundant than in the lower member north of the lake. The sandstone contains up to 40 percent quartz and plagioclase, with the remainder being fine-grained lithic

clasts, presumably of volcanic origin, and minor matrix. Also it is finer-grained, better sorted and more thinly bedded than the sandstone north of the lake. Because of the finer grain size, primary textures are poorly preserved.

Mafic conglomerate and sandstone form a major unit immediately north of Borthwick Lake and local interbeds elsewhere. These units are identical to the volcaniclastic sandstone and conglomerate except for a higher content of mafic to intermediate clasts.

The similarity of most clasts in the volcanic sandstone and conglomerate to lithologies in formation H suggests that most of the detritus was derived from formation H. However, source area must be outside of the exposed section, because, except for one or two low hills, formation H is completely covered by sandstone and conglomerate (Ayres, in preparation). North of Borthwick Lake the member probably was deposited rapidly in an alluvial fan and shallow-water environment with local agitation. This is supported by 1) topography of the pre-sedimentation surface, 2) thick bedding in some units, 3) local cross-bedding and ripple marks, 4) high lithic content of sandstone indicating immaturity, 5) numerous conglomerate interbeds and occurrence of pebbles in sandstone.

The member south of Borthwick Lake appears to be a more distal unit that deposited in a quiescent shallow-water environment. This is supported by laminar bedding, greater maturity, lack of conglomerate interbeds, and lack of cross-bedding.

The restricted occurrence of the mafic sedimentary rocks and their interbedding with more normal volcaniclastic rocks indicate a

different source. Because the mafic unit occurs in the centre of the caldera, the source is probably within the caldera and represents renewed mafic to intermediate volcanism near Borthwick Lake. This volcanism may have formed cones that separated the northern and southern parts of the sandstone and conglomerate member, at least on the plane of the exposed section.

The depositional environment, immaturity, composition, and extent of the sandstone and volcanic conglomerate support a restricted depositional basin whose extent was controlled by formation H. This basin is most likely the caldera produced during formation H volcanism. The deposition of the sediments indicates that the caldera was not completely filled by products directly produced by volcanism.

The abundant chert and the general fine-grained nature of the upper member suggests that it was deposited in a quiet aqueous environment, probably a lake that occupied the caldera.

ENVIRONMENT OF VOLCANISM

Formation E, which represents the early mafic phase of cycle 2 is pillowed and appears to have been emplaced in a subaqueous environment. Following this phase, and associated with the development of the caldera, felsic to intermediate volcanism of formations G and H appear to have been subaerial. Clear cut environmental indicators such as pillows are lacking but the broad characteristics of formation H, the characteristics of flows in formations G and H, and the origin of formation I all support subaerial volcanism.

Formation H consists dominantly of felsic to intermediate pyroclastic rocks which are normally restricted to shallow-water and

subaerial environments. Formation of pyroclastic rocks is controlled primarily by gas content of the magma and the degree of exsolution of each gas phase. Explosive eruption probably occurs only when the volume of exolved gases approaches the volume of the magma, and this can occur only under low pressure conditions characterizing shallow-water and subaerial environments (McBirney, 1963; McBirney and Murase, 1971). Much pyroclastic debris is transported from the site of original emplacement (Parsons, 1969; Fisher 1960b, 1961, 1966) by various subaqueous and subaerial processes. In formation H many of the pyroclastic rocks have been transported short distances, but they lack bedding and sedimentary structures indicative of aqueous environments. This suggests rapid deposition by subaerial sheet flow or stream movement. Also the chaotic stratification in lahars of member H-2, which is similar to lahars in modern subaerial stratavolcanoes, suggests subaerial emplacement in erosion channels. If the secondary pyroclastic rocks are largely subaerial, then the primary pyroclastic rocks which occupy higher topographic areas and are the source for the secondary pyroclastic rocks, must also be subaerial.

The epiclastic rocks in formation H have a high content of rock fragments from coeval units and a restricted extent. Both features are indicative of subaerial stream deposition and not of deep-or shallow-water marine environments. The restricted occurrence of chert and argillite in member H-1 which is mainly primary and secondary pyroclastic rocks of probable subaerial origin indicates that quiet, shallow water, possibly lucistrine environments occurred during early stages of caldera filling.

The absence of pillows, pillow breccia, and hyaloclastic rocks in flows of formations G and H, also suggest subaerial emplacement.

These structures are not developed in all subaqueous flows, particularly those of more felsic composition, but their total absence in caldera flows may be an environmental indicator.

The nature of clasts in sandstone and conglomerate in the lower member of formation I indicates that detritus was eroded from formation H and, therefore, that the source was subaerial. Deposition of detritus probably occurred in a subaerial alluvial fan environment at the top of the caldera.

In summary, the dominance of felsic to intermediate pyroclastic rocks, the characteristics of secondary pyroclastic rocks of fluvial and laharic origins, and the local derivation of formation H and formation I epiclastic rocks suggest that volcanism was largely subaerial. The origin and extent of the upper member of formation I, and the occurrence of chert and argillite in formation H suggest that pyroclastic rocks were emplaced locally in shallow lakes that formed in the caldera during periods of volcanic quiescence.

ALTERATION AND METAMORPHISM

During the Early Precambrian, formation H and adjacent units were regionally metamorphosed under low to middle greenschist conditions (as defined by Winkler, 1967). Detailed analysis of this metamorphism is beyond the scope of this thesis. The following discussion summarises textural and mineralogical characteristics related to the two main types of volcanic alteration, and associated metamorphism: restricted buff alteration, and pervasive recrystallization.

Discordant to concordant buff alteration zones (assemblage 3, Table 5) are present near the top of the proximal vent facies of member H-1 and the northern proximal vent facies in member H-4. These zones are characterized by a lighter colour, higher muscovite content and stronger recrystallization. The alteration in member H-1 has affected mainly the upper tuff unit but the thickness of the alteration zone is not known because of poor outcrop. The alteration in member H-4 is up to 400 m thick and has affected all rock types in this member and possibly the lower conglomerate of formation I. Smaller, more discrete alteration zones occur in flows, and along the margins of metamorphosed quartz veins and fault controlled quartz-actinolite veins (Adams, 1976). All buff alteration zones, except the discrete zones in flows, have a close spatial relationship to metamorphosed Cu, Zn, Pb, Ag, and Au mineralization.

Mineralogically and texturally, the remainder of formation H differs from other felsic to intermediate units of similar metamorphic grade in the Favourable Lake metavolcanic-metasedimentary belt (Ayres, in preparation) and from greenschist facies, felsic to intermediate metavolcanic rocks at Lake of the Woods, northwestern Ontario. The most important differences characterising formation H are:

1) Primary textures are less well preserved in tuff and in some flows because of pervasive recrystallization to fine-grained, quartz-feldspar aggregates. This may in part reflect a high primary glass content, but the differences in groundmass textures of flows cannot be due simply to differences in glass content.
2) Very fine-grained biotite is more abundant whereas actinolite is generally absent.
3) Pervasive muscovite-rich buff alteration zones, which are characterized by stronger distruction of primary textures, occur in proximal vent facies sequences.
4) Prograde garnet occurs in the muscovite-rich rocks in the buff alteration zones.
5) Epidote, which should be a common phase at this metamorphic grade because of the breakdown of plagioclase, is relatively rare.
6) Pyrite and pyrrhotite are widespread.

These differences must reflect variations in one or more of, 1) the nature of the primary rock units, as for example glass content, 2) synvolcanic alteration, or 3) conditions of regional metamorphism.

The differences cannot be due to regional metamorphism because pressure and temperature conditions must have been essentially the same in formation H as in adjacent units. Furthermore a high primary glass content, although possibly responsible for less well preserved primary textures in tuff, cannot explain the destruction of primary textures in flows and large fragments, nor the widespread occurrence and habit of biotite. It is thus concluded that the differences probably reflect a pervasive, pre-metamorphism alteration

that was restricted to formation H, although the present mineralogy is the result of later regional metamorphism. The alteration was apparently caused by a fluid phase that had unrestricted access and mobility in formation H. This is most likely during or shortly after deposition, when porosity was high and the formation still contained some primary heat and gases which were emitted both from degassing of units and from the subjacent magma chamber.

It is thus proposed that the alteration was related to cooling and to fumarolic and hot spring activity at the surface of the unit. The pervasive biotite-rich alteration represents subsurface reactions that were facilitated by the high primary glass content. The buff alteration zones which occur close to proposed source vents, where degassing would be most intense, represent surface fumarolic or hot-spring activity. Extension of the buff alteration zone, in the north proximal vent facies of member H-4, into the basal conglomerate of formation I suggests rapid erosion of formation H and sedimentation contemporaneous with hot-spring or fumarolic activity. The extensive chert and ferruginous chert in the upper member of formation I probably reflects continued hot-spring activity.

CHEMISTRY

INTRODUCTION

Major and trace element chemical analyses (Table 11) were made on 26 samples (Fig. 5) as follows:

1) 3 samples from mafic to intermediate flows and 1 sample from a mafic to intermediate primary lapillistone unit, in formation G.

2) 11 samples from felsic to intermediate flows in members H - 2 and H - 4. Duplicate samples were collected from two flows (18 and 19; 476 and 478).

3) 9 samples from felsic to intermediate pyroclastic and epiclastic units in all members of formation H, and

4) 2 samples from the quartz diorite intrusion.

Samples 308 and H 3/22 are from widespread buff alteration zones and samples 19, 394 and 423 from smaller but similar zones in felsic flows.

Barth norms were calculated volatile-free after removing H_2O (total), CO_2 and S and recalculating analyses to 100 percent. Fe_2O_3/FeO is high in several samples and Fe_2O_3 was therefore adjusted to compensate for possible oxidation. The upper limit for Fe_2O_3 was determined from the following equation (Irvine and Baragar, 1971):

$$\% Fe_2O_3 = \% TiO_2 + 1.5$$

If the Fe_2O_3 value is less than this, no adjustment was made, but if it is greater the excess was converted to FeO. This adjustment however, may be invalid in alteration studies because oxidation may be part of alteration rather than due to subsequent metamorphism.

Plots of the chemical data on various diagrams (Figs 15, 18, 19, 20, 21, and 22) show considerable scatter which crudely

TABLE 11. Chemical analyses of samples from formations G and H

	FORMATION G				FORMATION H													
					FLOWS									VOLCANICLASTIC ROCKS				
	156	160	199	71	18	19	37	38	261	394	423	426	445	476	478	95	183	224	228	268	285
	MAJOR ELEMENTS (%)																				
SiO_2	58·20	52·30	52·05	53·05	65·20	72·05	64·20	68·20	66·00	66·05	68·90	64·00	72·75	66·50	66·55	59·90	69·05	57·10	65·60	68·65	62·90
Al_2O_3	16·12	15·33	16·13	17·14	15·77	14·93	16·80	13·60	15·44	17·47	19·38	17·46	14·89	15·18	15·61	15·86	13·58	17·93	14·44	16·41	16·12
Fe_2O_3	1·19	1·42	2·92	3·74	1·47	1·39	1·15	0·21	2·59	1·86	1·23	1·06	0·63	1·40	2·07	1·42	1·19	2·18	1·34	1·00	3·02
FeO	4·72	7·32	6·44	8·44	3·32	0·56	4·00	4·80	3·64	2·36	1·96	3·96	1·46	4·36	4·48	5·16	3·40	4·32	4·24	1·80	3·80
MgO	5·10	6·75	6·40	5·55	3·15	1·22	2·27	2·92	1·30	1·03	0·79	1·40	0·54	1·50	1·93	5·80	2·10	4·50	3·55	1·05	2·42
CaO	7·40	11·30	9·42	3·10	3·20	1·80	4·49	3·75	4·55	1·75	1·34	6·17	3·68	1·62	3·01	3·25	2·90	5·60	3·25	4·00	6·07
Na_2O	3·66	2·31	2·19	3·23	3·86	0·60	3·45	2·59	3·46	3·58	0·55	1·78	2·62	5·36	3·52	1·55	3·14	2·23	2·99	2·11	1·54
K_2O	0·95	0·32	1·32	0·10	1·22	3·61	1·50	2·34	1·32	3·08	3·79	1·77	1·06	1·56	1·66	2·92	2·36	3·44	2·68	2·48	1·62
H_2O	1·47	1·35	1·53	3·83	1·62	1·89	1·02	1·06	0·91	1·50	2·77	0·92	1·08	1·14	1·29	2·54	1·31	1·27	1·24	1·41	1·31
CO_2	0·21	0·34	0·23	0·15	0·07	0·24	0·48	0·39	0·07	0·04	0·20	0·04	0·04	0·07	0·01	0·11	0·01	0·16	0·11	0·02	0·12
TiO_2	0·58	0·52	0·88	0·99	0·57	0·48	0·56	0·51	0·53	0·82	0·66	0·78	0·64	0·59	0·61	0·65	0·46	0·61	0·63	0·59	0·69
P_2O_5	0·18	0·14	0·16	0·15	0·15	0·15	0·12	0·15	0·17	0·29	0·17	0·24	0·18	0·24	0·20	0·29	0·15	0·18	0·21	0·21	0·16
MnO	0·12	0·17	0·25	0·40	0·07	0·04	0·12	0·15	0·10	0·15	0·07	0·10	0·06	0·17	0·18	0·13	0·08	0·06	0·07	0·05	0·13
S	0·05	0·99	0·625	0·16	0·62	0·97	0·24	0·01	0·11	0·07	0·004	0·053	0·06	0·01	0·03	0·13	0·01	0·15	0·14	0·10	0·169
TOTAL	99·95	100·56	100·55	100·03	100·29	99·93	100·43	100·70	100·19	100·05	99·81	99·73	99·71	99·70	100·15	99·71	99·74	99·73	100·49	99·98	100·07
	TRACE ELEMENTS (ppm)																				
Sr	100	70	70	170	190	60	400	300	90	80	50	130	150	90	140	80	90	60	60	50	120
Rb	23	10	100	—	34	116	40	60	77	66	92	56	29	46	55	76	65	199	101	101	57
V	193	152	91	260	113	123	50	60	80	124	68	86	88	72	82	105	62	89	110	110	80
Ni	100	113	162	138	116	38	50	50	29	<10	10	20	27	42	15	54	36	45	51	21	38
Cu	80	115	163	55	13	20	50	40	38	12	10	24	23	15	24	49	40	42	38	26	90
Co	45	57	50	41	33	10	20	10	14	<10	11	12	—	17	11	25	17	22	20	<10	14
Zn	99	104	112	239	102	62	90	180	55	95	19	46	26	40	55	230	146	90	205	31	63
Pb	<10	<10	tr	<10	<10	<10	50	30	<10	20	—	—	—	—	—	25	<10	<10	25	<10	tr
	CALCITE-FREE BARTH NORMS (%)																				
Quartz	8·90	3·54	3·67	12·45	23·79	48·89	22·14	27·08	25·93	26·76	44·20	28·69	43·03	20·24	26·11	20·74	29·34	9·74	22·34	34·95	28·39
Corundum	—	—	—	7·42	2·95	8·29	1·60	0·39	0·51	6·45	14·33	2·24	3·60	2·56	2·91	5·61	1·06	0·88	1·35	3·74	1·35
Orthoclase	5·69	1·94	8·01	0·62	7·39	22·78	9·00	14·17	8·03	18·68	23·84	10·87	6·52	9·38	10·14	17·98	14·40	20·81	16·16	15·21	10·02
Albite	33·29	21·27	20·18	30·60	35·48	5·74	31·50	23·82	31·94	32·96	5·25	16·60	24·45	48·91	32·64	14·49	29·08	20·48	27·37	19·64	14·45
Anorthite	25·08	31·30	31·08	15·20	15·25	8·48	21·40	18·06	22·07	6·96	5·89	30·16	17·76	6·57	14·07	14·82	13·83	27·21	15·04	19·67	30·39
Calcic pyroxene	8·74	20·20	12·64	—	—	—	—	—	—	—	—	—	—	—	—	—	—	—	—	—	—
—Diopside	6·17	13·19	8·62	—	—	—	—	—	—	—	—	—	—	—	—	—	—	—	—	—	—
—Hedenbergite	2·57	7·01	4·02	—	—	—	—	—	—	—	—	—	—	—	—	—	—	—	—	—	—
Hypersthene	15·85	19·16	20·27	29·18	12·43	3·59	10·60	15·20	8·23	4·41	3·77	8·65	2·65	9·52	10·59	23·23	10·03	17·37	14·95	4·41	11·94
—Enstatite	11·18	12·51	13·82	16·17	8·90	3·59	6·60	8·26	3·69	2·92	2·32	4·01	1·55	4·21	5·50	16·67	5·96	12·70	9·99	3·01	6·98
—Ferrosilite	4·67	6·65	6·45	13·01	3·53	—	4·00	6·94	4·54	1·49	1·45	4·64	1·10	5·31	5·09	6·56	4·05	4·67	4·96	1·40	4·96
Magnetite	1·26	1·52	2·55	2·75	1·57	0·42	1·60	0·23	2·18	1·99	1·37	1·15	0·69	1·49	2·24	1·55	1·28	2·26	1·43	1·08	2·39
Ilmenite	0·81	0·74	1·26	1·46	0·81	0·71	0·80	0·73	0·75	1·17	0·98	1·13	0·93	0·84	0·88	0·94	0·66	0·87	0·89	0·85	1·00
Hematite	—	—	—	—	—	0·75	—	—	—	—	—	—	—	—	—	—	—	—	—	—	—
Apatite	0·38	0·30	0·34	0·33	0·32	0·34	0·22	0·32	0·37	0·62	0·38	0·52	0·39	0·51	0·43	0·63	0·32	0·38	0·45	0·46	0·35

TABLE 11 (continued)

	FORMATION H				
	VOLCANICLASTIC ROCKS			QUARTZ DIORITE	
	308	382	H3/22	84	398
	MAJOR ELEMENTS (%)				
SiO_2	69·50	65·90	56·25	65·70	65·55
Al_2O_3	15·18	15·60	16·42	15·61	16·02
Fe_2O_3	1·92	1·90	3·07	0·91	1·81
FeO	1·44	3·60	7·12	3·32	2·32
MgO	1·83	2·99	6·00	2·63	1·93
CaO	1·46	2·15	3·50	1·66	2·25
Na_2O	0·34	5·52	1·44	5·62	5·58
K_2O	3·49	0·54	3·22	1·34	1·56
H_2O	2·31	0·73	1·81	1·94	1·24
CO_2	0·51	0·06	0·07	0·09	0·23
TiO_2	0·60	0·72	0·74	0·59	0·58
P_2O_5	0·23	0·17	0·22	0·18	0·16
MnO	0·62	0·22	0·17	0·10	0·12
S	0·814	0·010	0·04	0·005	0·027
TOTAL	100·24	100·13	100·07	99·70	99·38
	TRACE ELEMENTS (ppm)				
Sr	50	60	50	80	250
Rb	113	25	94	30	32
V	87	89	140	90	70
Ni	27	53	60	20	31
Cu	44	24	25	33	59
Co	18	23	31	15	22
Zn	146	249	107	85	87
Pb	tr	tr	—	—	—
	CALCITE-FREE BARTH NORMS (%)				
Quartz	48·09	19·68	13·80	17·68	17·79
Corundum	10·23	2·66	5·54	2·58	1·60
Orthoclase	22·15	3·20	19·71	8·03	9·35
Albite	3·27	49·66	13·38	51·13	50·79
Anorthite	6·16	9·57	16·48	7·15	10·26
Calcic pyroxene	—	—	—	—	—
—Diopside	—	—	—	—	—
—Hedenbergite	—	—	—	—	—
Hypersthene	6·52	11·87	27·33	11·25	7·14
—Enstatite	5·42	8·27	17·14	7·36	5·40
—Ferrosilite	1·10	3·60	10·19	3·89	1·74
Magnetite	2·15	1·99	2·44	0·96	1·92
Ilmenite	0·90	1·00	1·07	0·83	0·82
Hematite	—	—	—	—	—
Apatite	0·52	0·36	0·48	0·38	0·34

Notes

1. FORMATION G. Flows, proximal vent facies: 158, 160, 199
   Primary lapillistone, distal vent facies: 71

2. FORMATION H. Flows, proximal vent facies
   member H-2: 394
   member H-4: northern facies 18, 19, 37, 38, 476, 478
   southern facies 261, 423, 426, 445

   Volcaniclastic rocks,
   Primary tuff — proximal vent facies
   member H-1: H3/22
   member H-4: 268
   — distal vent facies
   member H-1: 95
   member H-3: 228
   Fluvial tuff — distal to proximal vent facies
   member H-4: 285
   — distal vent facies
   member H-3: 224
   Fine primary lapilli-tuff — distal vent facies
   member H-2: 183
   Primary breccia fragment — proximal vent facies
   member H-4: 308
   Volcanic lithorenite — proximal to distal vent facies
   member H-2: 382

   Quartz diorite, northern pluton: 398
   southern pluton: 84

4. FORMATION H BUFF ALTERATION ZONES
   Flows: 19, 394, 423
   Breccia: 308
   Tuff: H3/22

5. Sample locations are plotted in Figure 5.

6. Modal analyses in Table 4.

7. Data for all samples, except 37 and 38, from this study.

. Data for samples 37 and 38 from Ayres (in preparation.)

indicates that formation H has undergone widespread alteration, as anticipated from mineralogical and textural studies. If unaltered, the plots should show relatively small scatter because formations G and H appear to be erupted from the same, or closely related magma reservoirs. The purposes of the chemical study were to establish, 1) the broad stratigraphic extent of alteration, 2) the relationship, if any, between lithology and alteration, 3) the major chemical changes to facilitate classification, and 4) a basis for future detailed study.

Metasomatism of Precambrian rocks metamorphosed under greenschist facies conditions can commonly be detected by high H_2O (total), CO_2 and S contents (Wilson et al., 1965). However, except for high S in some samples, volatile contents are relatively low and not indicative of metasomatism (Table 11). Ideally metasomatism should be studied by comparing altered samples with unaltered equivalents from similar lithologic units in the same area. This procedure could not be followed because of insufficient samples and because the alteration appears to have affected all parts of formation H. Consequently, calc-alkaline control suites were selected from both unmetamorphosed Cenozoic sequences and metamorphosed but apparently unaltered Early Precambrian sequences (see Figs. 15 and 17). Calc-alkaline suites were chosen because, after broad adjustments are made for chemical changes, the study samples appear to be calc-alkaline (Fig. 22). Prior to adjustment, the samples show a wide dispersion and straddle the tholeiite-calc-alkaline field boundary on the Al_2O_3 - normative plagioclase plot (Fig. 22) and on other diagrams used for classifying subalkaline rocks (e.g. Miyashiro, 1974; diagram not shown). Both Early Precambrian and Cenozoic suites were used because of possible primary chemical differences between Early

Precambrian and Cenozoic calc-alkaline volcanism (Baragar and Goodwin, 1969; Hart et al. 1970; Glikson, 1971; Jolly, 1975). Major differences proposed by Baragar and Goodwin (1969) are lower Al_2O_3, Fe_2O_3, Na_2O and K_2O, and higher FeO, MgO and volatiles in Early Precambrian rocks compared to Cenozoic equivalents.

Metasomatic changes involving depletion in CaO and Na_2O, and both enrichment and depletion, K_2O were the easiest to detect (Figs. 15 and 18; Table 12). Changes in other oxides were not as readily detected by graphical techniques, but their apparent behaviour can be summarized as follows:

1) SiO_2 appears unchanged in most samples but enrichment is inferred in several samples,
2) MgO and FeO appear to be depleted in some samples,
3) Al_2O_3 appears unchanged in most samples,
4) TiO_2 and P_2O_5 appear unchanged, and
5) MnO appears unchanged except in sample 308 which is from a buff alteration zone.

METASOMATISM

Lime and Alkalies

Changes in lime and alkalies can be broadly determined on a K_2O+Na_2O - Al_2O_3 - CaO ternary diagram (Fig. 15) in which formation H samples show a wide scatter and are mainly outside of the restricted field of unaltered Cenozoic and Early Precambrian calc-alkaline rocks. Most formation H samples plot above the unaltered field toward the Al_2O_3 corner. This could reflect addition of Al_2O_3 but except for a few samples, such as, 423 which contains 19.38 percent Al_2O_3 (Table 11), the raw chemical data do not support the major additions of Al_2O_3

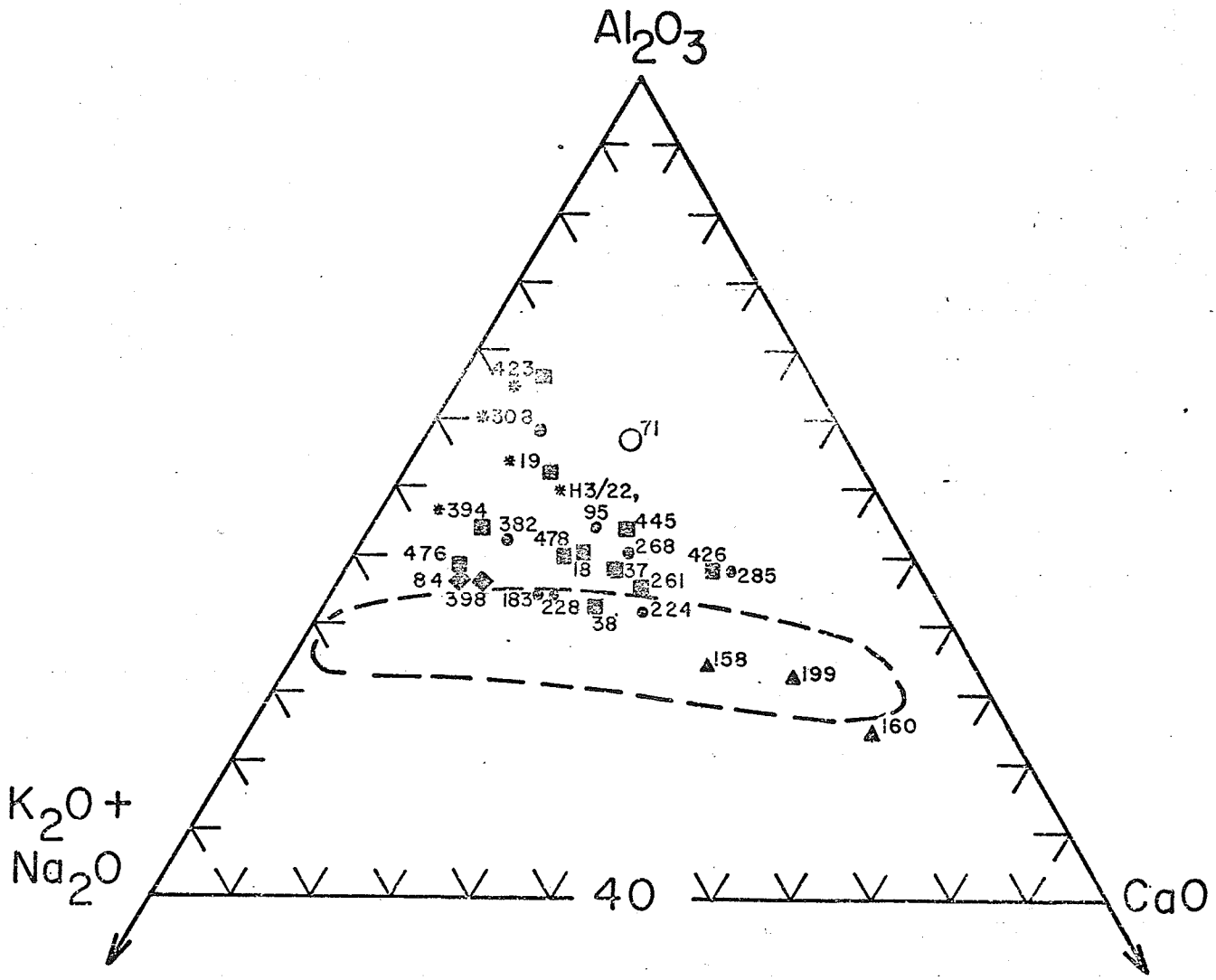

Fig. 15. Caption on next page.

Fig. 15. Portion of the $K_2O + Na_2O$ — Al_2O_3 — CaO ternary diagram showing the wide scatter of the study samples above the unaltered field.

Triangles - formation G mafic to intermediate flows; open circle - formation G mafic to intermediate primary lapillistone; squares - formation H felsic to intermediate flows; dots - formation H felsic to intermediate volcaniclastic rocks; diamonds - quartz diorite intrusive rocks; asterisks beside samples denote buff alteration.

The unaltered field enclosed by the dashed line was determined by plotting about 85 apparently unaltered but metamorphosed, Early Precambrian calc-alkaline samples (Andrews, 1964; Goodwin, 1967; Baragar and Goodwin, 1969; Jolly, 1975; Morrice, unpublished) and about 85 unaltered, unmetamorphosed, Cenozoic calc-alkaline samples from a wide range of island arc environments (Kuno, 1959; Fiske et al 1963; Ewart and Stipp, 1968; Jakes and White, 1969, 1972; Seigers et al., 1969; Taylor 1969, Gill, 1970: Rubel, 1971; Pichler and Zeil, 1972; Condie and Swenson, 1973; Higgins, 1973; Colley and Warden 1974; Keller, 1974; Lopez-Escobar, in press; Miyashiro, 1974). The unaltered field includes samples with silica content between 50 and 76 percent. The trend of the field defines the behaviour of the three parametres with increasing SiO_2, with low SiO_2 samples at the right end of the field and high SiO_2 samples at the left end.

necessary to produce the observed data points. Furthermore simple addition of Al_2O_3 would not cause such a wide scatter in the data. Thus this plot reflects mainly depletion of CaO and alkalies, although slight additions of Al_2O_3 may have taken place.

Four formation H samples plot in, but close to the upper boundary of the unaltered field (Fig. 15). Three of these (38, 183 and 228) have the lowest Al_2O_3 contents of formation H samples (Table 11) and this partly controls their position in the field. Although it is difficult to determine whether the Al_2O_3 content of these samples is primary or depleted, the position of these samples near the upper boundary of the field in conjunction with low Al_2O_3 indicates that CaO and/or alkalies are depleted. If CaO and alkalies had not been depleted then the samples should plot in the lower part of the unaltered field because of their low Al_2O_3 content.

Two samples (158 and 199) from mafic to intermediate flows in formation G also plot in the unaltered field (Fig. 15) and lack obvious changes in the three parameters. One flow sample (160) plots slightly outside the field due to possible CaO enrichment. The mafic to intermediate pyroclastic sample (71) plots above the field as a result of depletion in CaO and alkalies.

The semi-quantitative effect of changes in lime and alkalies can be illustrated by reference to Figure 16. In this figure an unaltered calc-alkaline dacite from Bougainville, Solomon Islands (Taylor, 1969), which has a similar SiO_2 content (65.1 percent SiO_2) to some of the formation H samples, has been subjected to various changes. Line 1 shows the shift in composition of the sample as total alkalies are depleted and Al_2O_3 and CaO remain constant. Line 2 shows the effect of decreasing CaO when the other components remain constant. Lines

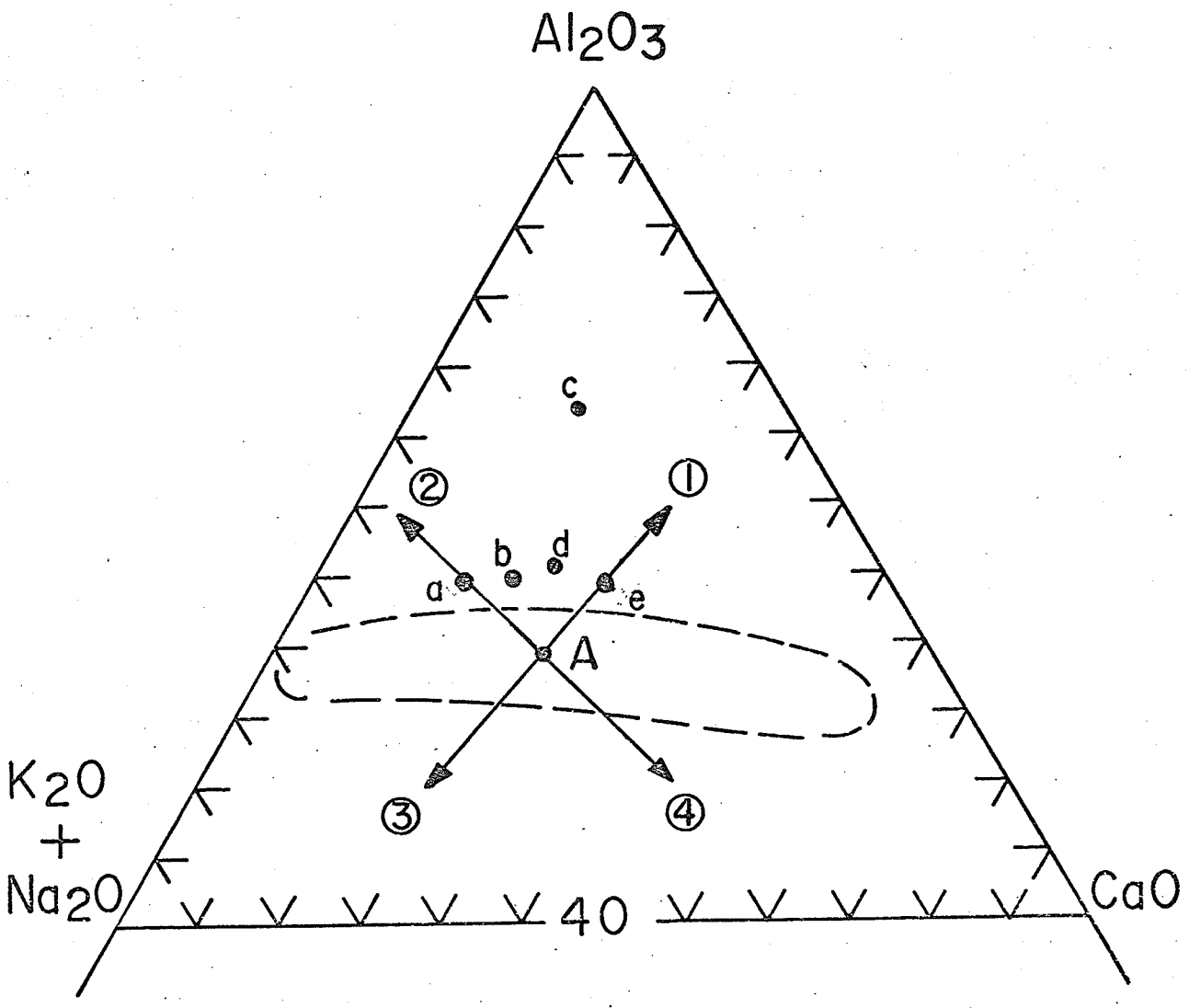

Fig. 16. Caption on next page.

Fig. 16. Portion of the $K_2O + Na_2O$ — Al_2O_3 — CaO ternary diagram showing the effects of changing total alkalies and CaO when Al_2O_3 remains constant. An unaltered calc-alkaline dacite (A), with 65.1 percent SiO_2, from Bougainville, Solomon Islands (Taylor, 1969) is used to illustrate the changes. The solid arrows indicate the directions in which the dacite composition would shift if: total alkalies were depleted — line 1; lime was depleted — line 2; total alkalies were enriched — line 3; or lime was enriched — line 4. Points a, b, c, d, and e illustrate the effect of specific total alkalies and lime depletions of 'A' and correspond to the field occupied by formations G and H samples in Figure 15. The changes made for these points are:

	CaO	Al_2O_3	K_2O+Na_2O	% Variation CaO	% Variation K_2O+Na_2O
A	5	16	7	—	—
a	2	16	7	-60	—
b	3	16	5.6	-40	-20
c	2	16	2.8	-60	-60
d	3.5	16	4.9	-30	-30
e	5	16	4.2	—	-40

3 and 4 show respectively the effects of increasing alkalies and increasing lime with the other components remaining constant. Lines 1 and 2 are the most pertinent to this study because most of the formation G and H samples plot between these lines above the unaltered field (Fig. 15) as a result of depletion of both CaO and alkalies with Al_2O_3 remaining constant. The changes are shown semi-quantitatively in Table 12.

The behaviour of the individual alkali oxides can be examined on the alkali igneous spectrum diagram (Figs. 17 and 18) of Hughes (1972). Hughes studied unaltered Phanerozoic igneous rocks, and found that rock suites defined trends with positive slopes on a K_2O+Na_2O versus (K_2O/K_2O+Na_2O) x 100 plot. These trends were confined to a portion of the diagram which he termed the igneous spectrum, and within which all unaltered rocks should plot. Stauffer et al (1975) proposed a modification in the lower boundary curve (Fig. 17) to include island-arc tholeiitic rocks previously omitted by Hughes, and this modified boundary is used in the present study. According to Hughes (1972), in samples that plot outside the igneous spectrum primary, K_2O and Na_2O contents have been modified. Hughes also observed that most spilites plot on the Na_2O side of the igneous spectrum (Fig. 17) and have accordingly undergone Na_2O metasomatism.

Examination by the author, of 94 Early Precambrian, intermediate, calc-alkaline metavolcanic rocks with low volatile contents, showed a very wide scatter (Fig. 17). Most samples plotted either in the ingeous spectrum or in the Na_2O field; many of the samples on the Na_2O side of the boundary were in the spilite field. The meaning of this distribution is not certain. It may reflect K_2O depletion or Na_2O addition, or both, of Early Precambrian samples which was not indicated

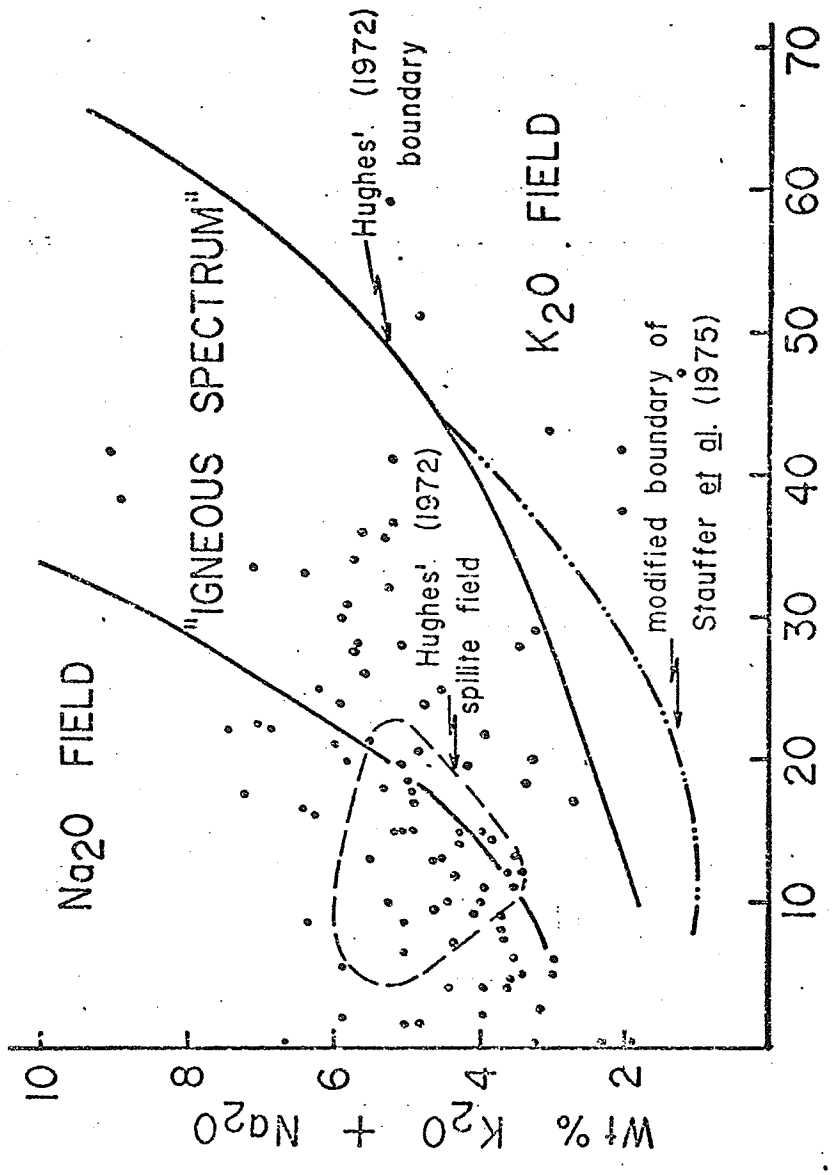

Fig. 17. Caption on next page.

Fig. 17. The alkali igneous spectrum diagram of Hughes (1972) with the revised lower boundary proposed by Stauffer et al (1975) to include island-arc tholeiitic rocks. In this diagram samples with strongly modified alkali contents would plot outside the igneous spectrum. The spilite field as defined by Hughes (1972) is shown also and generally falls outside of the igneous spectrum. For comparison 94 metamorphosed but apparently unaltered Early Precambrian calc-alkaline volcanic rocks are plotted (Andrews, 1964; Goodwin, 1967; Baragar and Goodwin 1969; Jolly 1975; Morrice unpublished). Many of the samples plot above Hughes' upper boundary and this may indicate either lower primary K_2O contents in the Early Precambrian samples, or more likely, Na_2O metasomatism that was not recognized by other tests.

by their volatile content (as is the case for the caldera samples), or lower primary K_2O contents in Early Precambrian rocks. Metasomatism appears to be the most acceptable alternative because when the samples are plotted by geographic areas (not shown in the diagram), they still have a wide scatter and do not define trends with positive slopes. Each geographic area represents one or more volcanic suites, and by analogy with unaltered suites, each suite should define a definite trend with a positive slope if the low K_2O is a primary feature. This suggests that present tests for alteration of Early Precambrian meta-volcanic rocks are inadequate.

When the study samples are plotted on the igneous spectrum diagram (Fig. 18) the most conspicuous feature is their wide range of K_2O/Na_2O ratios indicating strong alkali metasomatism. The nature of changes in Na_2O and K_2O are shown semi-quantitatively in Table 12.

Most samples plotting in the igneous spectrum (Fig. 18) either have primary K_2O and Na_2O contents, or metasomatic effects have been minor. Two samples (158 and 160) from mafic to intermediate flows in formation G plot close to positions of similar unaltered rocks studied by Hughes (1972) and probably have not been affected by alkali metasomatism (Table 11). Formation H samples, however, are more scattered and this probably indicates subtle, K_2O and Na_2O changes. Although some flows do plot in the strongly metasomatised fields, the predominance of flows over pyroclastic rocks in the igneous spectrum field suggests that flows will give a better approximation of primary Na_2O and K_2O contents than pyroclastic rocks. Most formation H samples within the igneous spectrum are flows (Fig. 18). Four flow samples (18, 37, 261, and 478) plot close to positions of similar unaltered rocks studied by Hughes (1972) and would appear to be unaltered (Fig. 18).

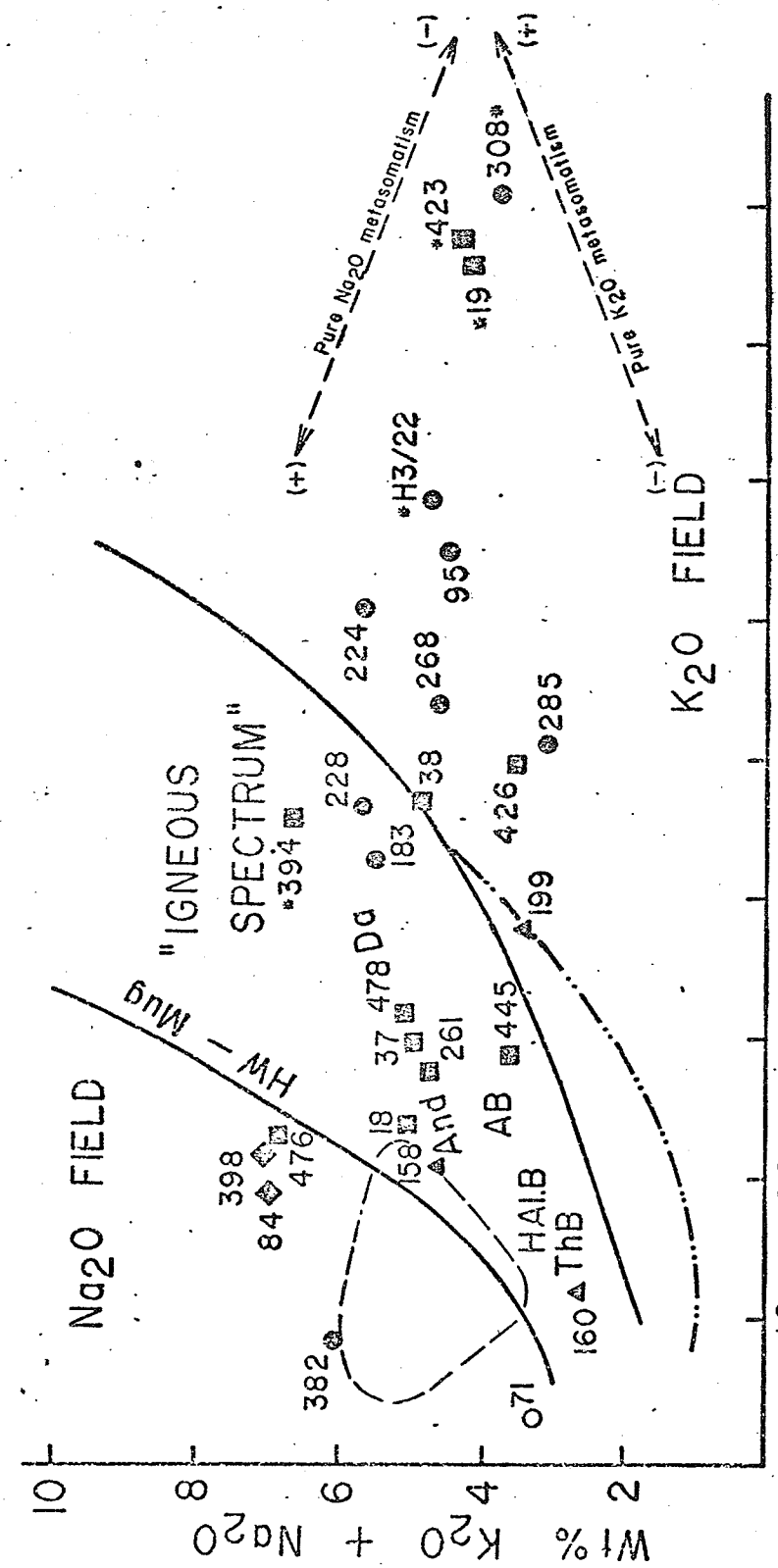

Fig. 18. Caption on next page.

Fig 18. The alkali igneous spectrum diagram of Hughes (1972) showing the wide lateral spread of the study samples indicating alkali metasomatism. Symbols as in Figure 15. Lines for pure Na_2O and K_2O metasomatism are shown and arrows and signs denote directions for addition and depletion.

Unaltered major rock types from Hughes (1972) are ThB - tholeiitic basalt, Hal.B - high-alumina basalt, AB - alkali-olivine basalt, And - andesite, Da - dacite, HW-Mug - hawaiite-mugearite.

However, they plot above the unaltered field in Figure 15 indicating small alkali depletions (Table 11). One sample from a buff alteration zone within a flow (394) probably had a similar primary mineralogy to sample 18, but it plots farther away from the positions of similar unaltered rocks (Hughes, 1972). This is probably the result of K_2O enrichment because the trend of the tie-line parallels the pure K_2O metasomatism trend. Sample 445 plots in the alkali-basalt field but mineragraphic work indicates that it probably originally plotted in the dacite field. This divergence is probably a result of Na_2O and K_2O enrichment because the trend of the tie-line is divergent to those for pure Na_2O and K_2O depletion.

Samples in the Na_2O field (Fig. 18) probably reflects Na_2O enrichment (Table 12). This is best shown by samples 476 and 468 from the same flow. The trend of the line joining these two samples parallels the trend for pure Na_2O metasomatism (Fig. 18). Sample 382 has probably undergone K_2O depletion in addition to Na_2O enrichment because the SiO_2 content is equivalent to that in dacite, and a line joining the sample to the unaltered dacite field has a divergent trend to those for pure Na_2O and K_2O metasomatism.

Samples in the K_2O field (Fig. 18) reflect K_2O enrichment and Na_2O depletion (Table 11). This is illustrated by samples 18 and 19 from the same flow. A line joining these samples defines a trend intermediate between the trends for pure K_2O and pure Na_2O metasomatism. If formation H samples originally plotted close to the unaltered andesite to dacite trend in the igneous spectrum (Hughes 1972; Fig. 18) as mineralogical observations suggest, then shifting of the samples to their present positions would define a trend slightly closer to that for pure Na_2O metasomatism. This suggests that Na_2O depletion

was slightly more dominant than K_2O enrichment.

Four of the five samples from the strongly recrystallized buff alteration zones (19, 308, 423, and H3/22) plot fartherest away from the igneous spectrum boundary in the K_2O field. This suggests that the intensity of recrystallization is directly proportional to Na_2O depletion and K_2O enrichment.

One mafic to intermediate flow sample (199) from formation G which is chemically similar, except for higher K_2O content, to sample 160 in the igneous spectrum, plots outside the igneous spectrum (Fig. 18). This is probably a result of stronger K_2O enrichment than Na_2O depletion because the trend of the tie-line parallels the pure K_2O metasomatism trend.

Table 12 shows semi-quantitatively the effects of lime and alkali metasomatism by reference to figures 15, 16 and 18. CaO and Na_2O+K_2O changes are determined by establishing for each sample the approximate starting point within the unaltered field in Figure 15 on the basis of SiO_2 content and using A in Figure 16 as a control. The majority of samples (for example, 476, 478, and 268) would probably replot close to A in the unaltered field (Fig. 16) because of similar SiO_2 contents. Thus, the changes in the study samples can be determined by comparing directly their position outside the unaltered field in Figure 15 with the changes in A in Figure 16. A few samples (for example 71) would replot away from A, but the changes can be approximated by transposing alteration trends from A to the point. Na_2O and K_2O changes are determined from Figure 18. Although Al_2O_3 contents may have changed in some samples, they are not shown in Table 12 because they are difficult to quantify. Such changes are probably small.

TABLE 12. The nature of CaO, $K_2O + Na_2O$, and K_2O changes and their relation to normative corundum content and normative plagioclase and their composition.

SAMPLE NO.	CHANGES IN				NORMATIVE CORUNDUM	NORMATIVE PLAGIOCLASE/CHANGE IN COMPOSITION	
	CaO	K_2O+Na_2O	Na_2O	K_2O			
			FORMATION G				
			(i) Pyroclastic rocks				
71	--	+,o	+,o	o	7.4	-	33.2
			(ii) Flows				
158	o	o	o	o	o	o	43.0
160	o,+	o	o	o	o	o,+	59.5
199	o	+	o,-	+	o	o,+	60.6
			FORMATION H				
			(i) Pyroclastic rocks				
95	-	-	-	o,+	5.6	+	50.5
183	o	o	-,o	+,o	1.1	o	30.2
224	o,-	o,+	-	+	0.9	+	57.2
228	o,-	o,+	o	o,+	1.4	-	35.5
263	o,-	-	-	o,+	3.7	+	50.0
285	o	--	--	o	1.3	+	67.8
*308	--	-	--	+	10.2	+	65.2
382	--	o	+	-	2.7	-	16.2
*H3/22	--	-	--	+	5.3	+	55.2
			(ii) Flows				
18	-	-	-	-	2.9	o	30.1
*19	--	-	--	+	8.2	+	59.6
37	o	-	-	-	1.8	+	40.6
38	o	-	-	+	0.3	+	43.0
261	o	-	-	-	0.5	+	41.0
*394	--	+	o	+	6.4	-	17.4
*423	--	--	--	+	14.2	+	52.9
426	o	--	--	o	2.2	+	64.5
445	o	--	--	-	3.6	+	42.1
476	--	+	+	o,-	2.6	-	12.0
478	-	-	-	-	2.9	o	30.1
			(ii) Quartz diorite intrusive rocks				
84	--	+	++	o,-	2.5	-	12.3
398	--	+	++	o,-	1.6	-	16.8

Key to Symbols

o = no detectable change

+ = small increase; ++ = large increase * = buff alteration zone

- = small decrease; -- = large decrease

Changes in lime and alkalies can have profound effects on normative mineralogy. Normative corundum is low or absent in unaltered rocks, but is relatively high in samples that are strongly depleted in CaO and/or alkalies. These depletions cause excess Al_2O_3 because not all of the available Al_2O_3 should be incorporated in normative plagioclase and orthoclase; the greater the depletions the higher the normative corundum content. The same depletions can also cause higher normative quartz contents because less SiO_2 is incorporated in normative plagioclase and orthoclase. Lime and alkali depletions also affect the normative plagioclase composition, which becomes more albitic if CaO is depleted and Na_2O enriched and more anorthitic if CaO is enriched and Na_2O depleted. The effect of metasomatism on normative corundum content and normative plagioclase composition is shown in Table 12. The effect on normative quartz is not shown because the effect of SiO_2 metasomatism, as will be discussed below, is difficult to determine.

The behaviour of CaO, Na_2O and K_2O in the major lithofacies of formations G and H can be summarized as follows:

1) Mafic to intermediate flows from formation G show only limited alteration with possible CaO enrichment in sample 160 and K_2O enrichment and possible Na_2O depletion in sample 199.

2) The single sample of mafic to intermediate primary lapillistone in formation G (71) is depleted in CaO and possibly enriched in Na_2O.

3) Felsic flows from formation H have undergone variable metasomatism ranging from weak depletions in CaO and alkalies to strong depletion in CaO and Na_2O, and moderate depletion and enrichment in K_2O.

4) Pyroclastic rocks from formation H have undergone stronger and more widespread changes than flows because of their greater permeability and higher surface area and glass content. As in flows the nature of the changes vary, although most samples show CaO, and Na_2O depletion and both depletion and enrichment of K_2O.

5) Quartz diorite intrusions appear to be strongly depleted in CaO, enriched in Na_2O, and possibly slightly depleted in K_2O.

6) The buff alteration zones are characterized by strong CaO depletion and either strong Na_2O depletion and moderate K_2O depletion or strong K_2O enrichment with no detectable change in Na_2O.

Ferromagnesian Elements and Silica

Determination of MgO, FeO (total) and SiO_2 variations by graphical techniques is difficult because of, 1) their wide primary variation, 2) lack of a suitable constant against which to study these elements, and 3) lack of obviously unaltered samples. In Figures 19 and 20 MgO and FeO are plotted against SiO_2. In both diagrams, the samples show a negative correlation which may be a primary feature because this trend characterizes differentiated, unaltered rock suites, or it may indicate reciprocal changes in ferromagnesian elements and SiO_2.

This correlation may be a primary feature, although the wide scatter of points, particularly in the 65 to 75 percent SiO_2 range indicates metasomatic modification. Four samples (19, 308, 394 and 423) from the buff alteration zones have very low MgO and total FeO contents. Sample 19 is from the same flow as sample 18 and comparison of these samples, suggests that the buff alteration zones represented by these samples are depleted in MgO and FeO and possibly enriched in SiO_2. An exception to this depletion is sample H3/22 which

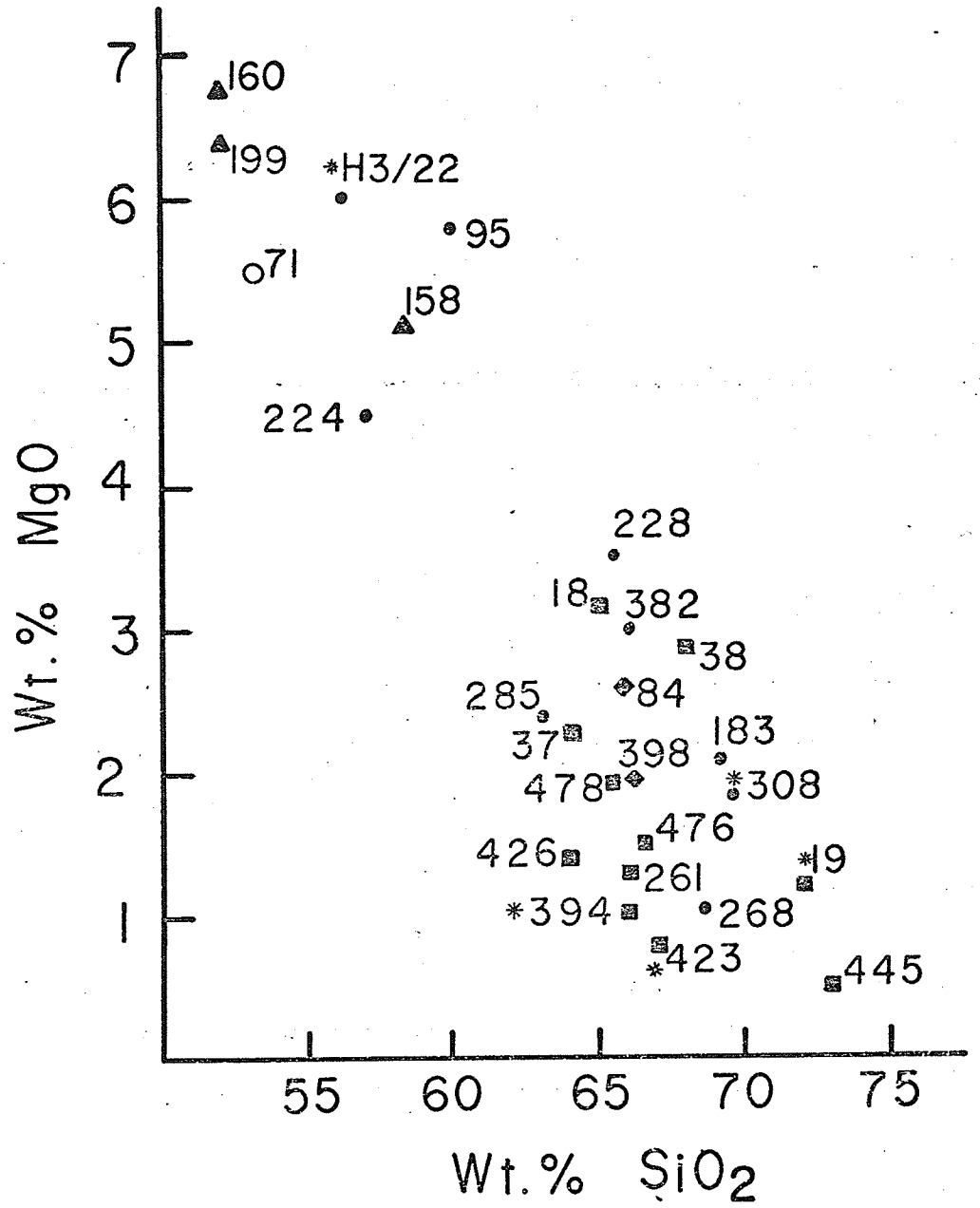

Fig. 19. Silica - magnesia variation diagram showing the wide variation of both silica and magnesia contents. Symbols as in Figure 15.

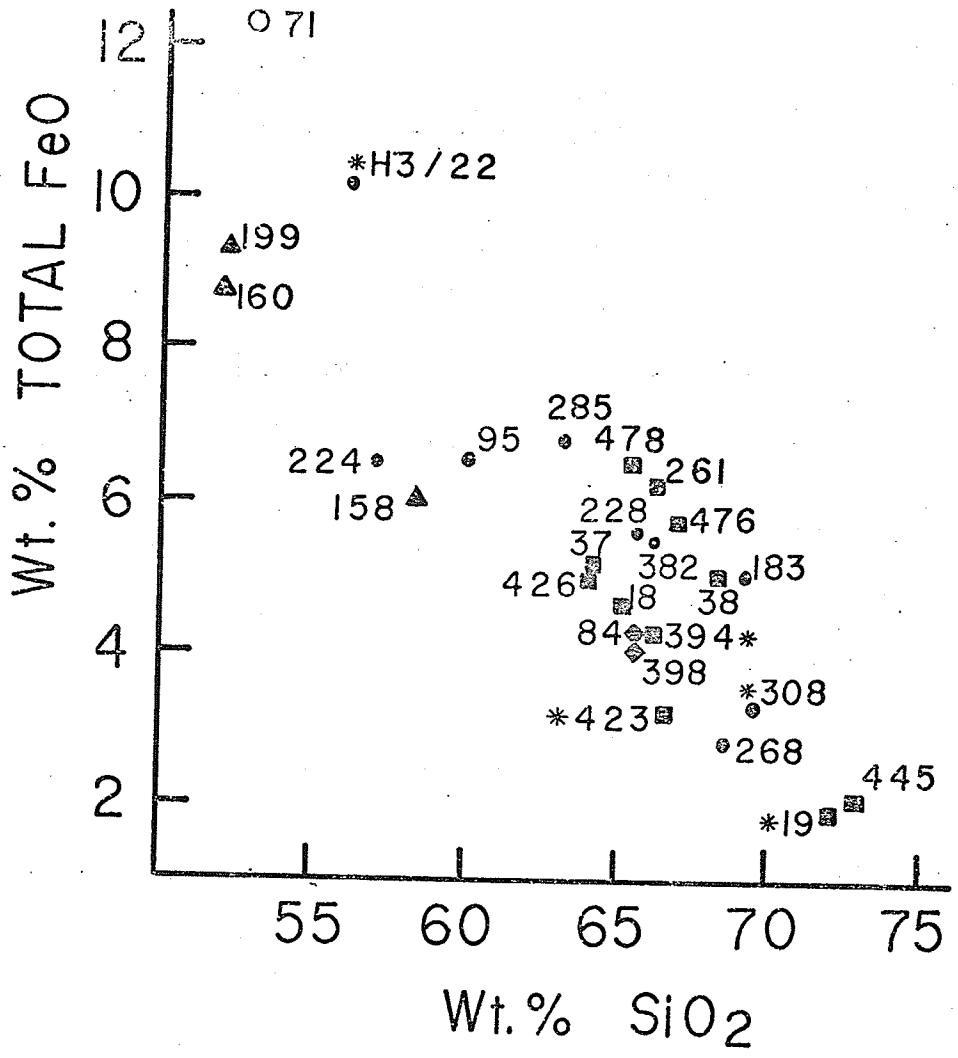

Fig. 20. Silica - total FeO variation diagram showing the wide variation of silica and total iron contents. Symbols as in Figure 15.

appears to have been enriched in MgO and total FeO because these oxides have the same abundance as in mafic to intermediate flows from formation G (Figs. 19 and 20).

Mafic to intermediate flow samples from formation G do not show MgO, total FeO and SiO_2 changes on these diagrams. A sample (71) from a mafic to intermediate pyroclastic unit has a higher total FeO content than flows (Fig. 20) of equivalent SiO_2 content, and the FeO content may have been metasomatically increased.

In summary, it is apparent that determination of metasomatic changes of other elements on SiO_2 variation diagrams is difficult because of the strong possibility that SiO_2 itself was mobile. Although the scattered plot of formation H samples is indicative of metasomatic change it is impossible to determine whether MgO, total FeO or SiO_2 were mobile. Changes can be determined only in the buff alteration zones using samples from the same flow (18 and 19) as the basis for comparison. These zones appear to be depleted in MgO and total FeO and enriched in SiO_2, except sample H3/22 which appears to have enriched MgO and total FeO.

CLASSIFICATION

Classification of metasomatized rocks is difficult unless the chemistry can be readjusted to primary values by comparison with unaltered equivalents. Although this is obviously impossible in the present study, the samples can be broadly classified by determining the effect of chemical changes on classification parameters and by comparing the more strongly altered with the least altered samples. In the alkalies-silica diagram of Irvine and Baragar (1971), all samples plot in the subalkaline field (Fig. 21). The wide scatter and lack of a definite trend is due to metasomatism, but the metasomatism probably merely shifted points within the subalkaline field.

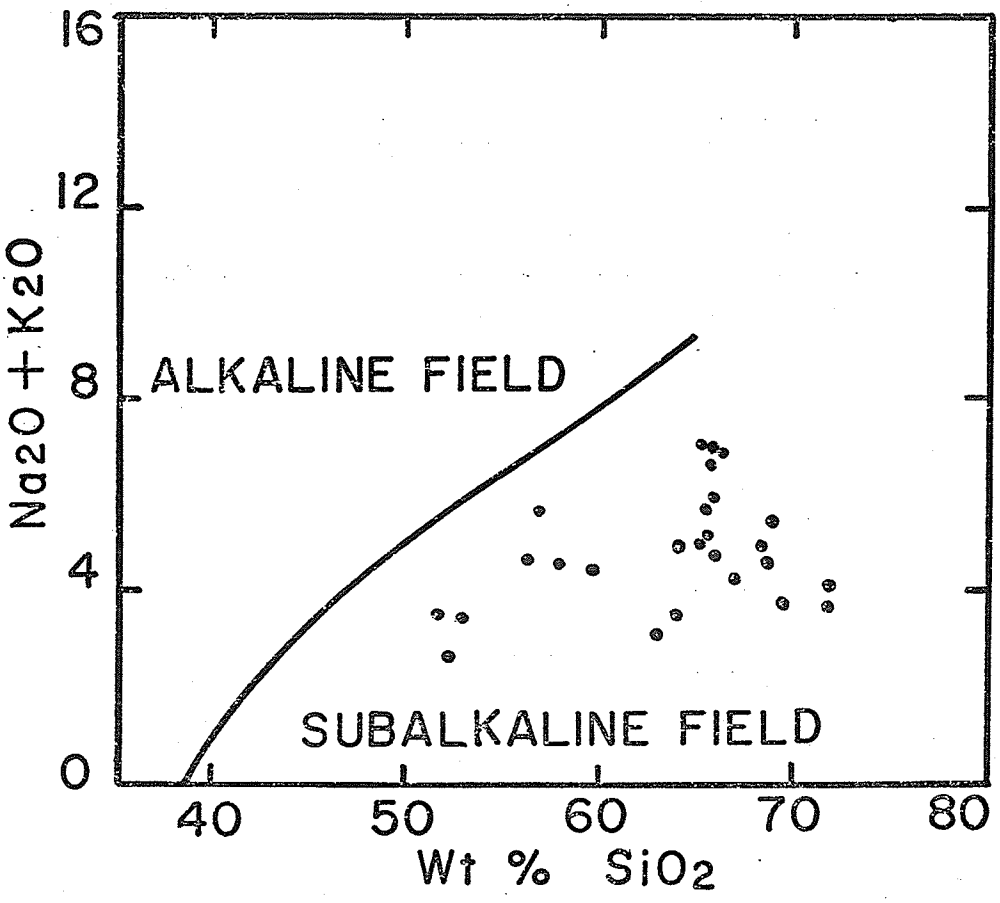

Fig. 21. Alkalies - silica plot showing the distribution of the study samples in the subalkaline field. The dividing line used is that proposed by Irvine and Baragar (1971).

The strong alkali depletion in many samples (Table 12) could not have shifted any samples from the alkaline to the subalkaline field. The maximum observed alkali depletion is about 60 percent and the most strongly depleted samples plot in the lower part of the subalkaline field.

The subalkaline field comprises tholeiitic and calc-alkaline suites. The most significant chemical difference between these two suites is their Al_2O_3 content which is shown by the Al_2O_3 - normative plagioclase diagram (Fig. 22). Even though Early Precambrian calc-alkaline metavolcanic rocks appear to have lower Al_2O_3 contents than their Cenozoic counterparts (Baragar and Goodwin, 1969) they can still be identified on this diagram (Irvine and Baragar, 1971).

Formation H and G samples are widely scattered in Figure 22 and plot in both the tholeiitic and calc-alkaline fields. The variation is mainly in the normative plagioclase parameter and reflects CaO and Na_2O metasomatism which modifies normative plagioclase composition, (Table 12), if Al_2O_3 remains constant. The relative change in normative plagioclase composition due to this metasomatism is illustrated in Figure 22 by arrows attached to the more altered samples. The arrow gives the direction in which samples would shift if normative plagioclase compositions were readjusted to their primary values; the magnitude of shift is not known. No arrow is assigned to samples in which the shift is relatively minor.

In formation H weakly metasomatized samples have normative plagioclase compositions between An_{20} and An_{40}. Most metasomatized samples with higher normative An contents shift to lower values when readjusted, whereas those with lower An contents shift to higher values. Most of the altered samples would probably replot in the An_{20} to An_{40} composition

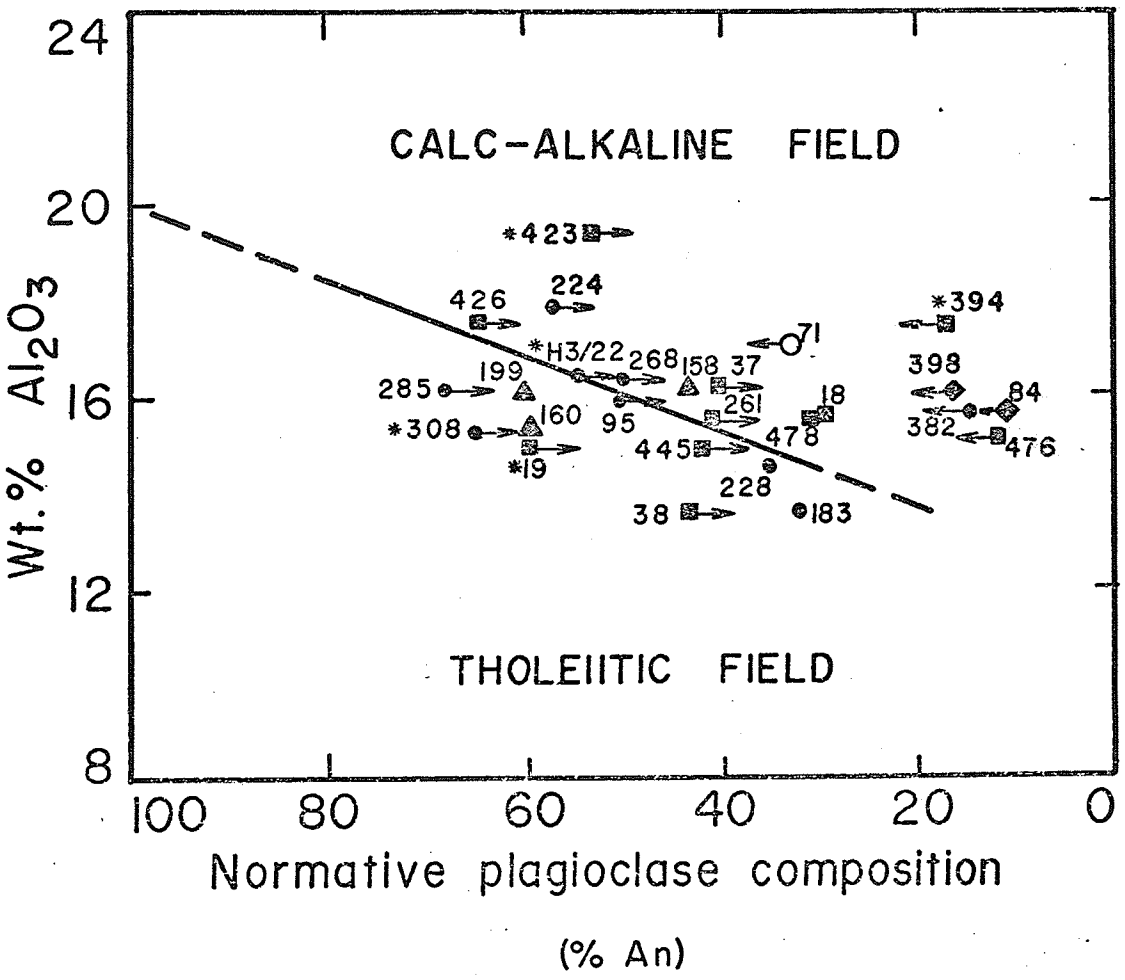

Fig. 22. Alumina - normative plagioclase composition diagram of Irvine and Baragar (1971). Because of metasomatism the study samples are scattered in both the tholeiitic and calc-alkaline fields. The arrows associated with most samples indicate the direction in which the sample point would shift if the normative plagioclase composition could be readjusted to the primary value. The magnitude of the shift is not known (Table 12). Arrows are not given to samples in which the readjustment is relatively minor. Symbols as in Figure 15.

range and would be in the calc-alkaline field. Of the 8 formation H samples in the tholeiitic field, most would shift into the calc-alkaline field. Several samples however, especially 38, 183, and 228, would remain in the tholeiitic field because of low Al_2O_3 contents. Considering the nature of formation H, it is unlikely that both calc-alkaline and tholeiitic suites are present. Those samples that remain in the tholeiitic field after adjustment, probably have been depleted in Al_2O_3; these samples have the lowest Al_2O_3 contents analysed (Table 11).

Samples from mafic to intermediate flows in formation G also plot in both the tholeiitic and calc-alkaline fields (Fig. 22). Sample 158 which plots in the calc-alkaline field lacks detectable CaO and Na_2O changes, and its normative plagioclase composition (An_{43}) would not be changed. Samples 160 and 199 plot in the tholeiitic field but both samples have been altered. Sample 160 is apparently enriched in CaO and 199 depleted in Na_2O. If normative plagioclase compositions (An_{60}) are readjusted to primary values the samples would shift towards the field boundary, but the magnitude of change is probably not great enough for them to shift into the calc-alkaline field. The mafic to intermediate pyroclastic sample (71) which has a decreased normative plagioclase composition, plots in the calc-alkaline field. This sample would probably replot between An_{43} and An_{60} in the calc-alkaline field. Thus formation G appears to comprise both tholeiitic and calc-alkaline suites but this dual nature may be an artifact of alteration. Slight changes in Al_2O_3 or more changes in normative plagioclase composition could result in all samples plotting in the same field.

Without knowing the magnitude of changes in normative plagioclase composition and the degree of MgO and total FeO metasomatism it is difficult to determine rock types. However formation H was probably andesite and dacite and formation G probably basalt and andesite.

PROCESSES OF METASOMATISM

Although water is an important catalytic agent in greenschist metamorphism, pore and adsorbed water probably will transport elements only a few millimeters (Winkler, 1967). Therefore, this grade of metamorphism is probably largely isochemical and the rocks are a closed thermodynamic system. An exception to this rule occurs when intensive shearing accompanies metamorphism (Stauffer et al, 1975). In formation H, metamorphic grade is greenschist facies and foliation is not strongly developed. Yet strong metasomatism has occurred. This anomaly plus mineralogical features mentioned previously and other features summarized below, suggest that metasomatism pre-dated regional greenschist facies metamorphism. These include:

1) the almost ubiquitous occurrence but variable extent of alteration in formation H,
2) the restriction of alteration and strong recrystallization to formation H,
3) the development of the formation in a caldera that would have been a natural locus for vent related hydrothermal activity, such as hot springs and fumaroles,
4) the dominantly clastic nature and high glass content of the formation must have made it susceptible to alteration,
5) the occurrence of buff alteration zones near former volcanic centres suggesting hot spring or fumarolic activity associated with the vents, and

6) the common occurrence of alteration in similar Cenozoic environments.

Two types of metasomatism are recognizable in formation H: restricted buff alteration and more widespread, less intense alteration. The buff alteration zones occur near proposed volcanic centres at the top of members H-1 and H-4, as local patches within flows, and as selvages adjacent to fault-controlled quartz-actinolite-sulphide veins that may have formed during volcanism. The location and intense metasomatism of these zones suggest that they resulted from localized hydrothermal activity probably related to fumaroles or hot springs. The fault-related alteration may have had a complex history with metasomatism beginning during volcanism and continuing through to regional metamorphism (Adams, 1976).

The more widespread metasomatism affected most of formation H, and required unlimited mobility of the fluid phase. This mobility would have been facilitated by the dominantly clastic nature of the formation, and to a lesser extent by faults formed during volcanism, and by flow features such as autobreccia, internal flow foliation, vesicles, and cracking of the glass during cooling. The fluids may have been 1) magmatic, 2) meteoric, or 3) a combination of magmatic and meteoric. Meteoric water probably predominates in such widespread alteration. This proposal is based on experimental studies (Burham, 1967) and recent studies by Craig (1966, 1969) of the Red Sea and Salton Sea geothermal systems which concluded that magmas do not contain large quantities of water and that meteoric water is the dominant fluid phase in geothermal systems. Cold meteoric water was probably heated by hot country rocks and by mixing with ascending magmatic gases which would have caused circulation upwards

through the porous parts of the formation.

The reactive capacity of the fluids depends upon numerous variables, particularly fluid chemistry, rock composition, temperature, pressure, and time. Formation H, primary pyroclastic rocks and flows apparently consisted largely of glass, a phase particularly unstable and susceptible to chemical reaction (Boles and Coombs, 1975). Temperature controls the rate of the reactions and, in conjunction with porosity, the circulation of the fluid phase. Heat may have been derived from: 1) low level magmatic sources such as the quartz diorite intrusions or the underlying magma chamber, 2) retained volcanic heat produced by the concentration and rapid accumulation and burial of volcanic products in this area, and, or 3) retrograde hydration reactions which are exothermic and self-accelerating provided that material can be supplied and removed with the rate of reaction (Zen and Thompson, 1974).

CALDERA ORIGIN

Any model formulated to explain the restricted occurrence of formation H must consider, 1) the overall shape of the confining structure, 2) the nature and origin of lateral boundary structures, 3) the nature and signficance of volcanic products occupying the structure, 4) co-extensive distribution of the northern proximal sedimentary facies of formation I with formation H, and 5) the restriction of pre-greenschist facies alteration to formation H.

The confining structure could be due to three possible processes, some of which could be combined:

1) pre-depositional erosion,
2) post-depositional tectonic disruption, or
3) syn-volcanic collapse of part of a volcano.

EROSION

Formation of the depression by pre-depositional erosion does not appear to be a tenable model for the following reasons:

1) no erosional debris from the underlying basaltic sequence is present near the base or margins of the structure,
2) the structure is bounded by faults, and
3) the model imposes no constraints for restricting felsic tc intermediate volcanism to the depression and such a relationship would be fortuitous.

TECTONIC DISRUPTION

The metasedimentary-metavolcanic sequence has undergone tectonic deformation and the restricted occurrence of formation H may be the result of tectonic faults. The ends of the formation are truncated by faults (Fig. 5), but, the age of the faults is uncertain. Syn-volcanic faults are undoubtedly present in the metavolcanic sequence but they would be difficult to recognise

because of subsequent metamorphism and deformation. Furthermore many synvolcanic faults were probably reactivated during tectonic deformation. Because of this potential reactivation of old faults tectonic fault movement is not a priori evidence that the fault is of tectonic origin.

Study of fault traces bounding the formation is hampered by poor exposure. The folded north end of the formation is truncated by a north to northeast-trending fault (Fig. 5) that has major late tectonic movement probably post-dating folding. However, the fault could have been initiated much earlier.

Fault relationships at the south end of formations G, H and I are complex (Fig. 5). The upper boundary fault bifurcates downwards. The southern branch is well exposed in outcrop as a cataclastic and schistoze zone up to 10m wide, and foliations in adjacent rocks parallel the fault trend. The northern branch is not exposed and its presence is interpreted from abrupt lateral facies changes in adjacent rocks. Regional study by Ayres (in preparation) suggests that these faults are truncated on the lower (east) side by a late north-trending fault that is best developed in granitic batholiths south of Setting Net Lake. This fault apparently terminates immediately north of the upper boundary faults (Fig. 5). In the lower part of the sequence the boundary faults trend northeast and east and are offset about 600m north of the upper boundary faults (Fig. 5). The downward (eastward) extent of the lower boundary faults is not known because of poor outcrop and intrusion by the Setting Net Lake stock. The faults are overlain by the upper part of the sequence and there is no apparent offset in the overlying units.

The apparent truncation of the lower boundary faults by the

upper part of formation H could be explained by two tectonic models: 1) the upper and lower boundary faults were once the same but were offset by the later north-trending fault, or 2) the lower boundary faults and north-trending fault formed an intersecting pair bounding a mafic wedge. Both models appear untenable because there is no evidence for the northward extension of the north-trending fault. Furthermore, the first model requires left lateral movement along the north-trending fault, but work by Ayres (in preparation) indicates that movement further south is dominantly right lateral. Therefore, the offset between the upper and lower boundary faults is probably not a tectonic feature. The lower southern boundary faults are most likely synvolcanic and related to deposition of formation H.

Although the upper southern boundary faults have undergone tectonic movement, truncation of formations H and I entirely by late faults is difficult to explain unless there was considerable lateral tectonic movement in reference to the original horizontal surface.

The tectonic model imposes no constraints for the near-vent character of formation H and the facies distribution within the formation, the restricted depositional environment of formation I, or the pervasive pre-greenschist alteration restricted to formation H.

VOLCANIC COLLAPSE

Because of the shortcomings of the previous models, it is proposed that the structural depression is a cross-section of an overturned caldera or graben formed by volcanic collapse. Calderas formed in this way are quasi-circular depressions greater than 1.5 km in diameter (Macdonald, 1972) and associated with pre-existing vents,

whereas volcanic grabens are linear down-faulted depressions commonly associated with rift zones. The overall shape and dimensions of the cross-section of the structural depression are compatible with those of recent calderas such as Vatukoula, Fiji (Denholm, 1966), Aoba (Warden, 1970) and Ambrym (McCall et al, 1971), New Hebrides, and Krakatoa, Indonesia (Williams, 1941; Williams and McBirney, 1968).

Although the origin of the boundary faults is difficult to determine because of tectonic deformation, available evidence indicates that the lower boundary faults at the south end of formations G and H are synvolcanic. Units in the upper part of formation H extend across the faults without apparent offset. The apparent truncation of formation G and the lower parts of formation H thus reflects deposition within a caldera formed by collapse; the boundary fault was the wall of the caldera. The amount of collapse on this boundary was about 1000 m. The upper boundary faults have undergone tectonic movement, but they probably also represent the original caldera boundary. The offset between the southern upper and lower boundary faults suggests outward enlargement of the caldera as volcanism continued. Thus the total collapse at the south end would be 1600 m. The thinning of formation H northward suggests that the collapse was analogous to the trap door type of caldera (Ridley, 1971) in which collapse is concentrated on one side with the other being hinged.

Formation H is a vent facies with source vents located within the structure as in numerous recent calderas. Thus, this model explains the restricted nature of the felsic to intermediate volcanism. Following termination of the volcanism, the caldera was apparently still a negative area and this controlled the distribution of formation I.

The cross-section through the caldera provides an opportunity to study the nature and significance of infilling products and history of volcanism (Fig. 23).

Stage 1. Early subaqueous to subaerial shield-building mafic volcanism (formation E).

Stage 2. Following termination of mafic volcanism there was a hiatus during which formation F was deposited. Volcanism resumed to the north with the construction of a major pyroclastic cone (northern part of formation G).

Stage 3. Collapse at the summit or on the flanks of the shield volcano; restricted volcanism within the caldera. During collapse the nature of the volcanism changed, producing effusive to explosive mafic to intermediate products (southern part of formation G) followed by dominantly explosive felsic to intermediate products (formation H) which infilled most of the caldera. Collapse occurred in a series of stages that more or less kept pace with infilling.

Stage 4. Cessation of felsic to intermediate volcanism and collapse, followed by fumarolic activity and rapid erosion of the upper part of formation H. Detritus was deposited in an alluvial fan and shallow-water environment confined by the top of the caldera.

Stage 5. Quiescent interval during which chert, tuff, and argillite were deposited in a lake confined by the caldera.

Similar caldera collapse on shield volcanoes with subsequent volcanism restricted to the caldera have been reported from calderas in the Hawaiian Islands (Williams and McBirney, 1968), Masaya caldera, Nicaragua (Williams and McBirney, 1968), Ambrym (McCall et al 1971) and Aoba (Warden, 1970) calderas, New Hebrides. In many recent

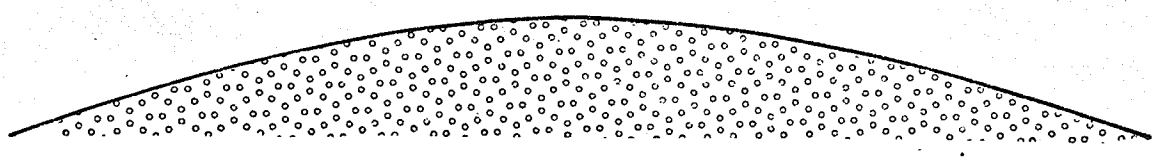

STAGE I. Subaqueous to subaerial mafic shield volcanism

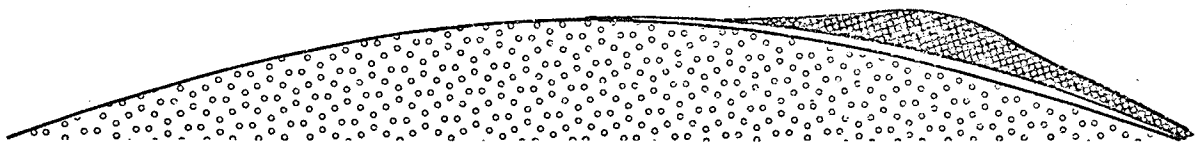

STAGE 2 Cessation of mafic shield volcanism followed by local sedimentation and cone-building intermediate volcanism

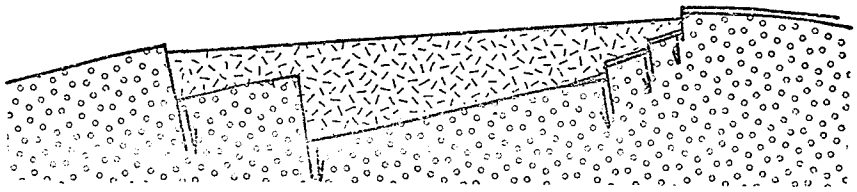

STAGE 3 Collapse of the shield volcano and infilling of the caldera by explosive intermediate to felsic volcanism

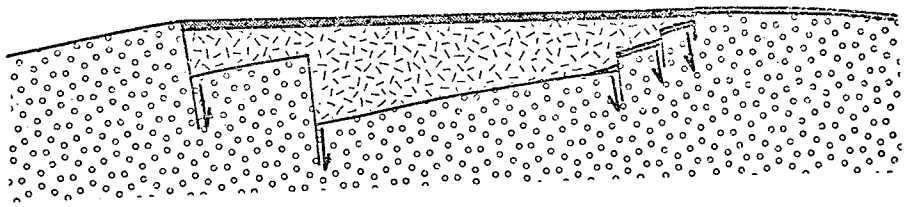

STAGES 4 and 5 Cessation of caldera-filling volcanism followed by fumarolic activity, erosion, and sedimentation at the top of the caldera

Formation E — mafic flows

Formation F — marble, chert and siltstone

Formation G(northern part) — intermediate pyroclastic rocks

Formation H — felsic to intermediate pyroclastic rocks and flows (includes the southern part of formation G)

Formation I — siltstone, sandstone and conglomerate

Fig. 23. Stages of development prior to, during, and following volcanic collapse.

volcanoes, formation of calderas heralds changes in volcanism, with eruption of more felsic and pyroclastic products.

Recognition of the four members and the proximal and distal vent facies of formation H not only elucidates the phases and nature of volcanism, but also the relationship between the phases of volcanism and stages of collapse forming the caldera. The apparent lack of collapse breccias (Lipman, 1976) and the stratigraphic relationships within formation H suggest that volcanism and collapse were synchronous. Although it is difficult to determine the mechanism controlling collapse, synchronous volcanism and collapse probably indicate that collapse resulted from the eruption of felsic to intermediate products within the caldera, thereby removing support from the underlying magma chamber.

The southern part of formation G and member H - 1 represent the first major period of volcanism which was associated with the first period of collapse. Early volcanism during this period comprised effusive, mafic to intermediate phases and explosive felsic to intermediate phases. As volcanism continued the explosive, felsic to intermediate phase became the dominant phase. Although the northern margin of the caldera probably formed during this period of collapse, it is obscured by subsequent faulting and the intrusion of quartz diorite and gabbro sills. Collapse appears to have been greatest at the southern margin of the caldera. Proximal vent facies units and the majority of source vents are near the southern margin of the caldera and the units are thickest in the south because of accumulation against the wall of the caldera or differential collapse. These units decrease in thickness to the north and interfinger with distal vent facies units in the northern part of the caldera.

Member H-2 comprises effusive and explosive felsic to intermediate phases and represents the second major period of volcanism; it extends most of the way across the present cross-section of the caldera. It is the only member exposed at the north end of the caldera which may indicate that this period of volcanism was accompanied by a second period of collapse which enlarged the caldera northward. Source vents are near the northern margin of the caldera and as a result, proximal vent facies units accumulated against the wall of the caldera. To the south the proximal vent facies interfingers with distal vent facies lahars which eventually pinch out near the southern margin of the caldera.

Member H-3 occurs in the southern and central parts of the caldera and is a distal vent facies which represents the third major period of volcanism. Although proximal vent facies units are not exposed in the present cross-section of the member, the thick accumulation of pyroclastic rocks suggests that volcanism was dominantly explosive. The southern part of the member accumulated against the southern wall of the caldera which may indicate further collapse on this margin, during this period of volcanism. The northward thinning and eventual pinching out of the member suggests that collapse was greatest in the south and central parts of the caldera.

Member H-4 occurs in the southern and central parts of the caldera and represents the fourth and final major period of volcanism and collapse. The member consists of a northern and southern proximal vent facies and a central distal vent facies. Stratigraphic relations indicate that volcanism was earlier in the north than in the south. The northern vent facies, which forms a modified cone, was produced by dominantly explosive volcanism. There does not appear to have been

concomitant volcanic collapse. The southern proximal vent facies, which was produced by both explosive and effusive volcanism, overlies the initial southern boundary of the caldera because collapse at this stage enlarged the caldera southward. Units in this facies accumulated against the upper, southern wall of caldera because of the close proximity of source vents to the margin of the caldera.

Active volcanism was followed by a period of fumarolic and hot spring activity and erosion of formation H. Detritus in the lower part of formation I was deposited in alluvial fan and shallow-water environments confined by the top of the caldera which had not been completely filled by volcanism. This period of sedimentation was followed by a more quiescent period of lacustrine sedimentation represented by the upper part of formation I. The lake was probably within the northern part of the caldera.

The location of many of the source vents near the margins of the caldera may indicate that they are related to boundary faults controlling collapse, as in the Masaya caldera, Nicaragua (Williams and McBirney, 1968).

Evidence for collapse has not been found in formations that underlie formation G. This does not discount the collapse model because 1) synvolcanic boundary faults would be difficult to locate in meta basaltic sequences because of their uniform appearance and poorly defined stratigraphy, 2) boundary faults may have been destroyed by felsic and mafic intrusions (Fig. 1), or 3) more likely there was major offset along the Setting Net Creek fault (Fig. 5).

CONCLUSIONS

In the past, volcanological research in Early Precambrian metavolcanic-metasedimentary sequences has focused mainly on regional stratigraphy and geochemistry. This has provided a framework that should be used for more detailed research on the stratigraphy. Study of formation H shows the importance of detailed stratigraphic analysis for deciphering volcanological development of Early Precambrian volcanic sequences. This type of analysis is a prerequisite for a comprehensive understanding of the geochemical characteristics and variation within volcanic sequences.

Formation H is unique because it represents a cross-section of a felsic to intermediate vent facies sequence occupying a volcanic depression, probably a caldera, steeply overturned by Late Precambrian isoclinal folding. The formation consists predominantly of a complex accumulation of felsic to intermediate pyroclastic rocks that, despite recrystallization during regional greenschist facies metamorphism, can be broadly subdivided into primary and secondary types. Primary pyroclastic rocks contain lithic and vitric fragments and were not moved from their original site of emplacement after ejection. Secondary types consist of lithic fragments that were transported from their original sight of emplacement during or shortly after the eruptive stage and prior to lithification. Glass and pumice are rare in secondary pyroclastic rocks because they are readily broken down during transportation. Transportation of pyroclastic fragments, closely following volcanic emplacement, is probably a common process on the upper slopes of stratovolcanoes because initial deposits are unconsolidated, depositional slopes are unstable, and rainfall and earthquakes during the eruption add to instability. Transportation that probably involved reworking by

sheet, rill, and stream erosion and mass movement by debris flows can be recognized in formation H.

On the basis of major, systematic, vertical, lithologic changes and genetic variations, four vent facies members can be recognized. The members in turn are subdivided into proximal vent facies and distal vent facies on the basis of lateral lithologic and genetic variations. Proximal vent facies comprise flows and primary pyroclastic rocks that were deposited close to source vents. Distal vent facies comprise primary tuff, fluvial and laharic pyroclastic rocks, and minor volcanic epiclastic rocks that were deposited further away from the source vents. Both of these subdivisions are useful because they elucidate the history of volcanism, the relationship between volcanism and volcanic collapse, and the location of source vents in the cross-section of the caldera.

The members represent four major periods of volcanism, each of which was apparently coeval with a period of collapse. Collapse was probably the trapdoor type with the magnitudes of collapse being greater at the south boundary of the caldera than at the north. The concentration of proximal vent facies near the northern and southern boundaries of the caldera indicate that source vents were located in the caldera and that they were peripheral features some of which may have been related to boundary faults controlling collapse. Felsic to intermediate volcanism was dominantly explosive, except in the proximal vent facies in member H-2 and the southern proximal vent facies in member H-4 where effusive phases were as equally important as explosive phases. Following volcanism formation I sediments deposited in shallow-water and alluvial fan environments confined by the top of the caldera which had not been completely filled by volcanism.

Felsic to intermediate volcanism was apparently subaerial. This is indicated by the composition and explosive nature of volcanism, the absence of pillows, the high degree of reworking in distal vent facies, the absence of submarine sedimentary features, the local occurrence of conglomerate in formation H, the probable deposition of many lahars in erosion channels, the erosion of the upper part of formation H, and the deposition of extensive formation I conglomerate in an alluvial fan environment.

Texturally, mineralogically, and chemically, formation H differs from other greenschist facies felsic to intermediate metavolcanic rocks in the area, suggesting that it underwent an episode of metasomatism prior to the regional metamorphic event and probably during volcanism. Textural and mineralogical features include intense destruction of primary textures, high biotite content, presence of muscovite-rich buff-alteration zones, widespread pyrite occurrence and the local presence of garnet in the buff-alteration zones. Chemically there is a marked depletion in lime and total alkalies, and depletion and enrichment in Na_2O and K_2O, and magnesia and total iron appear to have been mobile. Isolated changes in silica could not be proven but can not be discounted. The origin of metasomatism was probably hot spring activity.

Classification of metasomatised samples is meaningless unless chemical changes can be determined. When these changes were taken into account it was found that formation H was originally calc-alkaline, andesite and dacite although samples now span the tholeiitic to calc-alkaline field boundary.

REFERENCES

Adams, G.W. 1976. Precious metal veins of the Berens River Mine, northwestern Ontario. Unpubl. MSc. thesis, Univ. of Western Ontario. London.

Andrews, P.W. 1964. Chemical characteristics of some volcanic rocks of the Superior Province of the Canadian Shield. Unpubl. MSc. thesis, Univ. of Manitoba, Winnipeg.

Ayres, L.D. 1969. Early Precambrian stratigraphy of part of Lake Superior Provincial Park, Ontario, Canada, and its implication for the origin of the Superior Province. Unpubl. Ph.D thesis, Princeton Univ., New Jersey.

_____ 1970. Setting Net Lake area. Ontario Dept. Mines, Prelim. Map P. 538 (revised).

_____ 1972. Northwind Lake. Ont. Dept. Mines N. Aff. Prel. Map P. 756.

_____ 1974. Geology of the Trout Lakes area. Ont. Div. Mines Geol. Rep. 113, 119p.

_____ 1977. Importance of stratigraphy in early precambrian volcanic terranes: Cyclic volcanism at Setting Net Lake, northwestern Ontario. Geol. Assoc. Con., Spec. Pap. 16, pp 243-264.

Baragar, W.R.A. and Goodwin, A.M. 1969. Andesites and Archean volcanism in the Canadian Shield. In: Proceedings of the andesite conference, Bull. 65, Oregon Dept. Geol. and Min. Industries. pp 121-142.

Boles, J.R. and Coombs, D.S. 1975. Mineral reactions in zeolitic Triassic tuff, Hokonui Hills, New Zealand. Geol. Soc. Amm. Bull. 86, pp 163-173.

Burnham, C. Wayne. 1967. Hydrothermal Fluids at the magmatic stage. In: Geochemistry of hydrothermal ore deposits. (H.L. Barnes, Ed.) Holt, Rinehart, and Winston Ltd., pp 34-36.

Christiansen, R.L. and Lipman, P.W. 1966. Emplacement and thermal history of a rhyolite fava flow near Forty Mile Canyon, southern Nevada. Geol. Soc. Am. Bull. 77, pp 671-684.

Colley, H. and Warden, A.J. 1974. Petrology of the New Hebrides. Geol. Soc. Am. Bull. 84, pp 1635 - 1646.

Condie, K.C. and Swenson, D.H. 1973. Compositional variation on three Cascade stratovolcanoes: Jefferson, Rainier and Shasta. Bull. Volc. 37. pp 1 - 26.

Craig, H. 1966. Isotopic composition and origin of the Red Sea and Salton Sea brines. Science, 154, p 1444.

_____ 1969. Geochemistry and origin of the Red Sea brines. In: Hot brines and recent heavy metal deposits in the Red Sea. (E.T. Deggens and D.A. Ross, Eds.) Springer Verlag, New York, pp 225-242.

Denholm, L.S. 1966. Structural and Economic aspects of the Vatukoula caldera, Fiji. Bull. Volc. V 29, pp 223 - 233.

Ewart, A. and Stipp, J.J. 1968. Petrogenesis of the volcanic rocks of the central North Island, New Zealand, as indicated by a study of Sr 87/ Sr 86 ratios, and Sr, Rb, K, Cl and Th abundances. Geochim. Cosmochim. Acta, 32, pp 699 - 736.

Fisher, R.V. 1960a. Criteria for recognition of laharic breccias, Southern Cascade Mountains, Washington. Geol. Soc. Am. Bull. 71, pp 127-132.

_____ 1960b. Classification of volcanic breccias. Geol. Soc. Am. Bull. 71. pp 973-982.

_____ 1961. Proposed classification of volcaniclastic sediments and rocks. Geol. Soc. Am. Bull. 72, pp 1409 - 1414.

_____ 1966. Rocks composed of volcanic fragments and their classification. Earth Sci. Rev. 1, pp 287-298.

Fiske, R.S., Hopson, C.A., and Waters, A.C. 1963. Geology of Mt. Rainier National Park, Washington. U.S. Geol. Surv. Prof. Pap. 444, 93p.

Gill, J.R. 1970. Geochemistry of Viti Levu, Fiji and its evolution as an island arc. Contrib. Mineral. Petrol. 27, pp 179 - 203.

Glikson, A.Y. 1971. Primitive Archean element distribution patterns: chemical evidence and geotectonic significance. Earth Planet. Sci. Lett. 12, pp 309-320.

Goodwin, A.M. 1967. Volcanic studies in the Birch-Uchi Lakes areas of Ontario. Ont. Dep. Mines Misc. Pap. 6, 96p.

Goodwin, A.M. and Ridler, R.H. 1970. The Abitibi orogenic belt. In: Symposium on basins and geosynclines of the Canadian Shield. (A.J. Baer, Ed) Geol. Surv. Can. Pap. 70-40, pp 1-30.

Hart, S.R., Brooks, C., Krogh, T.E., Davis G.L., and Nava, D. 1970 Ancient and modern volcanic rocks: a trace element model. Earth Planet. Sci. Lett. 27, pp 17-38.

Higgins, M.W. 1973. Petrology of Newberry volcano, Central Oregon. Geol. Soc. Am. Bull. 84, pp 455-487.

Hughes, C.J. 1972. Spilites, keratophyres and igneous spectrum. Geol. Mag. 109, pp 513 - 527.

Irvine, T.N. and Baragar, W.R.A. 1971. A guide to the chemical classification of the common volcanic rocks. Can J. Earth Sci. 8, pp 523 - 548.

Jakes, P. and White, A.J.R. 1969. Structure of the Melanesian arcs and correlation with distribution of magma types. Tectonophysics. 8, pp 223 - 236.

_____ 1972. Major and trace element abundances in volcanic rocks of orogenic areas. Geol. Soc. Am. Bull. 83. pp 29-40.

Jolly, W.T. 1975. Subdivision of the Archean lavas of the Abitibi area, Canada, from Fe-Mg-Ni-Cr relations. Earth Planet. Sci. Lett. 27, pp 200-210.

Keller, J. 1974. Petrology of some volcanic rock series of the Aeolian arc, Southern Tyrrhenian Sea: Calc-alkaline and shoshonitic associations. Cont. Min. Pet., 46, pp 29-49.

Kuno, H. 1959. Origin of Cenozoic petrographic provinces of Japan and surrounding areas. Bull. Volc. 29, pp 195-222.

Lipman, P.W. 1976. Caldera-collapse breccias in the western San Juan Mountains, Colorado. Geol. Soc. Am. Bull. 87, pp 1397-1410.

Lipman, P.W., Christiansen, R.L., and O'Connor, J.T. 1966. A compositionally zoned ash flow sheet in southern Nevada. U.S. Geol. Survey Prof. Paper 524 - F, 47p.

Lopez-Escobar, L., Frey, F.A., and Vergara, M. in press. Andesites in central-south Chile: Trace element abundances and petrogenesis. Bull. Volc.

Macdonald, G. 1972. Volcanoes. Prentice-Hall Inc., New Jersey, 510p.

McBirney, A.R. 1963. Factors governing the nature of submarine volcanism. Bull. Volc. 26, pp 455-469.

McBirney, A.R. and Murase, T. 1971. Factors governing the formation of pyroclastic rocks. Bull. Volc. 34, pp 372-384.

McCall, G.J.H., Le Maitre, R.W., Malahoff, A., Robinson, G.P., and Stephenson, P.J. 1971. The geology and geophysics of the Ambrym caldera, New Hebrides. Bull. Volc., 34, pp 681-696.

Miyashiro, A. 1974. Volcanic rock series in island arcs and active continental margins. Am. J. Sci. 274, pp 321-355.

Parsons, W.H. 1969. Criteria for the recognition of volcanic breccias: A review. In: Igneous and metamorphic geology. (L. Larsen, V. Manson, M. Prinz, Eds.) Geol. Soc. Amer. Mem. 115, pp 263-304.

Pettijohn, F.J., Potter, P.E., and Siever, R. 1972. Sand and Sandstone. Springer Verlag, Berlin, 618p.

Pichler, H. and Zeil, W. 1972. The Cenozoic rhyolite-andesite association of the Chilian Andes. Bull. Volc. 35, pp 423-452.

Raudsepp, M. 1975. Metagabbro sill complex, Favourable Lake area. In: Centre for Precambrian Studies Annual Report, Pt - 2 Research, Univ, Manitoba, pp 114-120.

Ridley, W.I. 1971. The origin of some collapse structures in the Canary Islands. Geol. Mag. 108, pp 477-484.

Ross, C.S. and Smith, R.L. 1961. Ash flow tuffs: their origin, geologic relations and identification: U.S. Geol. Survey Prof. Pap. 366, 81p.

Rubel, D.N. 1971. Independence volcano: A major Eocene Eruptive Centre, northern Absaroka volcanic province. Geol. Soc. Am. Bull. 82, pp 2473-2494.

Siegers, A., Pichler, H., and Zeil, W. 1969. Trace element abundances in the Andesite Formation of northern Chile. Geochim. Cosmochim. Acta., 33, pp 882-887.

Smedes, H.W. and Prostka, H.J. 1972. Stratigraphic framework of the Absaroka Volcanic Supergroup in the Yellowstone National Park region. U.S. Geol. Survey Prof. Paper 729 - C, 33p.

Stauffer, M.R., Mukherjee, A.C., and Koo, J. 1975. The Amisk Group: an Aphebian island arc deposit. Can. J. Earth Sci. 12, pp 2021-2035.

Taylor, S.R. 1969. Trace element chemistry of andesites and associated calc-alkaline rocks. In: Proceedings of the Andesite Conference, Bull. 65, Oregon Dept. Geol. and Min. Industries, pp 43-64.

Waldron, H.H. 1967. Debris flow and erosion control problems caused by the ash eruptions of Irazu volcano, Costa Rica. U.S. Geol. Surv. Bull. 1241-1, 37p.

Warden, A.J. 1970. Evolution of Aoba caldera, New Hebrides. Bull. Volc. 34, pp 107-140.

Williams, H. 1941. Calderas and their origin. Univ. Calif. Publs. Geol. Sci. 25, pp 239-346.

Williams, H. and McBirney, A.R. 1968. An investigation of volcanic depressions. Pt - 1 Geologic and geophysical features of calderas. National Aeronautics and Space Administration Res. Grant NRG - 38 - 003 - 012, Prog. rept., 87p.

_____ 1969. An investigation of volcanic depressions, Part 1, Airfall and intrusive pyroclastic deposits, and Part 11, Subaerial pyroclastic flows and their deposits. National Aeronautics and Space Administration Res. Grant NRG - 38 - 003 - 012, Prog. rept., 100p.

Wilson, H.D.B., Andrews, P., Moxham, R.L., and Ramlal, K. 1965. Archean volcanism in the Canadian Shield. Can. J. Earth Sc. 2, pp 161 - 175.

Wilson, H.D.B., Morrice, M.G. and Ziehlke, D.V. 1974. Archean continents. Geoscience Can. 1, No. 3, pp 12-30.

Winkler, H.G.F. 1967. Petrogenesis of Metamorphic Rocks (2nd edition). Springer - Verlag, New York, 237p.

Zen, E-an, Thompson, A.B. 1974. Low grade regional metamorphism; mineral equilibrium relations: Ann. Rev. Earth and Planet. Sc. 2, pp 179-212.

LEGEND

POST FORMATION H INTRUSIONS

17 Unmetamorphosed diabase dike

16 Granitic intrusive rocks

a. Setting Net Lake stock

b. minor dikes

15 Gabbro sill

FORMATION J

14 Undifferentiated mafic and ultramafic volcanic and intrusive rocks

FORMATION I

13 Shallow-water facies sedimentary rocks: undifferentiated volcanic sandstone, conglomerate, argillite and siltstone, intermediate tuff, chert and ferruginous chert

UNCONFORMITY

FORMATION H Felsic to intermediate pyroclastic rocks, flows, volcanic epiclastic rocks, and related intrusions

12 Fine-grained mafic dikes

11 Quartz diorite intrusive rocks

10 Intrusive alloclastic breccia

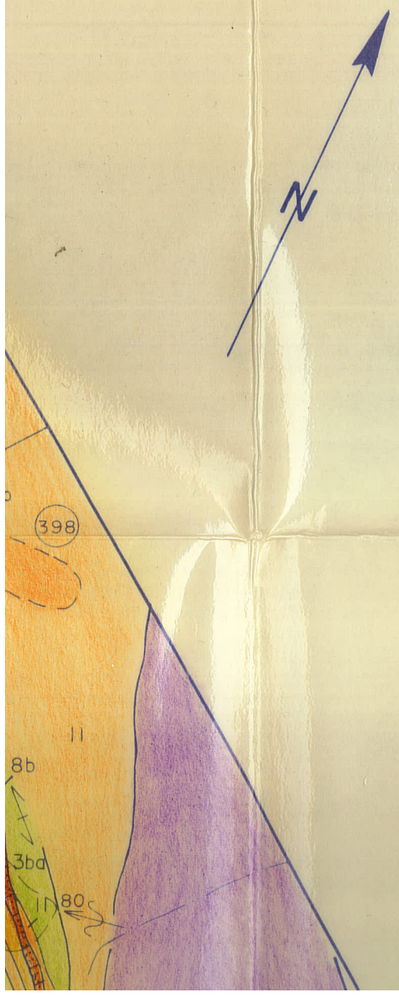

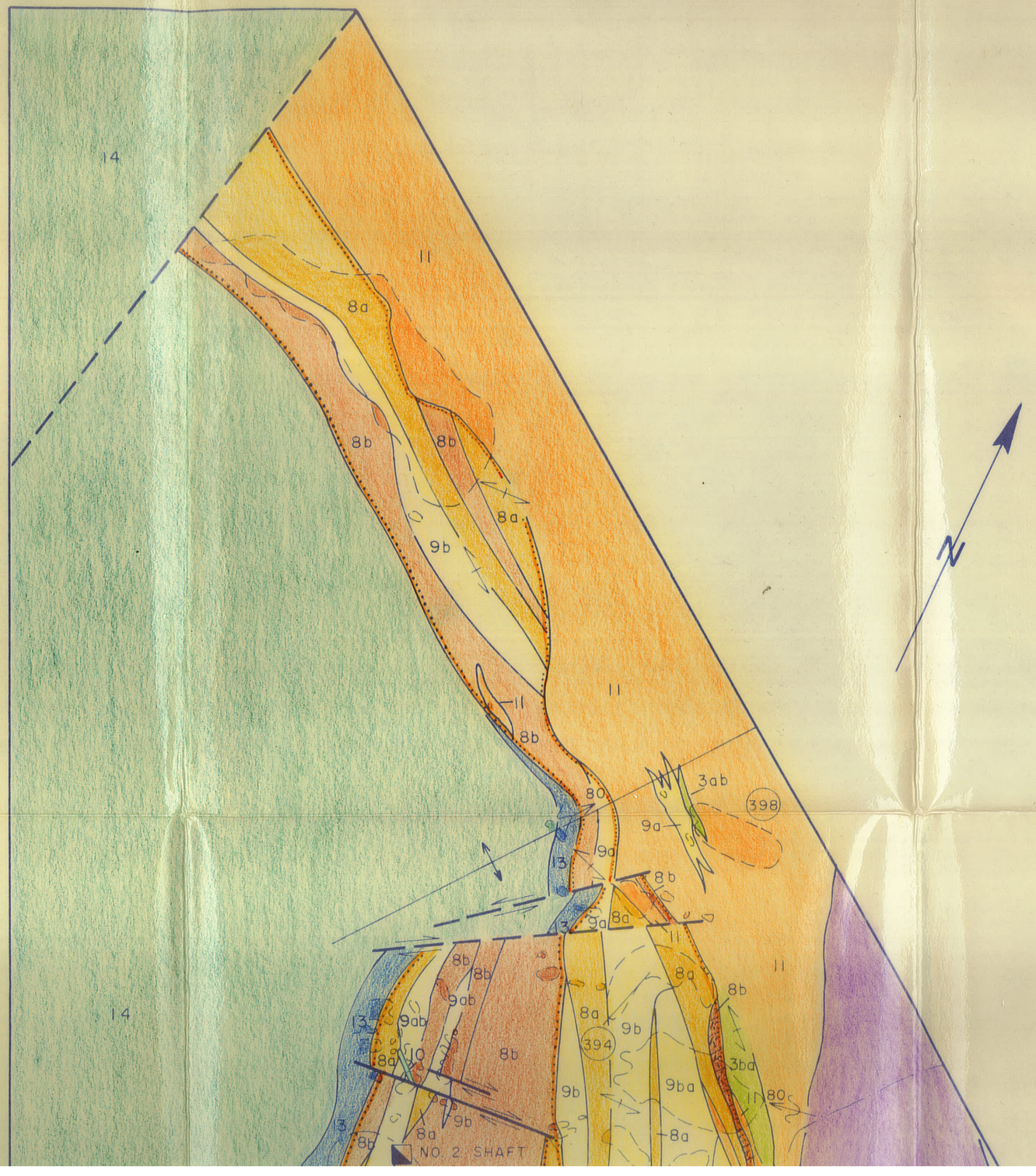

POST FORMATIC

17 Unmet

16 Graniti

a. S

b. r

15 Gabbr

FORMATION

14 Undiff

FORMATION I

13 Shallo
sands
chert

FORMATION H

12 Fine-

11 Quartz

10 Intrusi

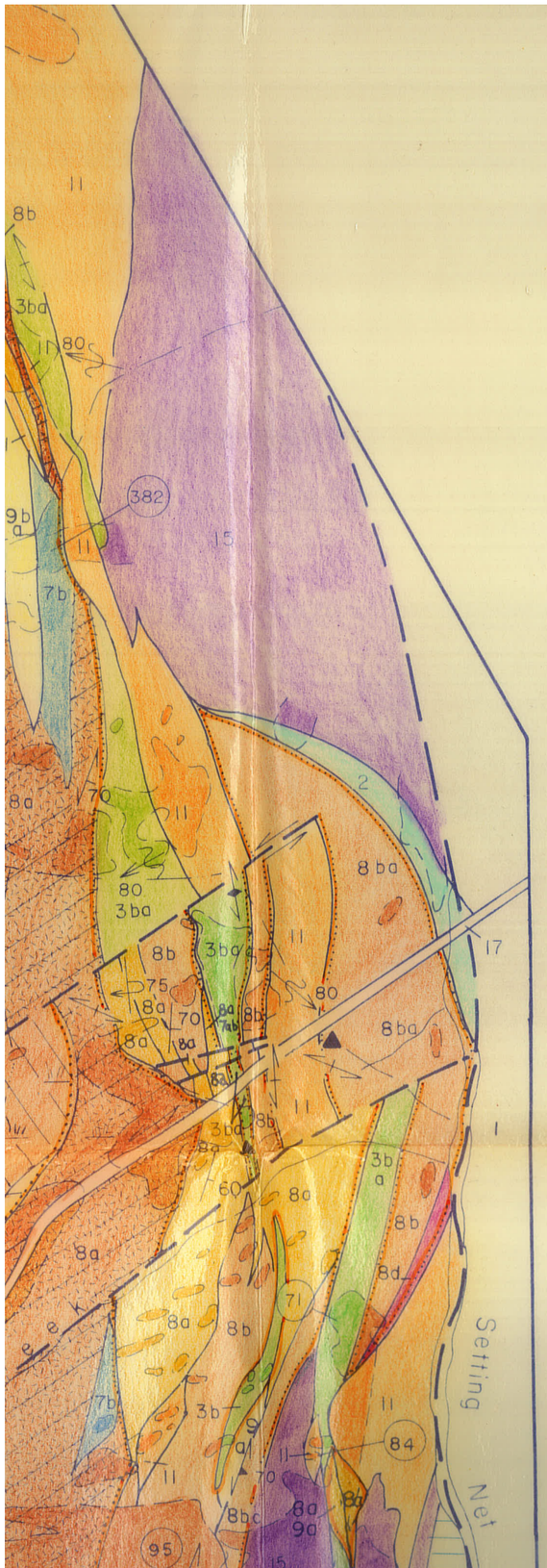

CALDERA SEQUENCE

FORMATION H Felsic to intermediate pyroclastic rocks, flows, volcanic epiclastic rocks, and related intrusions

12 Fine-grained mafic dikes

11 Quartz diorite intrusive rocks

10 Intrusive alloclastic breccia

9 Flows

- a. Aphyric
- b. Porphyritic with plagioclase phenocrysts
- c. Porphyritic with plagioclase and quartz phenocrysts
- d. Autobreccia

8 Pyroclastic rocks

Primary pyroclastic rocks

- a Tuff
- b Lapilli-tuff, lapillistone
- c Agglomerate
- d Breccia

Secondary pyroclastic rocks

Fluvial

- a Tuff
- b Lapillistone

Laharic

- a Lapilli-tuff, lapillistone
- b Tuff-breccia

NO. 2 SHAFT

NO. 1 SHAFT

Borthwick

Creek

Setting Net

FORMATION

12 Fine-

11 Quart

10 Intrus

9 Flows

a.

b.

c.

d.

8 Pyroc

CALDERA SEQUENCE

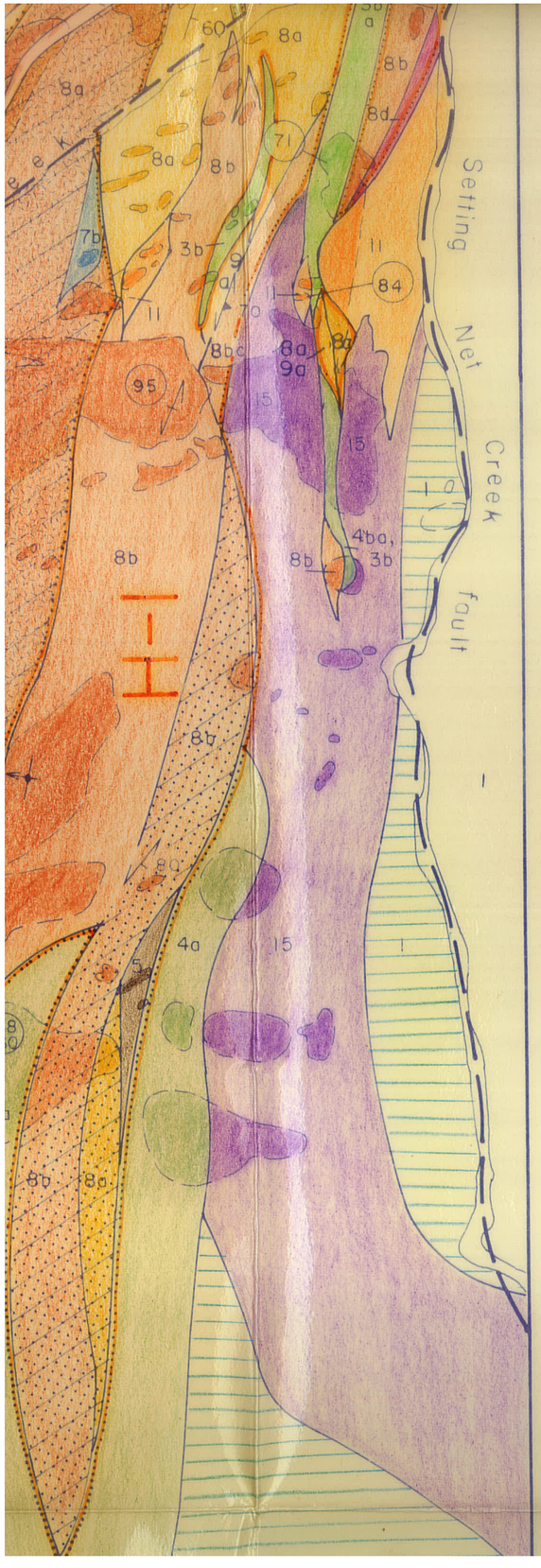

d Breccia

Secondary pyroclastic rocks

Fluvial

a Tuff

b Lapillistone

Laharic

a Lapilli-tuff, lapillistone

b Tuff-breccia

Undifferentiated pyroclastic rocks

a Tuff

b Lapilli-tuff, lapillistone

7 Volcanic epiclastic rocks

a. Argillite, graphitic argillite

b. Litharenite, feldspathic litharenite

6 Conglomerate

5 Chert and ferruginous chert

FORMATION G Mafic to intermediate flows and pyroclastic rocks

4 Flows

a. Massive, aphyric and porphyritic

b. Autobreccia

3 Pyroclastic rocks

a. Tuff

b. Lapilli-tuff, lapillistone

Borthwick

Borthwick

Lake

Creek

Setting Net Creek fault

H3

H2

H1

CALDERA SEQ

d

Sec

Und

a

b

7 Volca

a.

b.

6 Congl

5 Chert

FORMATION

4 Flows

a.

b.

3 Pyroc

a.

b.

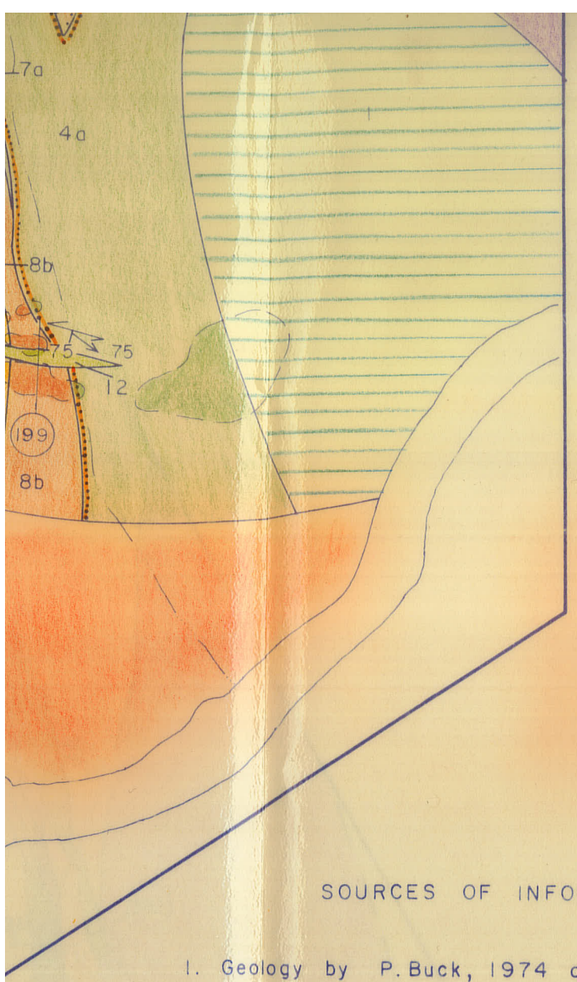

b. Lapilli-tuff, lapillistone

FORMATION F

2 Undifferentiated marble, chert, and siltstone

FORMATION E

1 Undifferentiated mafic volcanic rocks

FOOTNOTE: All rocks except the diabase dike have undergone greenschist grade metamorphism

SYMBOLS

- Small outcrop and outcrop, geological and member boundaries (H1-H4)
- Fault—defined, assumed
- Bedding, top unknown—inclined, vertical
- Bedding, top known—vertical, overturned
- Primary flow foliation
- Pillows
- Foliation, gneissosity, lineation
- Major fold axis—anticline
- Drag fold, minor fold, with plunge directions
- Shaft, Pb-Zn-Py-sulphide occurrences, gossans and pyrite veining
- Swamp
- Road, access trail
- Mine waste
- (18) Chemical analysis locations

SCALE

0 220 660 440meters 1320feet

SOURCES OF INFORMATION

1. Geology by P. Buck, 1974 and 1975.
2. Geological information adjacent to formations G and H derived from L.D. Ayres (in press).
3. Basemaps and aerial photographs derived from Forest Resources Inventory, Ministry of Natural Resources.

Fig.5 Geological map of formation H.

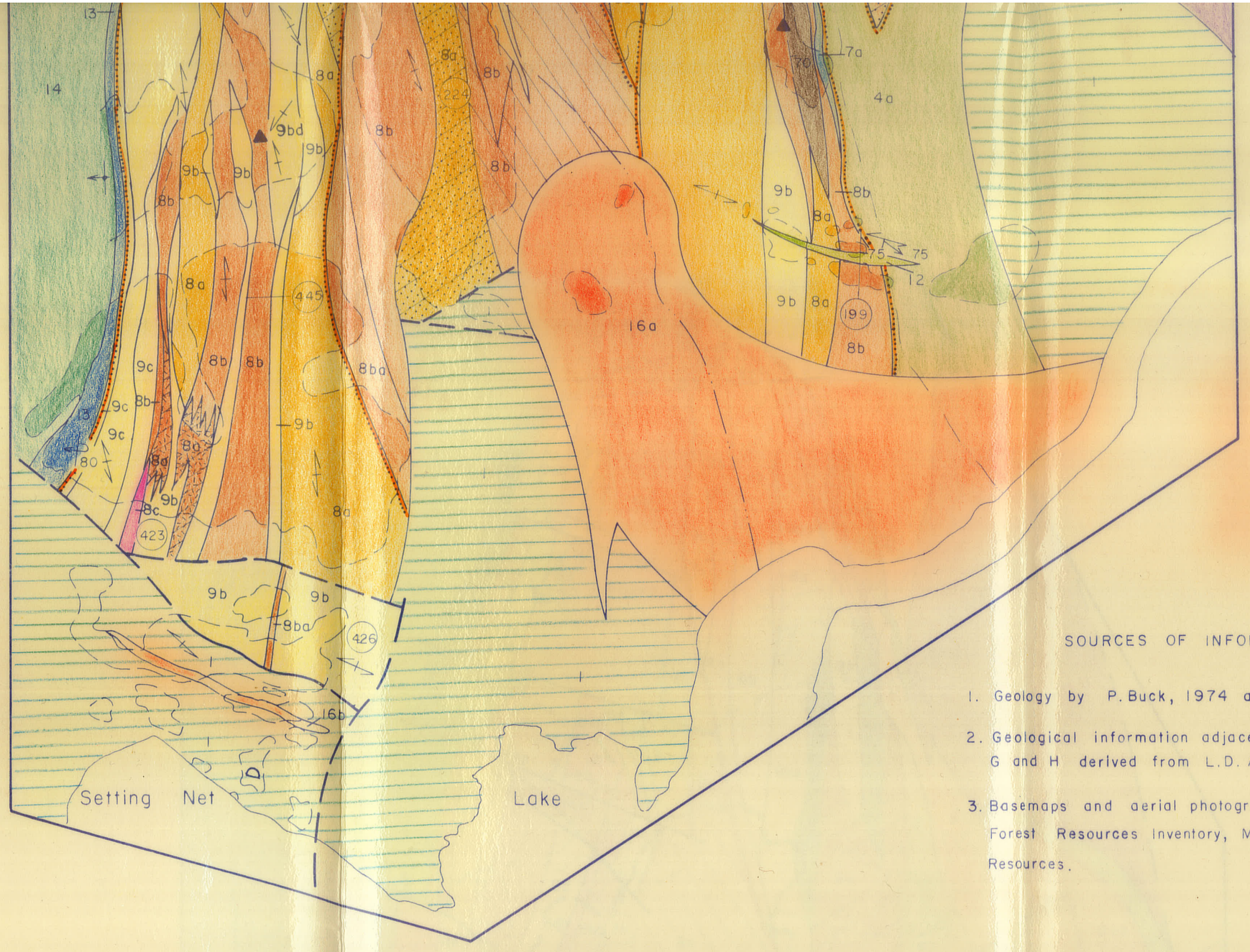

b. L

FORMATION

2 Undiff

FORMATION

1 Undiff

FOOTNOTE: All r

S

F

B

F

F

F

SOURCES OF INFORMATION

1. Geology by P. Buck, 1974 and 1975.
2. Geological information adjacent to formations G and H derived from L.D. Ayres (in press).
3. Basemaps and aerial photographs derived from Forest Resources Inventory, Ministry of Natural Resources.